

Kinematics and Controlling Mechanics of the Slow Moving Ripley Landslide

by

Matthew B. Schafer

A thesis submitted in partial fulfillment of the requirements for the degree of

Master of Science

In

Geotechnical Engineering

Department of Civil and Environmental Engineering

University of Alberta

© Matthew B. Schafer, 2016

Abstract

The Ripley Landslide is one of several slow moving landslides in the Thompson River Valley, near Ashcroft, British Columbia. Both the Canadian Pacific and Canadian National Railway main lines cross this landslide. As a result, the site is an important part of Canada's transportation network and has been investigated and monitored with the goal of developing an operational strategy to aid in the safe operation of the railroads.

A summary of the site investigation and monitoring results at the Ripley landslide are presented in this thesis, including information not used in previous publications. The monitoring results have been validated to ensure that the data are representative of the landslide behaviour. The updated geological and monitoring data are then analysed to develop cross sections and gain a better understanding of the kinematics of the Ripley Landslide and the mechanisms controlling its behaviour.

“For no man can lay a foundation other than the one which is laid...”

1 Corinthians 3:11

Acknowledgements

I would like to express my sincere gratitude to Dr. C.D. Martin and Dr. M.T. Hendry for their supervision and guidance in this thesis work. Their insight, guidance, and financial support were essential in completing the goals of this research. I would also like to thank Dr. R. Macciotta for his constant support and valuable advice.

Gratitude is also extended to all of the professors in the geotechnical group, particularly Dr. R. Chalaturnyk, Dr. D.H. Chan, Dr. G. Wilson, Dr. D.M. Cruden, and Dr. N.R. Morgenstern. Conversations with each of you during my time at the university have contributed to my professional and personal development.

My sincere appreciation is extended to Canadian National railway, Canadian Pacific Railway, Transport Canada, and the Geological Survey of Canada for their financial support of this project. I would like to thank Tom Edwards, Trevor Evans, Chris Bunce, Eddie Choi, David Huntley, and Peter Bobrowsky for their help.

Words cannot express my appreciation to my wife, Haley Schafer. Your unwavering love, support, and encouragement were instrumental in allowing me to pursue this great adventure. I look forward to supporting you and partnering with you in many adventures to come. Jack and Kerry Schafer are thanked for their encouragement and constant investment in me as loving parents. Thanks is extended to the Schafer and Van Daltsen families for their support throughout this research.

Gael Lemeil's collaboration while interpreting drilling results is appreciated. The field and instrumentation assistance of Jeffrey Journault was also very valuable. I am also thankful to my

other colleagues at the university, particularly Chris Davies and Eric Leishman, for their companionship through our course work together.

Funding for this project was provided through scholarships supplied by the Natural Sciences and Engineering Research Council of Canada (NSERC), Alberta Innovates Technology Futures (AITF), and the University of Alberta.

Table of Contents

1	Introduction.....	1
1.1	Research Purpose	2
1.2	Scope	2
1.3	Research Objectives	3
1.4	Organization of Thesis	3
2	Landslides in Varved/Rhythmic Glacial Sediments in Western Canada.....	5
2.1	Glaciolacustrine sediments.....	5
2.1.1	Instability in glaciolacustrine clays.....	8
2.2	The Ashcroft Thompson River landslides.....	9
2.2.1	History of the Ripley Landslide.....	10
2.2.2	Geological history.....	12
2.2.3	Characteristics of other Thompson River Valley landslides.....	12
2.3	Correlating movement rate with landslide conditions.....	15
3	Geology and Site Conditions	17
3.1	Geologic Context.....	17
3.2	Site investigations	20
3.2.1	Geophysical surveys	23
3.2.2	Borehole logging and observations during the site investigations	26
3.2.3	Variability in Bedrock Profile.....	29
3.2.4	Instrumentation	35
3.3	Summary	40
4	Pore Pressure and Displacements	42
4.1	Evaluation of pore pressure measurements.....	42
4.1.1	High frequency variation and barometric fluctuation.....	42
4.1.2	Evaluation of fully grouted installation method	46
4.2	Flow measurements of the Thompson River.....	49

4.3	Comparison of Displacement Measurements from ShapeAccelArray, GPS Monitoring, and Slope Inclinometer	53
4.4	Summary	60
5	Ripley Landslide Kinematics	62
5.1	Previously Proposed Cross Sections	62
5.2	The effect of bedrock profile on landslide mechanism	64
5.3	Surface displacement vectors	64
5.4	Additional displacement data at the Ripley Landslide	66
5.5	Vertical displacements of GPS 3	69
5.6	Cross sections of the Ripley Landslide	71
5.7	Implications of revised cross sections	73
5.8	Summary	74
6	Ripley Landslide Temporal Velocity	76
6.1	Calculating landslide velocity	78
6.2	Interaction of the Thompson River and the Ripley Landslide	82
6.3	Evaluating the proposed rapid drawdown mechanism of the Ripley Landslide	87
6.4	Factors affecting pore pressure in the Ripley Landslide	96
6.4.1	The Ripley Landslide as part of a regional groundwater flow basin	96
6.4.2	The effects of river level fluctuation on pore pressures at the Ripley Landslide	101
6.4.3	Analysis of weather data and its effects on regional bedrock pressures	106
6.5	Summary	108
7	Summary and Recommendations	110
7.1	Summary	110
7.2	Contributions of the Thesis	111
7.3	Conclusions	112
7.4	Recommended Future Research	113

List of Tables

Table 3-1 Depth and elevations of possible transition to Unit 2 encountered during the 2013 and 2015 site investigations at the Ripley Landslide (locations as per Figure 3-3)	29
Table 4-1 Comparison of horizontal displacement monitoring methods.....	57
Table 6-1 Equation coefficients and coefficients of correlation for the trend lines in Figure 6-11	92
Table 6-2 Equation coefficients and coefficients of correlation for the trend lines in Figure 6-12	95

List of Figures

Figure 2-1 Sample of glaciolacustrine clay from borehole drilled near Ashcroft, British Columbia (core photo courtesy of Dr. C.D. Martin; after Eshraghian et al. 2007)	6
Figure 2-2 Distribution of glacial lakes in Western Canada (after National Atlas of Canada 1972)	7
Figure 2-3 Index properties of glaciolacustrine silts and clays from the Ashcroft and Peace River regions (after Miller and Cruden 2002, Bishop et al. 2008)	8
Figure 2-4 Locations of landslides within the Thompson River Valley south of Ashcroft, BC (after Eshraghian et al. 2007, Hendry et al. 2015)	9
Figure 2-5 Comparison of slope geometry along three sections at the Ripley Landslide before and after the construction of the CP siding in 2005 (after Hendry et al. 2015)	11
Figure 2-6 Illustration of the typical failure mechanism observed in Thompson River Valley landslides near Ashcroft, B.C (after Eshraghian et al. 2007)	14
Figure 3-1 Regional stratigraphy considered while interpreting the borehole logs of the Ripley Landslide (after Clague and Evans 2003)	18
Figure 3-2 Coarse deposit within glaciolacustrine deposits at the Ripley Landslide	19
Figure 3-3 Location of boreholes drilled during the site investigation of the Ripley Landslide (after Macciotta et al. 2014)	22
Figure 3-4 Surface elevation model of the Ripley Landslide with locations of geophysics survey lines (after Huntley et al. 2014).	23
Figure 3-5 P-wave velocity contours interpreted from seismic refraction survey results along Line B of the Ripley Landslide (after Huntley et al. 2014, contours are in m/s)	25
Figure 3-6 Stratigraphy and instrumentation layout of the 2005 investigations of the Ripley Landslide	27

Figure 3-7 Stratigraphy and instrumentation layout of the 2013 and 2015 investigations of the Ripley Landslide	28
Figure 3-8 Rock slope along the West side of the Thompson River across from the Ripley Landslide.....	30
Figure 3-9 Andesite rock outcrop on southern boundary of the Ripley Landslide overlain by glacial till (Figure 3-3).....	31
Figure 3-10 Two possible interpretations of bedrock profile based on a set number of known points and seismic P-wave survey results.....	33
Figure 3-11 Andesite rock fragment obtained during the 2015 site investigation in BH15-03....	34
Figure 3-12 Comparison of the conventional and grouted-in installation methods of piezometers (after McKenna 1995).....	38
Figure 3-13 ShapeAccelArray on spool before installation has begun.....	39
Figure 3-14 Installation of ShapeAccelArray into BH15-04 in July 2015	40
Figure 4-1 Comparison of the variation of atmospheric pressure measured by an on-site barometer and a distant weather station.....	44
Figure 4-2 High Frequency Variation of Pore Pressure in the bedrock at a depth of 32.6 m and the shear zone at a depth of 15.6 m, and the Barometric Data provided by Environment Canada	45
Figure 4-3 Comparison of raw and barometric compensated pore pressure for a VW-piezometer at 20.4 m depth in BH13-01.....	46
Figure 4-4 Barometric compensated fully grouted piezometer readings at the Ripley Landslide in the first 18 months of monitoring over time (a) and with depth(b).....	47
Figure 4-5 Seasonal flow rate variation of the Thompson River as measured at Spences Bridge 50	

Figure 4-6 Correlation between the Thompson River elevation at the Ripley Landslide and the flow rate measured at Spences Bridge.....	52
Figure 4-7 Deflection recorded at the Ripley Landslide by a slope inclinometer in DH05-27 (a) and a ShapeAccelArray in BH13-02 (b) for the same time period in different years ...	54
Figure 4-8 GPS surface displacements recorded on the Ripley Landslide.....	55
Figure 4-9 River flow in the Thompson River measured at Spences Bridge for the period of November 15 to April 4 for the various periods of slope monitoring compared in Table 4-1.....	58
Figure 4-10 Comparison of displacement measurements of the SAA installed in BH13-01 and the GPS displacement units placed across the Ripley Landslide.....	60
Figure 5-1 Cross sections of the Ripley Landslide by Hendry et al. (2015) showing rupture surfaces, estimated stratigraphy, measured piezometric elevations (see Figure 3-3 for locations).....	63
Figure 5-2 Surface displacement vector inclinations observed by three GPS monitoring units installed on the Ripley Landslide (see Figure 3-3 on p.28 for unit locations).....	66
Figure 5-3 Incremental displacements (in mm) along Section 2 (Figure 3-3) between March 3, 2015 and July 13, 2015; Shear zones indicated in black with the cumulative displacement indicated beside them	68
Figure 5-4 Simplified visualization of a compound landslide (after Norrish and Wyllie 1996) ..	70
Figure 5-5 Revised cross sections of the Ripley Landslide showing rupture surfaces, river level range, instrumentation, and estimated stratigraphy	72
Figure 6-1 Seasonal variation of displacements recorded using SAA in BH13-02 (a), Thompson River Elevation (b), and Heat Degree Days (c) at the Ripley Landslide.....	77
Figure 6-2 Instantaneous velocity calculated from 6-hour SAA readings from BH13-02 using Equation 6-1.....	79

Figure 6-3 Fast fourier transform of instantaneous landslide velocity calculated from 6-hour SAA readings from BH13-02 using Equation 6-1	80
Figure 6-4 Fast fourier transform of landslide velocity during period of landslide inactivity in 2014 (Figure 6-1).....	81
Figure 6-5 Instantaneous landslide velocity calculated from the 16-day moving average of 6-hour SAA readings from BH13-02	82
Figure 6-6 Forces acting on the landslide mass that produce a net instability (F_s).....	83
Figure 6-7 Changes to landslide mass caused by variation in the river elevation adjacent to the landslide	84
Figure 6-8 Phreatic surface resulting from an increase and decrease in river level for a landslide mass with (1) high permeability, (2) moderate permeability, and (3) very low permeability.	85
Figure 6-9 Trend of 16-day velocity with volumetric flow of the Thompson River as measure at Spences Bridge	88
Figure 6-10 Displacements predicted based on river flow variation and the velocity trends presented in Figure 6-9 for the periods of July 1, 2013 to July 1, 2014 (a) and July 1, 2014 to July 1, 2015 (b).....	89
Figure 6-11 Landslide velocities for the movement seasons starting in 2013(a), 2014(b), and 2015(c) at the Ripley Landslide as a function of differential pressure as defined by Equation 6-4.....	91
Figure 6-12 Landslide velocities for the movement seasons starting in 2013(a), 2014(b), and 2015(c) at the Ripley Landslide as a function of river elevation.....	94
Figure 6-13 Regional map of the Thompson River valley and cross section A-A' centred at the Ripley Landslide (image and profile from Google Earth 2015).....	98

Figure 6-14 Isotope testing results with depth from BH15-01 (a) and BH15-03 (b) taken during the 2015 investigation of the Ripley Landslide (testing performed by Erin Schmeling)	99
Figure 6-15 Co-isotope plot of testing results from the Ripley Landslide (testing performed by Erin Schmeling)	100
Figure 6-16 Seasonal variation of Thompson River elevation at the Ripley Landslide	101
Figure 6-17 Variation of bedrock pressure as a function of river elevation	102
Figure 6-18 Deviation of bedrock pressures from linear river response over time as defined by Equation 6-3 (a) and Thompson River elevation adjacent to the Ripley Landslide with time (b).....	104
Figure 6-19 Non-linear pore pressures at the Ripley Landslide over time (a) and seasonal trends in temperature (b), rainfall (c), and snowfall (d) at Logan Lake.....	107

1 Introduction

There are many landslides located in river valleys across Western Canada. Glacial sediments deposited in valleys have been eroded by present day rivers which has resulted in relatively deep and steep valleys. These valleys are common locations to find deep seated translational slope instabilities which move at a wide range of rates (Clague and Evans 2003). Landslide hazard in these regions is among the highest in Canada (Evans 2005).

These landslides are a significant issue for Canadian railways. Railways generally manage these types of hazards in one of three ways: (1) avoid the hazard, (2) stabilize the hazard, or (3) use monitoring and signals to ensure that safe track conditions are maintained (Bunce and Chadwick 2012). There is a maximum grade restriction for the railway which makes moving the track to avoid hazards quite difficult. When stabilization is cost prohibitive or the effectiveness of stabilization is doubtful, the monitoring approach to risk management is often taken.

As the demands of society rise, the railways are under constant pressure to efficiently transport goods. From 1993 to 2013, the gross tonne-kilometres of freight in Canada increased from 4.29×10^{11} tkm to 6.95×10^{11} tkm (Statistics Canada 2016). These increased loads and increased traffic also increase the consequences of any potential track interruption. While monitoring a hazard ensures train safety, it does not decrease the chance of track interruption due to excess ground movement. Monitoring does provide valuable information on the behaviour of a given hazard. Current monitoring can be used to gain a better understanding of landslide mechanisms and be used to develop stabilization measures which are either more economically feasible or more effective.

1.1 Research Purpose

The Thompson River Valley in southern British Columbia is a critical corridor for the rail transport of goods in Canada. In 2012 it was estimated that CN and Canadian Pacific (CP) railways route as many as 40 trains per day over this section with train lengths up to 4.3 km (Bunce and Chadwick 2012). The economic losses resulting from an interruption of rail traffic in this corridor would grow exponentially with time out of service. There are also several translational landslides of various sizes which the railways cross in this region (Hendry et al. 2015). Understanding the mechanisms and behaviours of these landslides is essential in managing the risk to the safety of the railroad. The purpose of this research is to gain a better understanding of the mechanisms controlling the displacements at one of the translational landslides in the Thompson River Valley.

1.2 Scope

There has been multiple site investigation and monitoring programs carried out at different landslides within the Thompson River Valley (Eshraghian et al. 2007). Since 2005, the Ripley Landslide has been one of the most active landslides in the region (Bunce and Chadwick 2012, Hendry et al. 2015). The Ripley Landslide is the primary focus of this research. The scope of the thesis is a comprehensive analysis of the slope displacements and their relationship to pore pressures and river elevation. This study differs from previous investigations of the Ripley Landslide as it includes new site investigation information and a large database of high-frequency, pore pressure and displacement monitoring data.

Applying the information from the Ripley Landslide to the other landslides in the region is outside of the scope of this thesis. This research does not address the means of stabilization of

the slope, but does focus on developing an understanding of the landslide behaviour and mechanics that is required for the evaluation of stabilization designs. This research does not include the modelling of hydro-mechanical response, instead it focuses on monitoring results.

1.3 Research Objectives

The specific objectives of this project are summarized below:

- 1) Coordinate a site investigation and monitoring program on the Ripley Landslide to install new instruments and obtain high quality soil samples.
- 2) Summarize and synthesize the data collected from both recent and past investigations of the Ripley Landslide.
- 3) Develop cross sections of the Ripley Landslide based on site investigation results.
- 4) Validate the accuracy of instrumentation results obtained using fully grouted vibrating wire piezometers and ShapeAccelArrays installed in a slow moving landslide.
- 5) Establish the most likely landslide kinematics of the Ripley Landslide based on the synthesis of the available displacement measurements and field observations.
- 6) Evaluate factors and mechanisms that have been proposed to control the velocities of landslides in the Thompson River Valley using the results on the recent monitoring program.

1.4 Organization of Thesis

This thesis is organized into seven chapters, including this introduction chapter (Chapter 1).

Chapter 2 presents a review of previous research that has informed the understanding of the Ripley Landslide. This includes the previous research undertaken within the Thompson River

Valley; a summary of other regions with similar materials and stability issues; previous works which link pore pressures and the velocity of landslides.

Chapter 3 summarizes the site investigations which have occurred at the Ripley Landslide over the past decade. This includes detailed borehole logs, installed instrumentation, geophysical surveys, and field observations.

The use of a new installation method for pore pressure instrumentation and new technology for monitoring displacements are briefly discussed in Chapter 3.

Chapter 4 presents the validation of the new installation method and new monitoring technology to ensure their accuracy.

Chapter 5 presents the compilation of measured displacements and stratigraphy and a subsequent interpretation of the kinematics of the Ripley Landslide. This stratigraphy and kinematics are presented as cross sections of the landslide.

Chapter 6 presents an analysis of the interaction of river elevation, pore pressure, and landslide velocity. The correlations developed between these three factors are presented to assess the main factors controlling the velocity of the Ripley Landslide.

Chapter 7 closes the thesis with a summary of conclusions and the recommendations for future research in this area.

2 Landslides in Varved/Rhythmic Glacial Sediments in Western Canada

While the Ripley Landslide is the focus of this research, there is a history of instability in the region that extends over a century. Observations in the region and in other landslides occurring in glaciolacustrine sediments is beneficial in understanding the behaviour of the Ripley Landslide.

2.1 Glaciolacustrine sediments

Glaciolacustrine silts and clays were deposited in lakes formed during deglaciation by the blockage of natural drainage. These sediments typically contain alternating silt and clay layers resulting from the winter-summer cycle (Evans 1982, Smith and Ashley 1985). These alternating layers are referred to as varves. In glacial lakes, silts are deposited during the spring and summer months when the stream energy is higher due to increased runoff from the glacier. In winter months, the lake is frozen over and the clay particles have time to settle and form clay-rich layers (Eden 1955, Quigley 1980).

The rhythmic nature of these clays can be seen visually in Figure 2-1. Figure 2-1 also shows the difference between the varves on a microscopic scale. Figure 2-2 shows a map of western Canada indicating the areas previously covered by glacial lakes. These areas include both advance and retreat phase lakes (Cruden 2016).

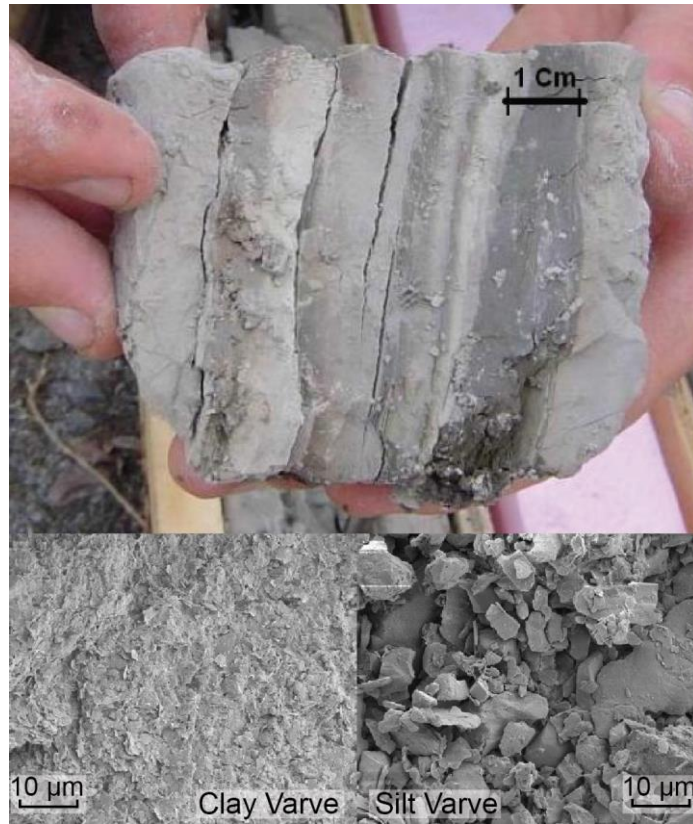


Figure 2-1 Sample of glaciolacustrine clay from borehole drilled near Ashcroft, British Columbia
(core photo courtesy of Dr. C.D. Martin; after Eshraghian et al. 2007)

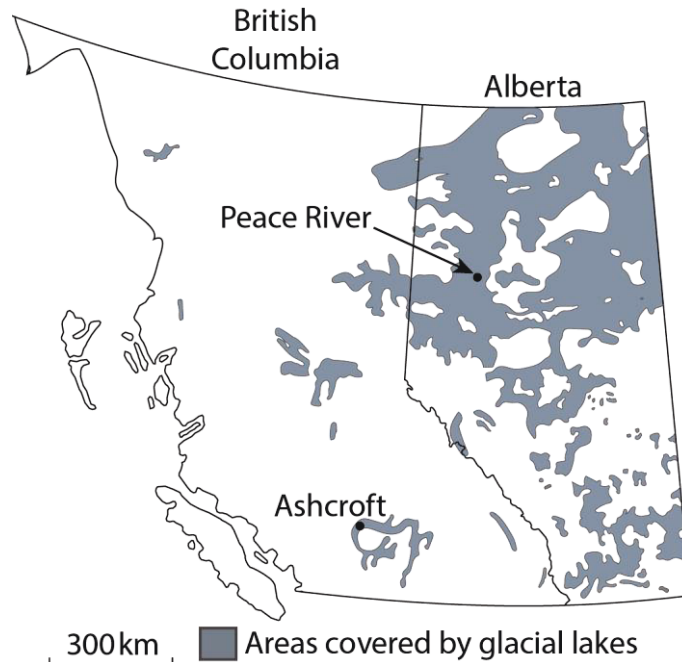


Figure 2-2 Distribution of glacial lakes in Western Canada (after National Atlas of Canada 1972)

Clague and Evans (2003) proposed that glacial over-riding may have sheared these sediments to their residual friction angle in some areas. Hendry et al. (2015) mapped nine slickenslides in a core of glaciolacustrine clay from a landslide in the Ashcroft region. Seven of these slickenslides were below the zone of recorded movement which indicates that the material has been presheared.

In addition to glacial shearing, the downcutting of rivers through these sediments leads to valley rebound. Valley rebound has been previously associated with bedding plane slip in soft, horizontally-bedded rocks (Matheson and Thomson 1973). It is logical that a heavily over-consolidated layered clay could experience similar interbed slip leading to discrete layers at residual strength.

The residual friction angle of clay rich layers is estimated to be between 7 and 14 degrees based on ring shear testing performed on samples from the Ashcroft region by Bishop et al. (2008).

Testing by Miller and Cruden (2012) found residual friction angles between 7 and 13 degrees for most samples taken in the Peace River region.

The layering of these clays can make them quite anisotropic. This was shown by shear testing by Eden (1955) on samples of varved clay from Ontario. Testing at different orientations had a significant effect on the shear strength of the soil.

The varying clay content in each varve is evident from the plasticity testing of these sediments. Figure 2-3 presents the index properties of various samples of glaciolacustrine from the Peace River and Ashcroft regions (Figure 2-2). The wide range of liquid limits observed in these sediments is due to the wide range of clay contents found in each varve.

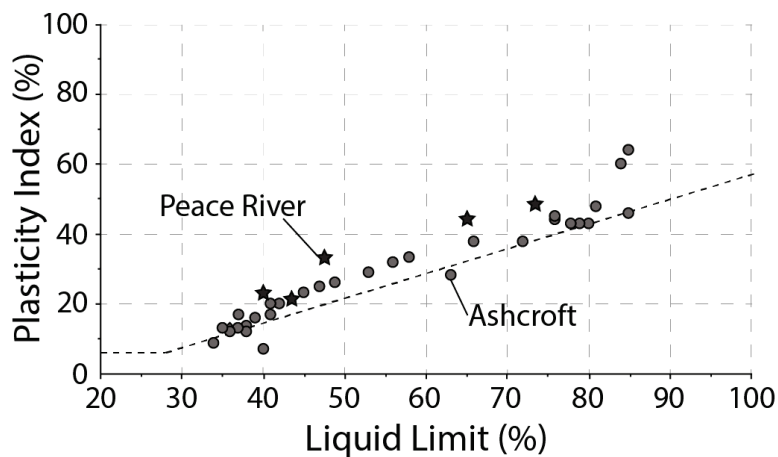


Figure 2-3 Index properties of glaciolacustrine silts and clays from the Ashcroft and Peace River regions (after Miller and Cruden 2002, Bishop et al. 2008)

2.1.1 Instability in glaciolacustrine clays

The Landslide Susceptibility Map of Canada by Bobrowsky and Dominguez (2012) lists river valleys and glaciolacustrine sediments as one of the three regions in Canada with high landslide potential. This high potential is likely due to the low residual strength of highly plastic layers in

the varved clays (Porter et al., 2002). The stratigraphy in the Peace River low lands and Ashcroft areas (Figure 2-2) contain glaciolacustrine clays and both areas have well documented histories of slope stability issues (Eshraghian et al. 2007, Miller and Cruden 2002, Hendry et al. 2015).

2.2 The Ashcroft Thompson River landslides

There are at least 14 landslides located within the Thompson River Valley between Spences Bridge and Ashcroft. The landslides range in volume from $0.6 \times 10^6 \text{ m}^3$ to $15 \times 10^6 \text{ m}^3$ (Hendry et al. 2015). Figure 2-4 shows the locations of these landslides.

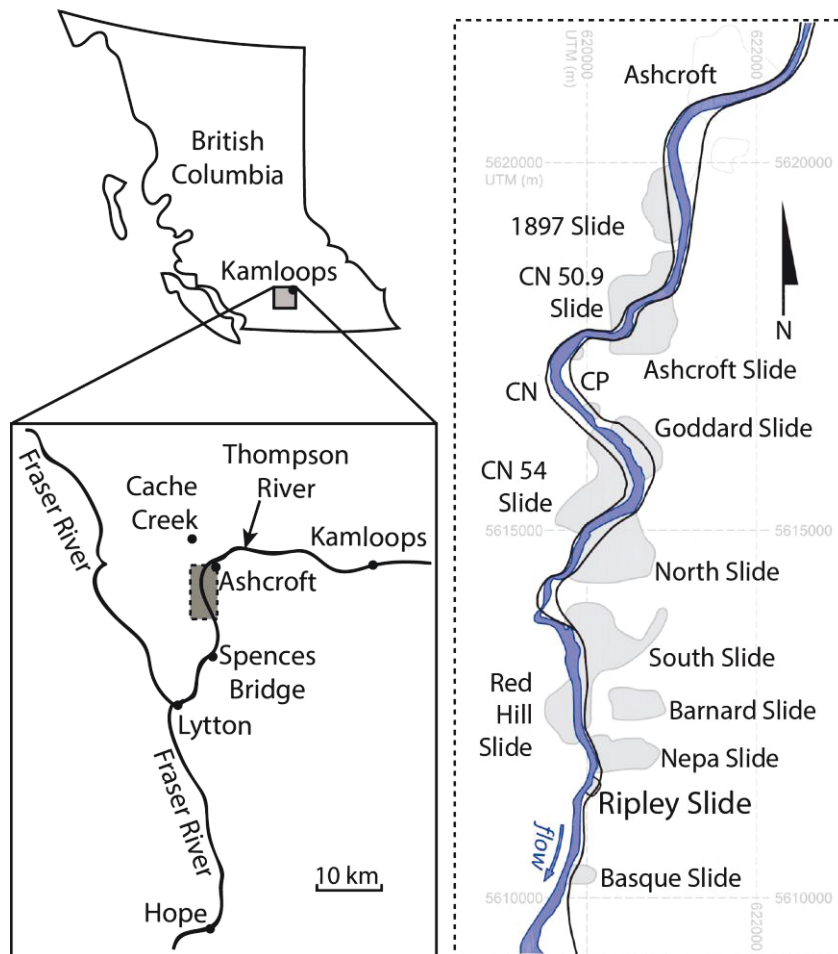


Figure 2-4 Locations of landslides within the Thompson River Valley south of Ashcroft, BC

(after Eshraghian et al. 2007, Hendry et al. 2015)

The area has been studied in the past with the goal of better understanding the mechanisms of these landslides and managing the associated risks in a proactive manner (Clague and Evans 2003, Eshraghian et al. 2007, Macciotta et al. 2014). Studies have been focussed on the general geology of the area, as well as investigations at specific landslides.

2.2.1 History of the Ripley Landslide

In 1951, Charles Ripley identified slope movements near what is now known as the Ripley Landslide. The observation of an offset in a fence located uphill from the CP track was the basis for the identification of the movement of the slope (Leonoff and Klohn Leonoff Ltd. 1994). Movement during the subsequent fifty years was not noticeable and was small enough that the regular maintenance of the track was sufficient to maintain the track alignment (Bunce and Chadwick 2012).

CP constructed a siding across the landslide in 2005. The construction included cutting into the slope and the building of a retaining wall (Bunce and Chadwick 2012). Figure 2-5 shows the topography of the slope before and after construction. This figure was produced using an airborne light detection and ranging (LiDAR) scan which was taken before construction and a ground based LiDAR scan, which was taken 7 years after construction. The scans have different resolution so the areas of cut and fill are not precise but give an indication of the relatively small changes in slope geometry which were involved in the construction process.

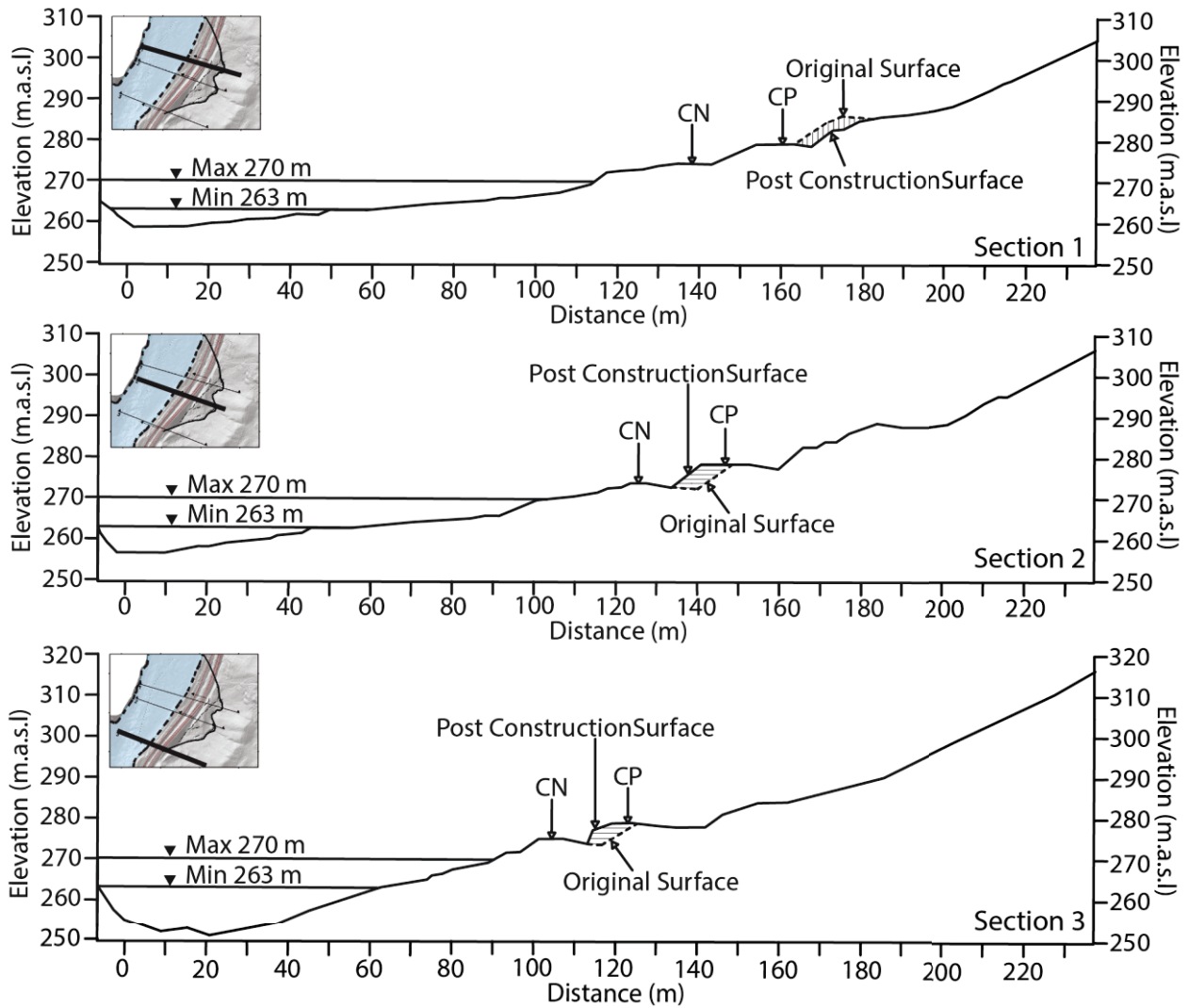


Figure 2-5 Comparison of slope geometry along three sections at the Ripley Landslide before and after the construction of the CP siding in 2005 (after Hendry et al. 2015)

In the winter of 2006 the track required lifting every three to six weeks to maintain alignment which is much higher frequency than regular maintenance. Tension cracks opened exposing the apparent back scarp of the landslide. Survey monitoring showed an apparent movement rate between 25-180 mm/year (Bunce and Chadwick 2012). This falls under very slow landslide classification according to Cruden and Varnes (1996).

The opening of tension cracks and increased maintenance requirements are signs that the Ripley Landslide was accelerating. After this apparent acceleration, the Railway Ground Hazard Research Program (RGHRP) began to direct resources towards this landslide. The site has since been monitored by various methods which are presented in detail in Section 3.2.4.

2.2.2 Geological history

The geologic processes that have resulted in the stratigraphy and topography of the Thompson River Valley are very complex. The surficial sediments in this valley were formed during three separate glacial periods (Fulton 1978). The time between these glaciations has resulted in unconformities between the sequences due to erosion and mass wasting (Clague and Evans 2003).

The Thompson River has eroded through glacial valley fill sediments. The sequence of sediments commonly found in this valley fill have been discussed in detail by Clague and Evans (2003) and Eshraghian et al. (2007). The stratigraphy includes ice contact, glaciolacustrine and glaciofluvial, alluvial, and colluvial sediments as well as till.

2.2.3 Characteristics of other Thompson River Valley landslides

Clague and Evans (2003) grouped the large landslides within the Thompson River Valley into three different mechanisms: (1) slow moving, rotational slumps with multiple intact back tilted blocks; (2) slow moving, primarily translational landslides; and (3) sudden rapid flowslides which involve the break up and flow of landslide debris.

Eshraghian et al. (2007) classified the modes of movement of the Thompson River Valley landslides as either retrogressive or reactivation movement. Retrogression involved rapid movements resulting from the extension of an existing rupture surface or sliding along a new

deeper surface. Reactivation movement involved slow movements along a previously active rupture surfaces. In the five landslides discussed, the movements were all occurring along rupture surfaces within the varved glaciolacustrine clays. These rupture surfaces also occurred within a narrow range of elevations (Eshraghian et al. 2007).

Eshraghian et al. (2007) developed a sequence of cross sections based on the CN50.9 landslide which illustrates the typical failure mechanism observed in the Thompson River Valley. Figure 2-6 further simplifies this to a more general sequence. This figure shows the multiple ways which a landslide can evolve over time. The formation of the original landslide (Stage 1 to Stage 2 in Figure 2-6) occurs as the river erosion cuts down through weak layers and also removes toe resistance from the slope. Following this, there are two main ways that the landslide could evolve: (1) continued river erosion can expose a new sliding plane which the existing landslide can move along (Stage 2 to Stage 3 in Figure 2-6); or (2) erosion or other factors allow the retrogression of the active rupture surface back into the slope (Stage 3 to Stage 4 in Figure 2-6). This sequence of events assumes that the weak planes extend back into the slope and that bedrock is below that layer. The sequence also assumes the presence of deeper presheared planes similar to those mapped by Hendry et al. (2015).

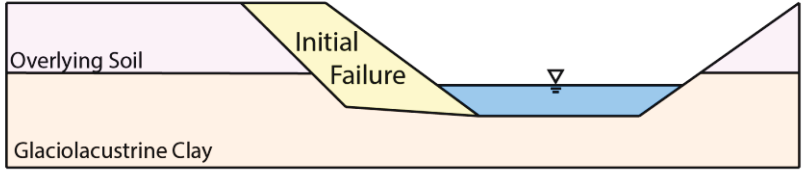
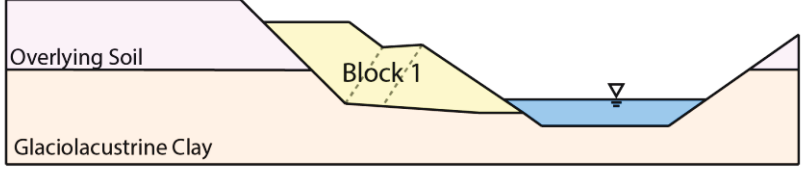
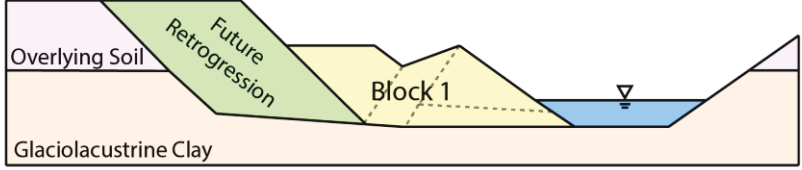
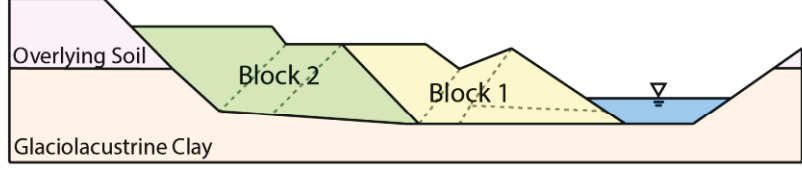
Stage	Simplified Cross-section	Description
1		<p>Before Failure River downcutting erodes through weak layer in glaciolacustrine clay.</p>
2		<p>Initial Failure At some point bank erosion has removed toe resistance and the initial slide occurs forming the original back scarp. Following failure, river continues downcutting and reaches a deeper weak layer.</p>
3		<p>Sliding on Deep Surface Block 1 deforms along deeper rupture surface. Removes confinement from slope and allows for extension of the deeper rupture surface back into the slope.</p>
4		<p>Retrogression Block 2 slides along the new back scarp of the slide. This pushes block 1 further along the deep rupture surface.</p>

Figure 2-6 Illustration of the typical failure mechanism observed in Thompson River Valley landslides near Ashcroft, B.C (after Eshraghian et al. 2007)

The causes of the instability in the Thompson River Valley have been discussed for over a century (Stanton 1898). Porter et al. (2002) identified four factors which appeared to control the stability of the landslides in the Thompson River Valley: (1) the shear strength of the glaciolacustrine clays; (2) bank erosion; (3) artesian pore pressures; and (4) river drawdown. Some of these factors, such as pore pressures and river drawdown, vary seasonally while the erosion occurs over a longer timescale.

2.3 Correlating movement rate with landslide conditions

The movement rates observed at the Ripley Landslide have been previously correlated to the elevation of the river (Bunce and Chadwick 2012). Eshraghian et al. (2007) suggested that the movement of the landslides within the Thompson River Valley were controlled by the interaction of the river level and the pore pressures within the landslides. Hendry et al. (2015) used pore pressure measurements from within the Ripley Landslide to calculate the Factor of Safety (FOS) over time. The FOS was then compared to the measured velocity over time and a correlation was developed.

Correlation of FOS and landslide velocity has been previously discussed by Skempton et al. (1989) and Cartier and Pouget (1988). Skempton et al. (1989) used the variation of shear strength with rate of displacement to explain the empirical correlation between FOS and landslide velocity. This concept was shown through the example of the Mam Tor Landslide in the UK. Cartier and Pouget (1988) also correlated the FOS and landslide velocity for an unstable slope in France. This method of interpretation was used in the Hendry et al. (2015) analysis of the Ripley Landslide.

The velocities of landslides have also been related to pore pressures. Calvello and Cascini (2006) used numerical modelling to predict the movements along a slip surface related to pore pressure variations caused by rainfall events. The numerical model was calibrated using an active colluvial slope in central Italy. This study was successful in predicting the maximum displacements of the slope but over predicted velocity at other times. The pore pressures were recorded at discrete times and the model was calibrated based on these pore pressure readings. There was a difference in modelling results depending on which set of recorded pore pressures Calvello and Cascini (2006) used for calibration. These differences highlighted a specific issue.

A large amount of high quality monitoring data is needed to better understand the mechanism of the landslide and properly calibrate a model.

Gundogdu (2011) has also looked at the relationship between pore pressure, FOS and movements of reactivated landslides. Gundogdu looked at case histories where concurrent displacement and pore pressure readings were available. A non-linear correlation between FOS, pore water pressure, and landslide velocity was found. Another interesting outcome of this study was the sensitivity of landslide movement rates to changes in pore pressure. Extremely slow landslides were found to be more sensitive. For example, the San Martino and Steinernase landslides showed an order of magnitude increase in landslide velocity with 1% and 2% increases in pore pressures, respectively.

3 Geology and Site Conditions

There have been various site investigation programs carried out at the Ripley Landslide (BGC Engineering 2006, Macciotta et al. 2014, Hendry et al. 2015). The main investigations which are discussed in this chapter were carried out in 2005, 2013 and 2015. Other landslides in the Thompson River valley have also been investigated (Eshraghian et al. 2007). The understanding of site specific geology of the Ripley Landslide and how it fits within the regional geology have been greatly increased as a result of these investigations. The purpose of this chapter is to summarize the findings of the investigations at the Ripley Landslide.

3.1 Geologic Context

The results of the site investigation programs at the Ripley Landslide are interpreted within the framework of a regional geological model. The Thompson River Valley consists of layers of Quaternary sediment deposited during three glaciations (Clague and Evans 2003). Figure 3-1 presents the regional stratigraphy used to develop a geological model for the Ripley Landslide. This stratigraphical sequence is only expected to be complete in areas of deep fills or when drilling on the terrace above the landslide. The approximate elevation of the Ripley Landslide is indicated on the figure as well as the approximate elevation of the rupture surface. Many areas within the Thompson Valley have been subject to a large amounts of erosion during glaciation and the subsequent downcutting of the Thompson River. This has resulted in many unconformities in the stratigraphic sequence so certain units can be found at a range of elevations in different locations in the region. This has been observed during the investigation of other landslides in the region (Eshraghian et al. 2007).

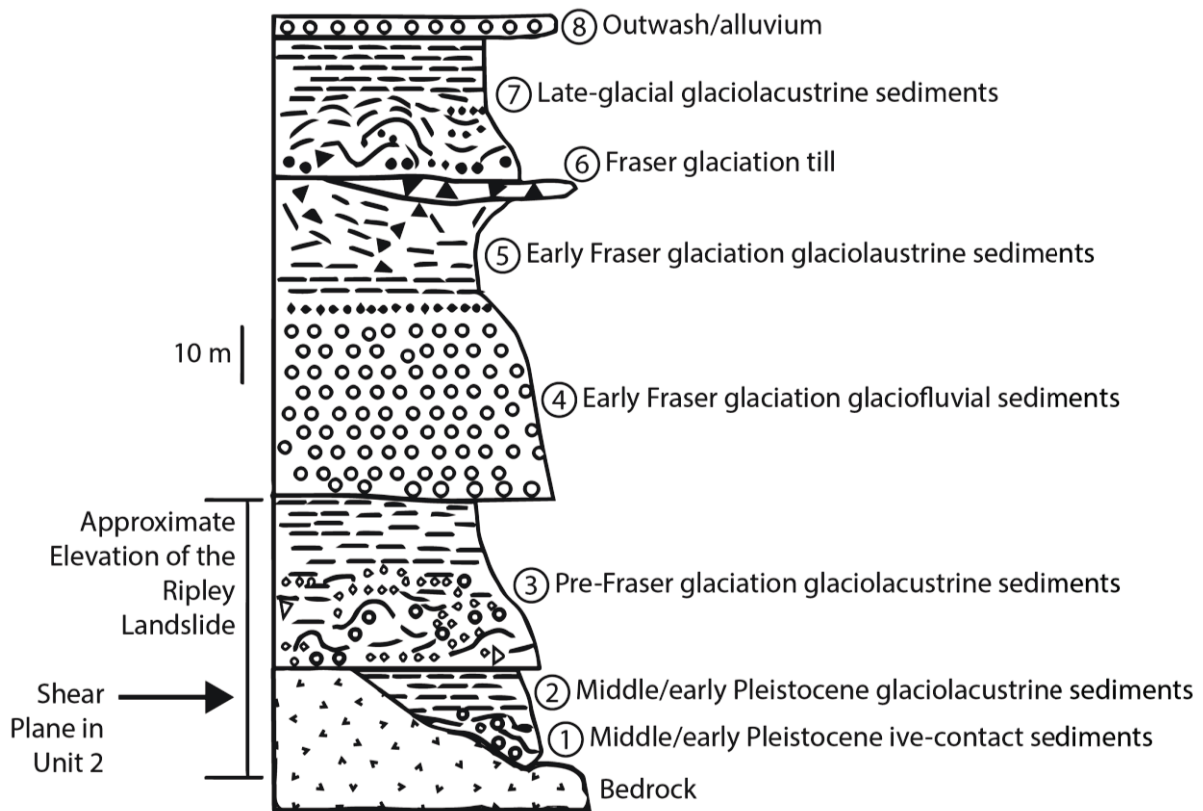


Figure 3-1 Regional stratigraphy considered while interpreting the borehole logs of the Ripley Landslide (after Clague and Evans 2003)

The primary concern of the investigations at the Ripley Landslide has been the second oldest of the glaciolacustrine deposits observed directly above the bedrock. Huntley et al. (2014) divided this layer into two smaller layers. The lower deposit was hypothesized to result from colluvium which was deposited into a pro glacial lake. The division between this lower “glaciolacustrine colluvium” and the overlying glaciolacustrine clay is marked by a coarse deposit of cobbles and sand which indicates a sharp change in the depositional environment. This coarse deposit was identified in both the 2013 and 2015 drilling investigations. The transition observed in the 2013 investigation can be seen in Figure 3-2.



Figure 3-2 Coarse deposit within glaciolacustrine deposits at the Ripley Landslide

Clague and Evans (2003) do not make this distinction and instead group these two layers into a single Unit 2. Further testing of the material above and below this transition is required to determine if the division between layers is needed based on the material properties of these two sublayers. It may be beneficial to combine these two layers during analysis if the mechanical and hydraulic properties of both deposits are very similar. For this report the two glaciolacustrine layers will be considered to be one layer.

Eshraghian et al. (2007) interpreted site investigation results from five of the major landslides within the Thompson River Valley. Eshraghian et al. (2007) identified Units 1, 2, 3, 6, and 8 at the South Landslide and Units 1,2,3, and 8 at the Basque Landslide. The stratigraphy of the Ripley Landslide is expected to be similar as it is located between the South and Basque Landslides.

The elevation of the transition between Unit 2 and Unit 3 is similar across the region based on site investigations (Eshraghian et al. 2007). The transition between Unit 2 and Unit 3 at the South Landslide and Basque Landslide were approximately 283 m and 271 m, respectively. The Unit 6 lower boundary is an unconformity and varies in elevation greatly (Clague and Evans 2003, Eshraghian et al. 2007). In locations at the Ripley Landslide where the top of Unit 2 is

encountered below 271 m, the overlying layer is likely not Unit 3. Unit 6 could potentially be found above Unit 2 at these lower elevations as its lower boundary is an unconformity. This is consistent with sections of the valley which were previously developed (Clague and Evans 2003) and sections of the adjacent landslides (Eshraghian et al. 2007).

3.2 Site investigations

An investigation was carried out in November 2005 prior to CP constructing a new embankment and retaining structure in 2005/2006 as part of a railway track siding extension. Displacement and pore pressures monitoring instruments were installed along the length of the proposed siding extension. Five of these boreholes were drilled on the Ripley Landslide (Figure 3-3). These consisted of two boreholes with slope inclinometers (DH05-24 and DH05-27) and two boreholes with vibrating wire piezometers (DH05-23 and DH05-26) and one which was not instrumented (DH05-25). These instruments were monitored twice a year following the construction of the siding (BGC Engineering 2006).

Another drilling and instrumentation program was performed in April 2013. The boreholes for this investigation (BH13-01 and BH13-02) were drilled near the same location as DH05-27 (Figure 3-3) in order to replace sheared inclinometer casings and upgrade the monitoring system. The displacement data from the 2005 investigation allowed the instrumentation to be concentrated around the previously identified shear zone. The instruments installed provide higher temporal resolution using a remote data acquisition system. An additional goal of this investigation was to retrieve high quality samples for material characterization.

A final drilling and instrumentation program was performed in February 2015. This investigation was planned and coordinated as part of this thesis. The goal of this investigation was to provide

deformation and pore pressure measurements at more locations on the landslide. This investigation also provided an opportunity to install new displacement monitoring equipment. The instrument installed during the April 2013 investigation was approaching the end of its reliable life based on the manufacturer's recommendation (Levesque 2015). The investigation was also used to investigate a potential separate landslide on the south end of the Ripley Landslide. The "secondary landslide" was hypothesized based on the abnormal vertical displacements observed by one of the global positioning system (GPS) displacement monitoring units on site (Hendry et al. 2015).

Figure 3-3 summarizes the layout of the boreholes drilled during the site investigations. Figure 3-4 shows the surface elevation model of the landslide and the location of geophysical survey lines.

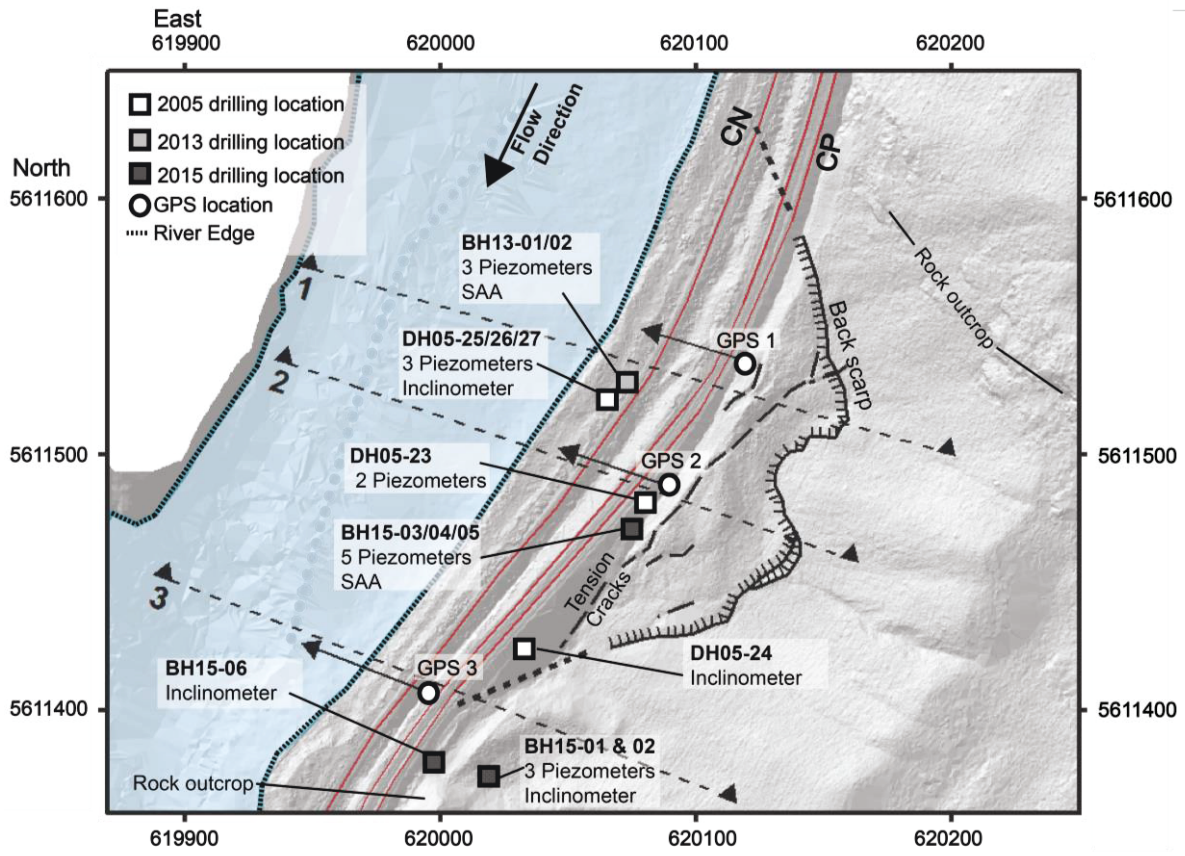


Figure 3-3 Location of boreholes drilled during the site investigation of the Ripley Landslide
(after Macciotta et al. 2014)

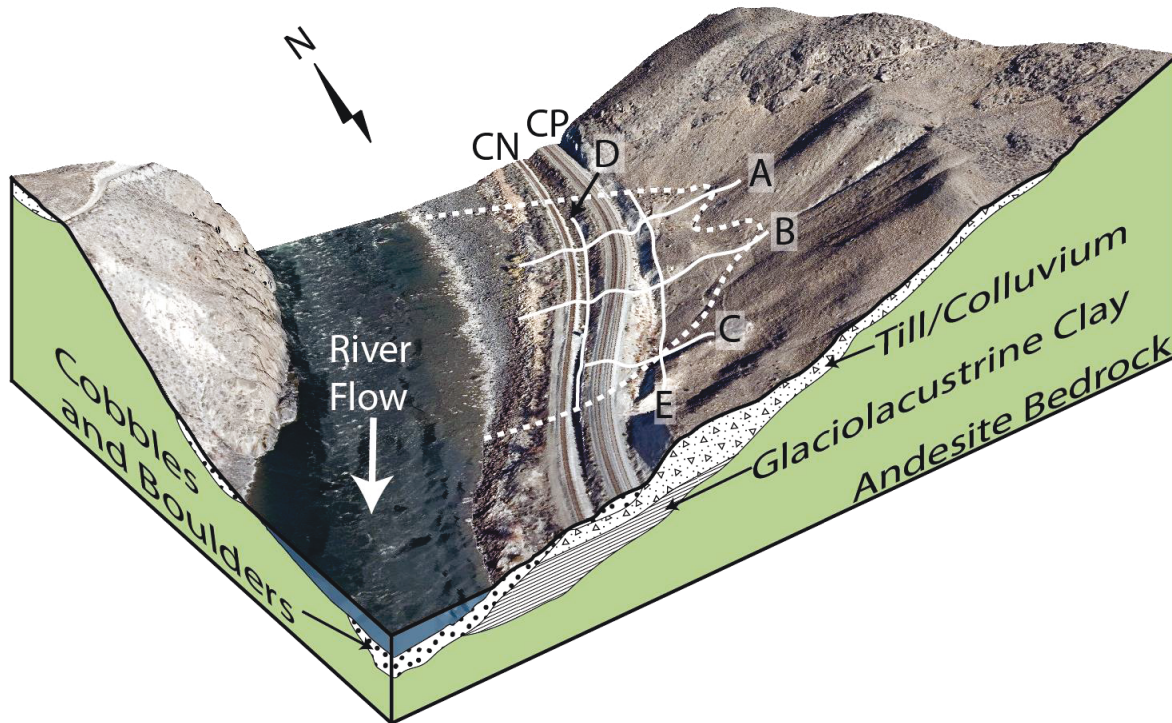


Figure 3-4 Surface elevation model of the Ripley Landslide with locations of geophysics survey lines (after Huntley et al. 2014).

3.2.1 Geophysical surveys

There have been several geophysical surveys carried out at the Ripley Landslide as part of the RGHRP led investigation. These have been coordinated by the Geological Survey of Canada and carried out by various consulting firms. Both land and water based surveys have been performed to aid in the understanding of the stratigraphy of the Ripley Landslide. The water based surveys have also provided information on the bathymetry of the Thompson River and the toe of the landslide.

The land based surveys included ground penetrating radar, seismic refraction, electrical resistivity tomography, and electromagnetic surveys. All of these surveys were carried out along the five different survey lines shown in Figure 3-4.

The interpretation of geophysical data is currently being coordinated by the Geological Survey of Canada (GSC) and is not within the scope of this project. However, the interpreted seismic refraction data was used to estimate bedrock profile in the vicinity of the boreholes. This data set was chosen to be used on its own as seismic refraction is a relatively effective and reliable method for estimating bedrock depth (Adeyeri 2014).

Figure 3-5 show a sample of the results of the seismic refraction surveys. The plotted contours are compression wave (P-wave) velocities. Higher P-wave velocities correspond to denser materials such as rock. Boreholes drilled near these geophysics surveys (Figure 3-3) were used to ground proof the seismic refraction results. The top of Unit 2 corresponded to P-wave velocities of approximately 3500 m/s. The top of bedrock corresponded to P-wave velocities of approximately 5000 m/s.

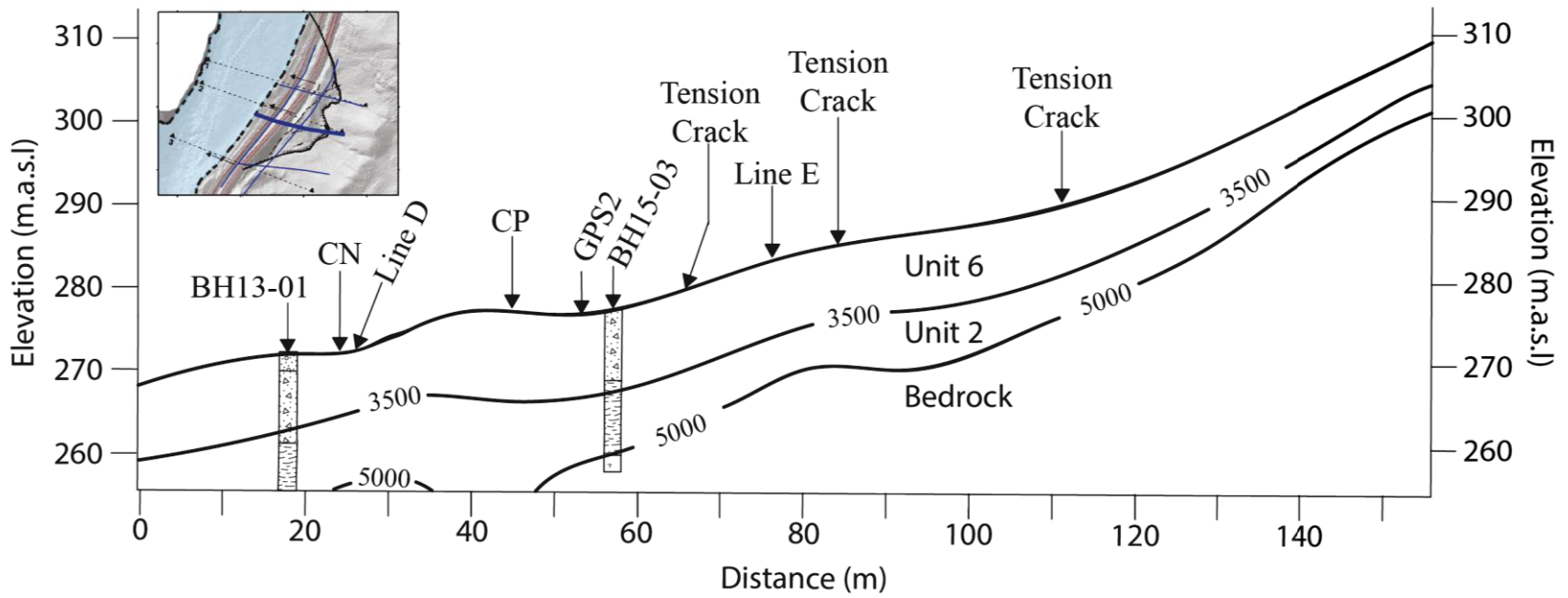


Figure 3-5 P-wave velocity contours interpreted from seismic refraction survey results along Line B of the Ripley Landslide
(after Huntley et al. 2014, contours are in m/s)

3.2.2 Borehole logging and observations during the site investigations

Figure 3-6 shows the stratigraphy that was encountered in each of the boreholes of the 2005 site investigations. Figure 3-7 shows the stratigraphy that was encountered in each of the boreholes of the 2013 and 2015 site investigations. These figures include the interpreted stratigraphical units based on the regional geological model presented in Figure 3-1. Holes drilled in close proximity to allow for instrumentation were grouped together as the stratigraphy was practically identical.

A till veneer belonging to Unit 6 overlies Unit 2 (Huntley 2014). This overlying unit was found to contain a significant fraction of clay based on field observations and the core recovered. Unit 3 is characterized as glaciolacustrine silt, sand, gravel and boulders (Clague and Evans 2003) and would not be clay rich. It is likely that boreholes drilled at higher elevations on the slope or terrace would encounter Unit 3 which was also encountered at the South Landslide and Basque Landslide as previously mentioned (Eshraghian et al. 2007).

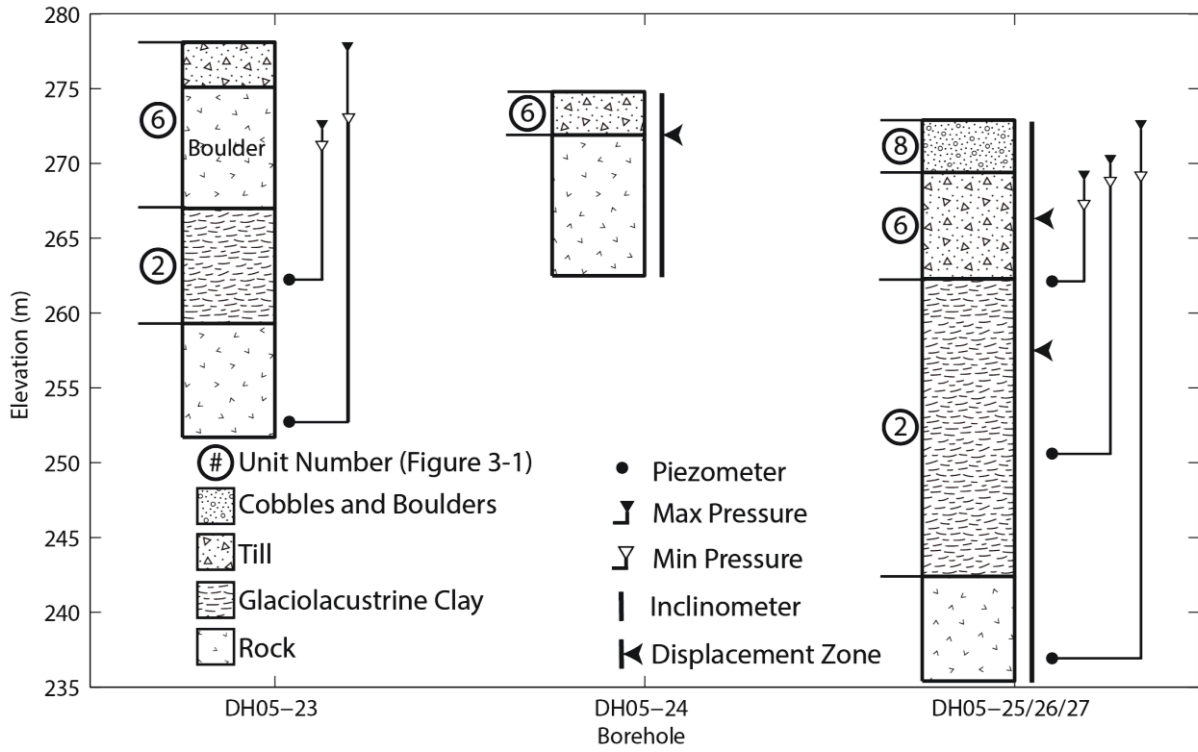


Figure 3-6 Stratigraphy and instrumentation layout of the 2005 investigations of the Ripley
Landslide

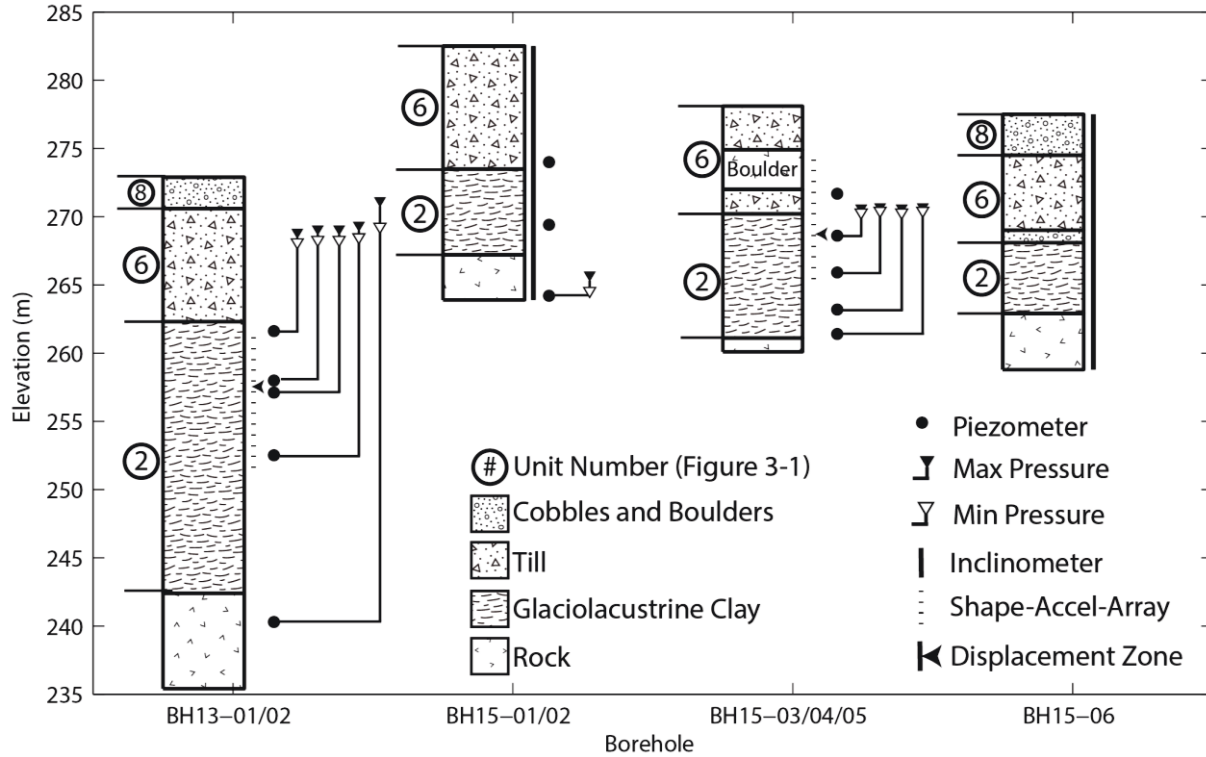


Figure 3-7 Stratigraphy and instrumentation layout of the 2013 and 2015 investigations of the Ripley Landslide

All drilling campaigns were carried out using 1.5 m long HQ size core barrels for sampling holes. All coring used water as the drill fluid. The additional holes at each location for instrumentation during the 2013 and 2015 investigations were drilled by setting 4" ODEX casing over the full depth of the hole.

In BH13-01 the average core recovery from 3.8 m to 10.8 m was 31% while average recovery from 10.8 m to 30.5 m was 97%. This sudden increase in core recovery was observed in the two sampling boreholes drilled as part of the 2015 site investigation. The drilling contractor also noted a contrast in stiffness at similar elevation when drilling the ODEX holes at the same locations. The depth of this transition for the various boreholes in the 2013 and 2015 investigations is summarized in Table 3-1. These elevations may represent the transition between

a normal to lightly overconsolidated upper strata and the underlying stiffer heavily overconsolidated glaciolacustrine clay (Unit 2).

Table 3-1 Depth and elevations of possible transition to Unit 2 encountered during the 2013 and 2015 site investigations at the Ripley Landslide (locations as per Figure 3-3)

Borehole	Transition in Recovery	
	Depth (m BG)	Elevation (m.a.s.l.)
BH13-01	10.8	262.3
BH15-01	9.0	273.5
BH15-03	7.9	270.2
BH15-06	9.4	268.1

3.2.3 Variability in Bedrock Profile

There are several bedrock outcrops in the vicinity of the Ripley Landslide at the locations shown on Figure 3-3. Bedrock is typically greenish coloured volcanic rock which has been identified as andesite (Huntley and Bobrowsky 2014). The bedrock valley slope on the opposite side of the river from the Ripley Landslide appears to be constraining the location of the Thompson River (Figure 3-8). In addition there is a large rock exposure at the South margin of the landslide that appears to be a bedrock outcrop (Figure 3-9).



Figure 3-8 Rock slope along the West side of the Thompson River across from the Ripley
Landslide



Figure 3-9 Andesite rock outcrop on southern boundary of the Ripley Landslide overlain by glacial till (Figure 3-3)

The variability of the elevation of the bedrock across the site is apparent from the borehole logs and geophysical surveys. The bedrock depths encountered in this investigation range from 2.9 m to 31.59 m with estimated elevations of 242.4 m.a.s.l. to 271.9 m.a.s.l. This is consistent with buried channels within bedrock profiles that are associated with river and subglacial flows during past glaciation (Ryder 1991). Such channels can produce very irregular bedrock profiles with steep channel walls.

Drilling closer to the centre of the valley (DH05-25/26/27 and BH13-01/02) identified bedrock at a depth of 30.5 m (Figure 3-6 and Figure 3-7). Figure 3-5 shows that the top of bedrock is shallower upslope. This was consistent in the geophysics sections. Based on these observations it is possible that the river is currently flowing along a depression in bedrock which was formed before the deposition of Unit 2.

There is also significant variation along the slope. BH05-23 and BH05-24 are at approximately the same distance from the river edge and similar elevation. The bedrock elevations at these locations are 259.3 m.a.s.l. and 271.9 m.a.s.l respectively (Figure 3-6). The geophysics surveys also show a large amount of variability in bedrock depth along the river axis.

The possibility that the rock segment observed in BH05-24 is not actually bedrock based on its elevation was considered. The SI installed at this location exhibited excess deformation at the clay to rock transition. This shear surface between the rock and overlying clay sediment have led to the conclusion that the rock segment is outside of the landslide mass. DH05-24 is located very close to the intersection of geophysics Line E and Line C. At this intersection the bedrock appears to be much shallower. For this reason it is hypothesized that the rock segment observed in DH05-24 is bedrock. This bedrock ridge or knob may be a factor which limits the lateral extents of the landslide. The bedrock outcrops observed on either side of the landslide indicated that the lateral extent was controlled by a shallowing of the bedrock towards the shoulders of the landslide (Hendry et al. 2015). The bedrock elevations observed during investigation support that hypothesis.

The variability of the bedrock elevation and possible presence of buried channels makes predicting the bedrock profile difficult. The boreholes drilled on the site (Figure 3-3) and the

rock slope on the adjacent bank are the only known points of bedrock elevation which can be used for developing a given section. The bedrock profile between these boreholes are interpolated based on seismic P-wave survey results (Figure 3-5). These surveys can be affected by geometric shielding effects (Perry 2016) which could result in irregularities in the bedrock profile, such as buried channels, being missed when developing sections (Figure 3-10).

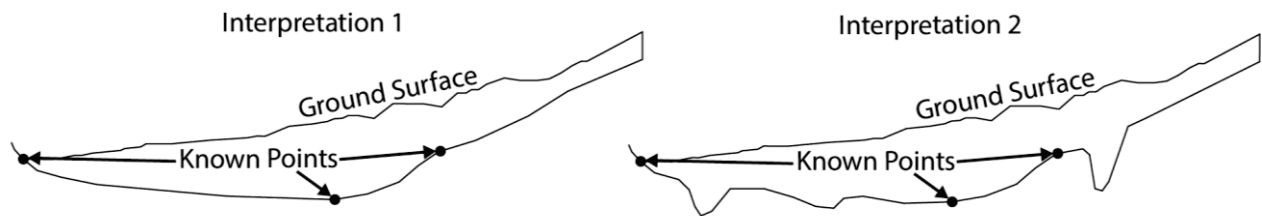


Figure 3-10 Two possible interpretations of bedrock profile based on a set number of known points and seismic P-wave survey results

A large section of rock was also encountered in BH05-23 with clay sediments above and below it. This rock segment could be a large boulder or series of large cobbles deposited as a rock fall or a rafted piece of bedrock. The rock was described as massive and extended from 3.0 m to 12.1 m below grade with core recovery mostly around 50%. There was a portion of this section from 5.5 m to 7 m which had a reported recovery of 100%. There are other boulders observed in the area which would be of similar size (1.5 m diameter).

The same large section of rock was encountered during the drilling of BH15-03. This hole was drilled approximately 7 m South of DH05-24. The rock section found in BH15-03 was smaller than that encountered in 2005 (~4.3 m). The largest fragment from the rock section encountered in BH15-03 can be seen in Figure 3-11. BH15-04 was drilled approximately 4 m further South from BH15-03. At this location the rock section encountered was even smaller based on the drill

response (~2.2 m). BH15-05 was drilled 4 m further South from BH15-04 and no rock section was encountered based on drill response and cuttings returned.

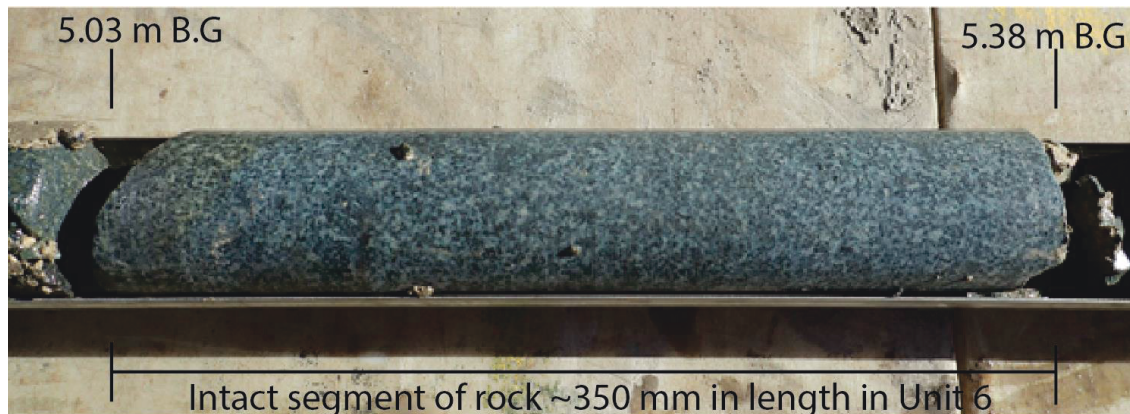


Figure 3-11 Andesite rock fragment obtained during the 2015 site investigation in BH15-03

Preliminary SI readings have shown that the primary slope displacement zone is below this section of rock and the rock is moving with the rest of the landslide mass. Based on the observed displacement it can be concluded that the rock section is not attached to bedrock. The origin of the rock is still uncertain. Given the recoveries reported for the 2005 investigation and the lack of large continuous segments of rock, it is likely that this portion of the stratigraphy is a deposit of cobbles within the glacial till.

There was also an interesting observation made during the mobilization to site. Two places along the track traversing the landslide were rougher while crossing them on the high rail truck. There was one section at the South end of the landslide near GPS3 and second section on the North end of the landslide. The track between these two points is typically quite smooth (Olson 2015). These rough patches appeared to be locations of increased vertical deformation based on visual inspection.

3.2.4 Instrumentation

2005

The 2005 investigation employed sand pack piezometers and traditional slope inclinometers. These methods have been used extensively throughout the geotechnical industry and have a long record of acceptable performance. Figure 3-6 shows the layout of the instruments installed in each of the boreholes. The areas of displacement and range of observed piezometric heads are included on Figure 3-6. Their location in plan view is shown in Figure 3-3.

Two piezometers were installed in DH05-23 at elevations of 262.1 m.a.s.l. and 252.6 m.a.s.l. Three piezometers were installed in DH05-26 at elevations of 237.2 m.a.s.l., 250.9 m.a.s.l. and 262.4 m.a.s.l.

Four of the five piezometers installed for this investigation became unreadable at some point between 30 and 48 months after install (BGC Engineering 2007, BGC Engineering 2009). The exact date of failure is difficult to determine due to the reading frequency. The fifth piezometer was a shallow piezometer was still functioning after 78 months of operation. This piezometer was installed above the shear zone and was not affected by slope displacements.

Inclinometer casings, 70 mm in diameter, were used to monitor the displacement of the slope. Inclinometer casings were installed over the entire depth of DH05-24 and DH05-27. These instruments were successfully read in April 2006 (BGC Engineering 2006). Readings were attempted again in March 2007. At this time the casings were blocked off and unusable. Estimated depths to the movement zone were established based on these measurements but exact quantities could not be determined.

The short lifespan of the displacement monitoring equipment lead to a recommendation by BGC Engineering Inc. (2007) to employ an “alternative displacement detection system”. A GPS monitoring system was installed on the site in 2008 to provide continuous surface deformation measurements (Bunce and Chadwick 2012). This system was designed to detect 12.5 mm of cumulative ground movement with a variability of ± 1 mm (Macciotta et al. 2014).

2013 and 2015

Methods with lower risk of failure and a longer life span were proposed for use in the 2013 and 2015 investigations as the poor site access greatly increases the cost of replacing instruments. Fully grouted vibrating wire (VW) piezometers and ShapeAccelArrays (SAA) were installed during these investigations to monitor the pore pressures and shear displacements along the landslide plane, respectively. The plan view of the location of the boreholes is shown in Figure 3-3. Figure 3-7 shows the layout of the instruments in each of the boreholes. The areas of displacement and range of observed piezometric heads are included on Figure 3-7.

Four piezometers were installed in BH13-01 at elevations of 261.6 m.a.s.l., 258 m.a.s.l., 252.5 m.a.s.l. and 240.3 m.a.s.l. One piezometer was installed in BH13-02 at an elevation of 257.1 m.a.s.l. An additional piezometer was also placed within the Thompson River adjacent to the Ripley Landslide to continuously monitor the elevation of the river. All piezometers in this investigation were VW piezometers with an accuracy of 0.35 kPa. A 9.7 m SAA with 0.3 m segment lengths was installed in BH13-02 between 261.3 m.a.s.l. and 251.6 m.a.s.l. This SAA has a typical accuracy of deformation value of approximately 0.9 mm (Measurand 2013).

Three piezometers were installed in BH15-01 at elevations of 274 m.a.s.l., 269.4 m.a.s.l. and 264.2 m.a.s.l. Five piezometers were installed in BH15-03 at elevations of 271.7 m.a.s.l.,

268.6 m.a.s.l., 265.9 m.a.s.l., 263.2 m.a.s.l. and 261.4 m.a.s.l. All piezometers in this investigation were VW piezometers with an accuracy of 0.35 kPa. Inclinator casings were installed over the entire depth of BH15-02, BH15-04, and BH15-06. These inclinometers were monitored for five months to characterize slope movements and identify depths that should be monitored using SAAs. In July 2015 a 9.2 m SAA with 0.3 m segment lengths was installed into the inclinometer casing in BH15-04 between 274.2 m.a.s.l. and 265 m.a.s.l. This SAA has a typical accuracy of deformation value of approximately 0.9 mm (Measurand 2013).

3.2.4.1 Grouted-in vibrating wire piezometers discussion

The conventional installation method of piezometers involves placing a piezometer tip in a high-permeability sand intake zone. The borehole is then sealed with a low-permeability bentonite seal above the sand intake zone. The remainder of the hole is filled with cement bentonite grout. The grouted-in installation method involves installing the piezometer tip and filling the entire borehole with cement-bentonite grout. The grouted-in method was originally proposed by Vaughan in 1969 but was not used in industry at that time (McKenna 1995). A comparison of these installation methods is shown in Figure 3-12.

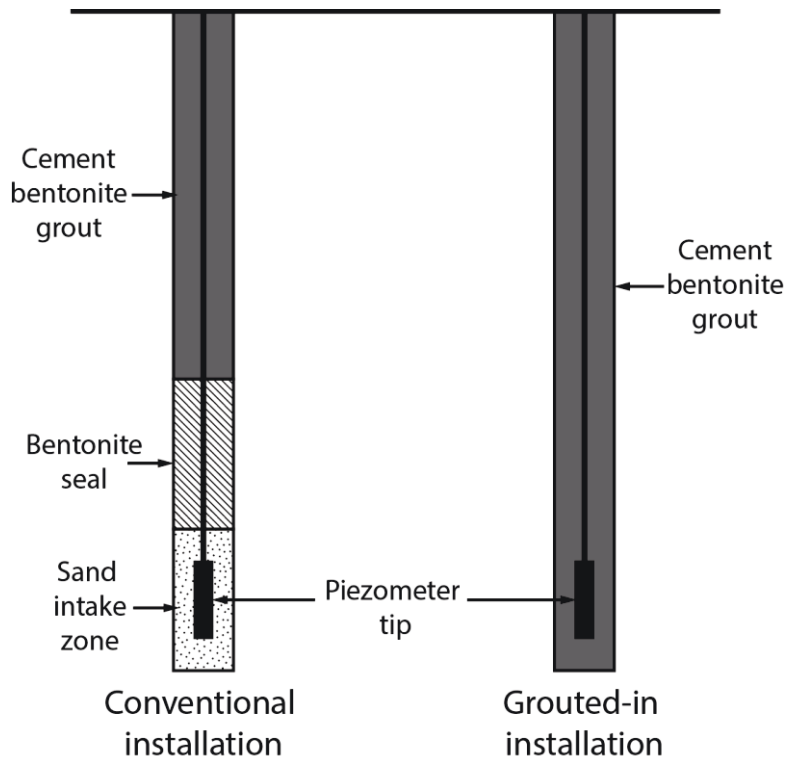


Figure 3-12 Comparison of the conventional and grouted-in installation methods of piezometers
(after McKenna 1995)

The main benefit of a fully grouted installation of piezometers is the simplicity and speed of installation (McKenna 1995). Comparisons of the measurements from fully grouted piezometers with traditional sand-pack piezometers have been completed by McKenna (1995) and Contreras et al. (2008). Mikkelsen (2003) also showed theoretically that the response time of fully grouted piezometers is not an issue and this was confirmed in the field by Simeoni (2011).

Past studies have cautioned against using fully grouted piezometers in areas where movement is expected (McKenna 1995). The primary concern with deformation is the potential for vertical cracking of the grout which could cause piezometers to communicate. Piezometer communication occurs when pressures from another depth are transmitted up through the grout column to a piezometer. The transfer of pressure along the grout column through cracks would

result in pressures being recorded from below or above the elevation of the piezometer. The identification of an upward or downward gradient could also be overlooked depending on the continuity of the grout cracks. Chapter 4 addresses this issue prior to further analysis and interpretation of the landslide behaviour.

3.2.4.2 ShapeAccelArray Discussion

An SAA consists of a series of rigid segments which each contain a gravity sensor (Measurand 2013). These sensors determine the tilt of each segment which allows for the calculation of the position of each joint relative to the base of the SAA. Figure 3-13 shows the SAA before installation. The rigid links can clearly be seen wrapped around a spool for easy transportation and handling. Figure 3-14 shows the installation of an SAA into one of the boreholes drilled during the 2015 investigation.

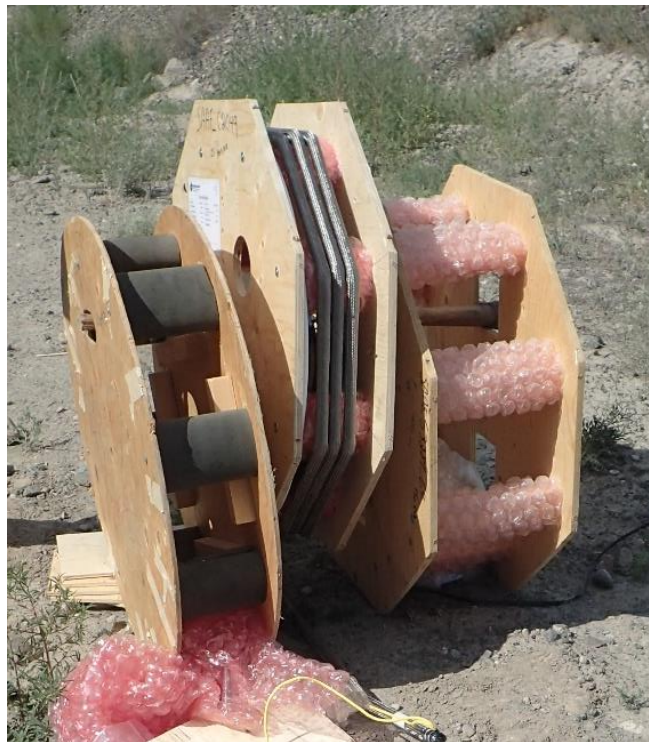


Figure 3-13 ShapeAccelArray on spool before installation has begun.



Figure 3-14 Installation of ShapeAccelArray into BH15-04 in July 2015

SAAAs have two main benefits which made it a good option for the Ripley Landslide. The SAA functions as an in-place inclinometer to allow for continuous and remote monitoring of the shear zone displacements. The in-place aspect of the instrument means that a slope inclinometer (SI) probe does not need to be passed through the casing. This increases the expected lifespan of the instrument.

The ability to remotely monitor the instrument is the second significant benefit to this technology. Frequent measurements in a remote area such as the Ripley Landslide are impractical without this type of technology.

3.3 Summary

Site investigations at the Ripley Landslide have been carried out in 2006, 2013 and 2015. A total of 13 boreholes were drilled during these investigations which consisted of six continuous coring

holes and seven holes drilled for the installation of instrumentation. Eighteen piezometers, five inclinometers and two SAAs were installed during these investigations to monitor the slope behaviour. A GPS displacement system was also installed on the site. There were 4 different types of land based geophysics surveys carried out along 5 different traverses of the landslide. Additional waterborne geophysics have been carried out as well.

Review of the site investigation results and field observations concluded that:

- 1) The strata overlying Unit 2 on the Ripley Landslide is most likely Fraser glaciation till (Unit 6)
- 2) The bedrock profile beneath the Ripley Landslide is extremely variable and difficult to predict.
- 3) New instrument technologies (SAA and grouted-in VW piezometers) are believed to be more suitable for use on the Ripley Landslide but require validation.

4 Pore Pressure and Displacements

In Chapter 3 the details of the instrumentation and their installation methods were presented. The results and methods of the 2005 are considered as base level information. Fully grouted vibrating wire (VW) piezometers and ShapeAccelArray (SAA) are comparatively new technologies. These were the technologies deployed during the 2013 and 2015 instrumentation. The reliability of these monitoring methods are evaluated in this chapter.

4.1 Evaluation of pore pressure measurements

An evaluation of the pore pressure measurements was conducted which included: (1) an analysis of the recorded data to determine if barometric pressure variations are the source of high frequency variation within the data, and (2) a review of the use of fully grouted piezometers in this moving landslide.

4.1.1 High frequency variation and barometric fluctuation

The unprocessed piezometer data from the piezometers grouted into the boreholes and the piezometer used to monitor the river elevation had a significant amount of high frequency variation. In the piezometer used to monitor the river, this variation was still present when the river level was below the piezometer, i.e., the piezometer was out of the river. This variation was attributed to barometric variation as the piezometer was dry at this time. Similar variations were also observed at the same time in the piezometers grouted in the boreholes. This led to the hypothesis that the high frequency variation in the pore pressure data recorded in the boreholes was at least partially the result of barometric pressure variation.

This hypothesis contradicts manufacturer literature (Slope Indicator 2013) which states that “barometric correction is not required in a sealed borehole”, such as the fully grouted piezometers installed in 2013. Contreras et al. (2012) stated that piezometer tips in fully grouted boreholes are not sealed and require barometric pressure correction. The hypothesis regarding the effects of barometric variation could be confirmed by performing a simple analysis.

Barometric pressure data is available from a weather station which was located 73 km from the Ripley Landslide (Environment Canada 2015). There was some concern about the applicability of the barometric data set being used to represent changes at the Ripley Landslide due to this distance.

The reading frequency of pore pressures was also increased in January 2015 to be greater than the barometric pressure logging frequency. This necessitated the installation of an on-site barometer to monitor the variation in atmospheric pressure. The barometer installed at site has been operating since the July 5, 2015. The data from the barometer were compared to the weather station data to ensure that the barometric pressure variations at the weather station are in fact representative of the changes on site.

It should be noted that the pressures recorded on site were consistently 8.5 kPa higher than those recorded at the weather station. This difference is caused by the elevation used for the elevation compensation equation programmed into the data logging system (Ryder 2016). The value used for the program corresponds to the average elevation in Edmonton (671 m.a.s.l.) while the barometer is located at a much lower elevation (277 m.a.s.l.).

Figure 4-1 shows that the variations of both data sets are in excellent agreement and the weather station data is representative of the site conditions.

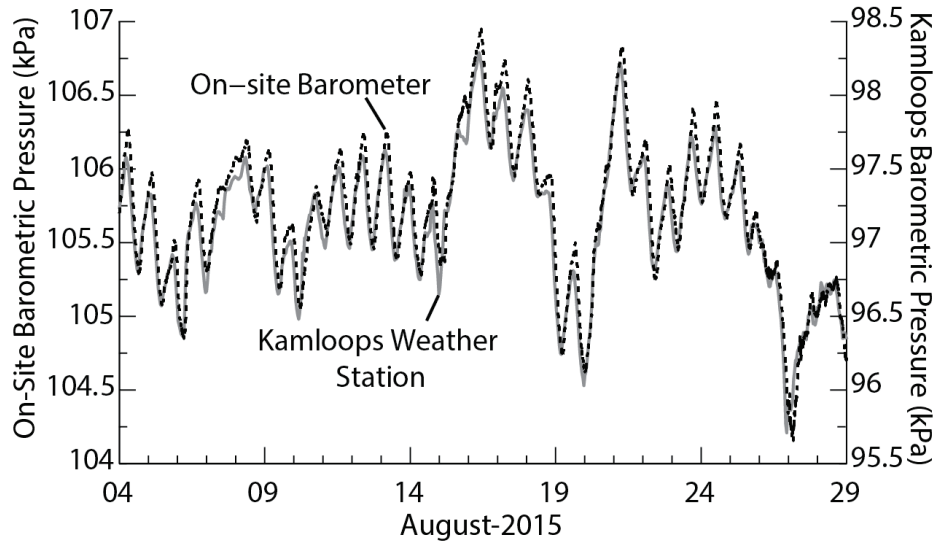


Figure 4-1 Comparison of the variation of atmospheric pressure measured by an on-site barometer and a distant weather station

This comparison shows that the variation measured at a weather station 73 km away is representative of the variation observed on site. Consequently, the variations in pressure from the weather station can be used to establish the variations at the site.

The raw pore pressure and barometric pressure data (Environment Canada 2015) were filtered using a 10-day moving average which removed the high frequency variation of each data set. The difference between the raw data and the filtered data was then compared to determine if the high frequency variation of pore pressure correlated strongly to the high frequency variation of barometric pressure. Figure 4-2 shows the difference between the raw and filtered data for the barometric data and the pore pressures measured by piezometers installed in the bedrock and at the rupture surface.

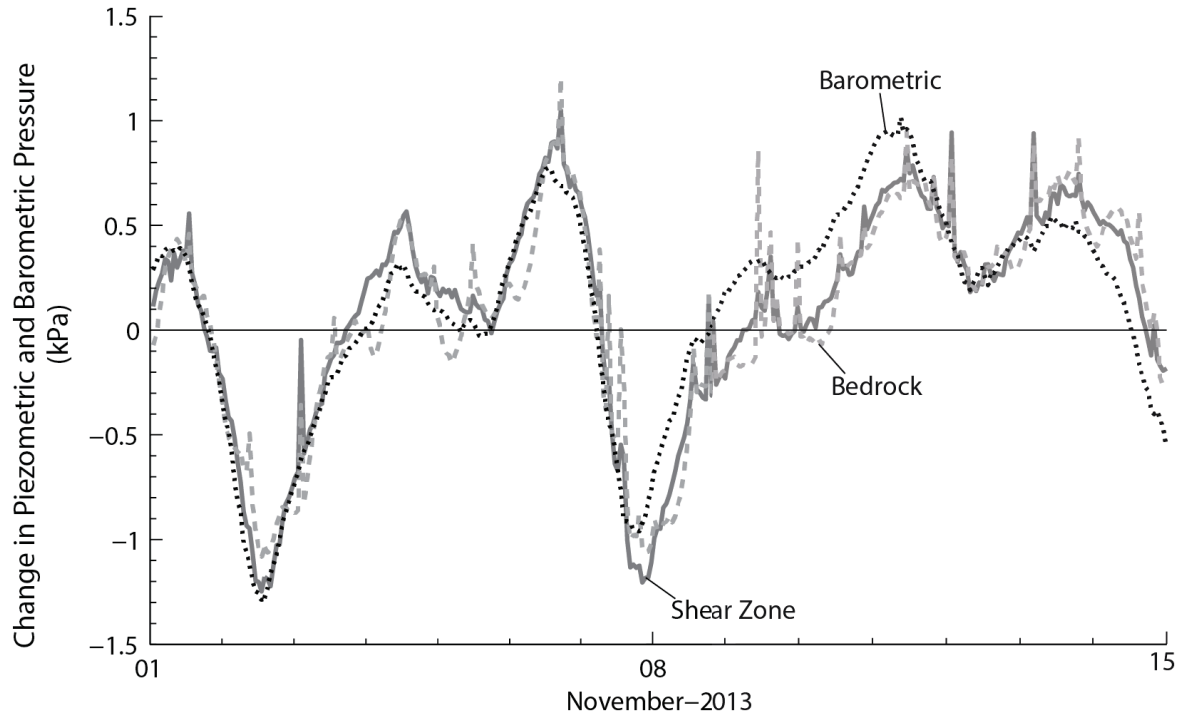


Figure 4-2 High Frequency Variation of Pore Pressure in the bedrock at a depth of 32.6 m and the shear zone at a depth of 15.6 m, and the Barometric Data provided by Environment Canada

The value of barometric variation was multiplied by a scalar factor of 0.8 to match the amplitude of the pore pressure variation. This was established using the visual inspection method (Marefat et al. 2015). The high frequency variation resulting from barometric pressure change can be compensated for by subtracting the barometric variation from the raw pore pressure data.

Figure 4-3 shows raw data from one of the piezometers installed at a depth of 20.4 m in BH13-01. This depth corresponds to the approximate midpoint of Unit 2. This figure also shows the pore pressure trend produced by applying the barometric compensation.

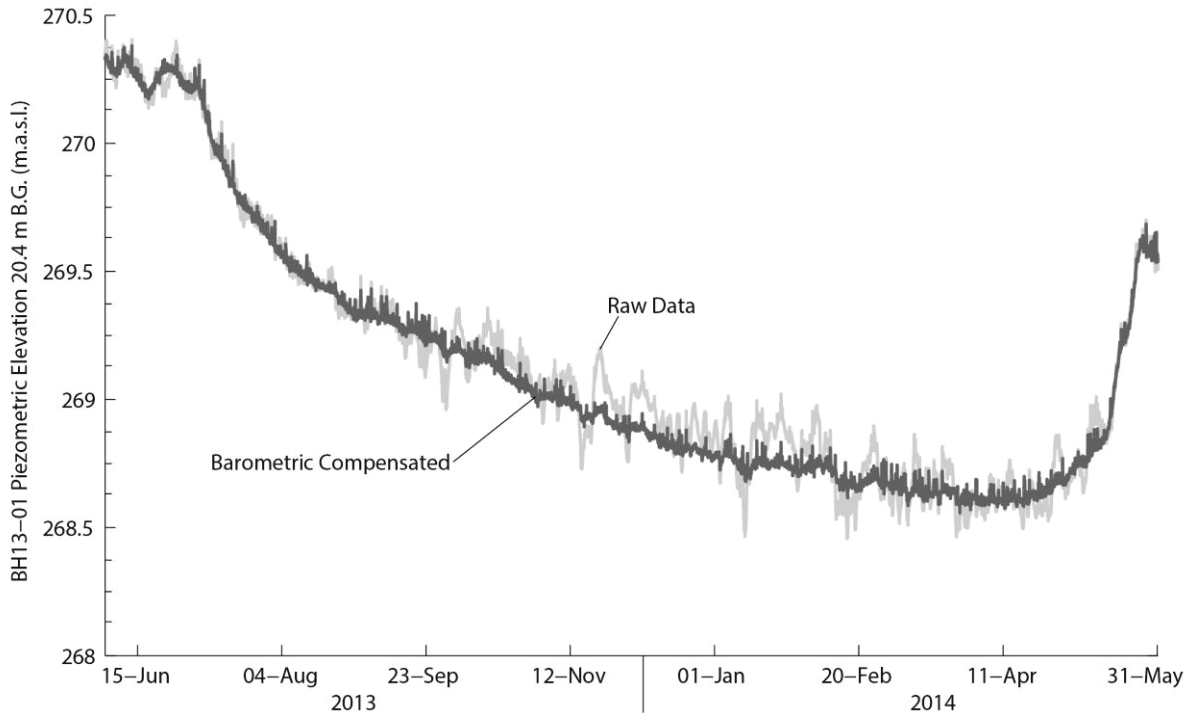


Figure 4-3 Comparison of raw and barometric compensated pore pressure for a VW-piezometer at 20.4 m depth in BH13-01

4.1.2 Evaluation of fully grouted installation method

There are three main concerns with the use of fully grouted piezometers: (1) proper selection of the grout mix, and (2) the interpretation of the initial pore pressures, and (3) the potential for vertical grout cracks allowing piezometers to communicate. These concerns are addressed below.

Grout Selection

The grout mix selected for a piezometer installation is very important. Theoretically, a piezometer would yield the most representative measurements if it is embedded directly into the soil. To mimic this, the grout mix should have the same permeability and stiffness as the adjacent soil (Contreras et al. 2008). The effect of the grout would be negligible if the properties matched the soil.

The grout mix used for piezometer installation during the 2013 and 2015 investigations was the mix recommended for medium to hard soils (Mikkelson 2003). This grout mix has an estimated 28-day compressive strength of 345 kPa and a modulus of approximately 70 GPa. There are not sufficient testing data available for the surrounding soils to determine the suitability of this grout mix for the soil conditions at the Ripley Landslide.

Initial Equalization Time

There were high initial pressures observed in the piezometers installed in the clay at the Ripley Landslide. These readings do not follow the seasonal patterns of pore pressure and are likely not representative of the layer in which they are installed. This can be seen in the highlighted region of the shear zone readings in Figure 4-4a.

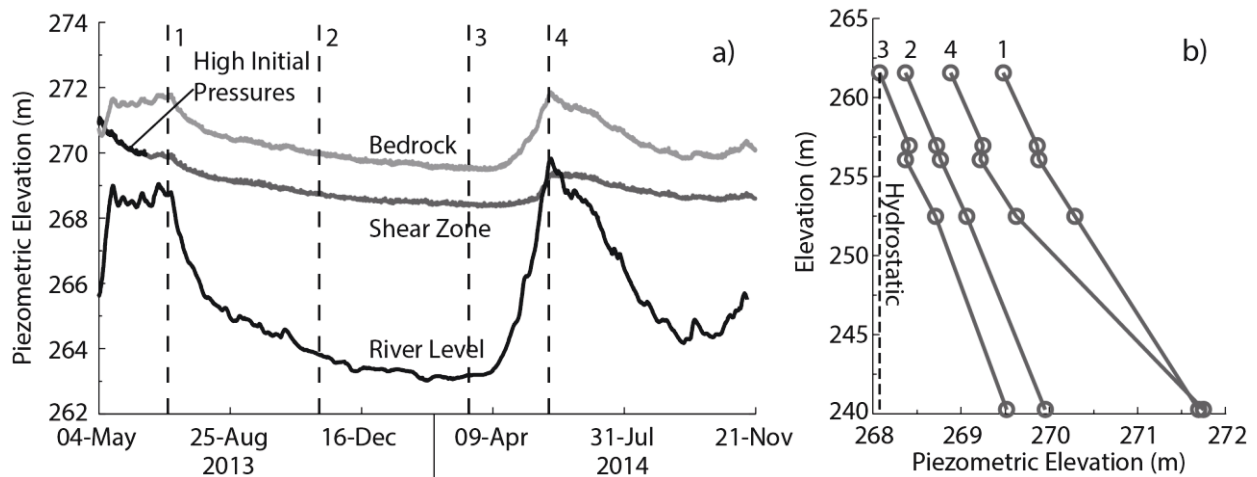


Figure 4-4 Barometric compensated fully grouted piezometer readings at the Ripley Landslide in the first 18 months of monitoring over time (a) and with depth(b)

These high readings gradually dissipate and eventually follow a similar trend to the pressures in the bedrock. These high pressures were not recorded in the bedrock. This means that the bedrock either (1) did not develop these high pressures or (2) the high initial pressures dissipated before the logger began taking readings.

The placement of the grout is potentially the reason for a higher than equilibrium pressure in the clay (Contreras et al. 2012). The unit weight of the fresh grout would result in a high fluid stress within the borehole. This will result in an increase in pore pressures in an area around the borehole. This assumes that the permeability of the clay leads to an initial undrained response to the load applied by the grout placement. Once the grout cures, the excess pore pressures gradually dissipate through the surrounding soil and rock.

Hvorslev (1951) described the concept of the Stress Adjustment Time Lag. The concept is that stress changes at the location of the sensor alters the moisture content and pressure of the soil adjacent to the sensor. The time required for the stress induced pressures to dissipate is defined as the stress adjustment time lag.

The stress adjustment time lag is a function of permeability of the soil (Hvorslev 1951). This is a logical dependence, as water needs to seep either into or out of the adjacent soil to equilibrate the pressures. This is a possible explanation of why the initially high pressures were not observed in the bedrock. The higher permeability of the fractured bedrock would allow any excess pressures to dissipate very quickly.

The exact time required for the disequilibrium pressure in the clay to dissipate is difficult to determine. The pore pressure readings in the clay appear to match the seasonal trends observed in the bedrock approximately two months after installation.

Grout cracking

Another concern for the use of grouted-in piezometers is the formation of cracks within the grout as ground movements occur. Piezometers installed at various depths would be able to communicate if cracks formed.

The Ripley Landslide has an upward gradient which has been measured in both the sand-pack and grouted-in piezometers. Analysis of these gradients with time has not identified any hydraulic connections between these piezometers. This is evident in Figure 4-4b where piezometer communication would be represented by a vertical line. Hence, at present all evidence from the monitoring results indicates these piezometers are providing representative pore pressures.

4.2 Flow measurements of the Thompson River

The Thompson River annually changes elevation at the Ripley Landslide by up to 6 m in response to the spring snow melt in the surrounding mountains. This rise in the river level starts in late April to early May and occurs over a two month period. The 2013-2015 river flow fluctuation can be seen in Figure 4-5.

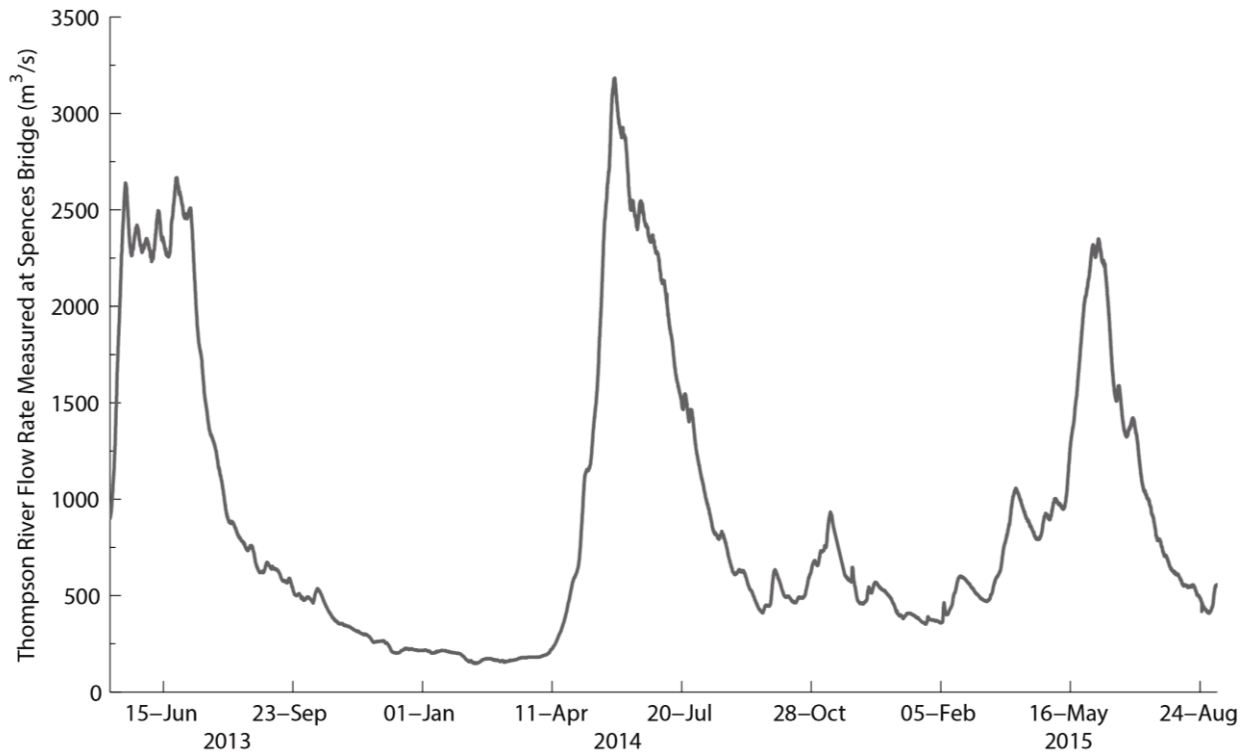


Figure 4-5 Seasonal flow rate variation of the Thompson River as measured at Spences Bridge

Consistent and strong correlations have been observed between the river elevation and the movement of the landslide (Hendry et al. 2015). However, to determine if these correlations are consistent through the year, the continuous river elevation was needed throughout the year.

A well-calibrated rating curve can estimate the variation of river level throughout the year based on measured flow data. A rating curve requires river discharge volume to calculate an approximate river elevation. There is a river monitoring station installed at Spences Bridge, 30 km downstream of the Ripley Landslide, which measures the river discharge volume every 20 minutes (Environment Canada 2015). Hendry et al. (2015) suggested that the river monitoring station at Spences Bridge could be used as a proxy for the river elevations at the Ripley Landslide.

However, the rating curve proposed by Hendry et al. (2015) was developed using three survey data points at the Ripley Landslide. To establish a stronger correlation between the water flows at Spences Bridge and the Ripley Landslide, a piezometer was installed in the Thompson River at the Ripley Landslide on May 4, 2013. The piezometric elevation recorded by this piezometer was considered to be equal to the river surface elevation.

This piezometer provided approximately 3,500 data points between May 4, 2013 and May 26, 2014. The rating curve used by Hendry et al. (2015) was updated by computing the residual sum of squares of the power law with respect to the piezometer data. The revised rating curve is given by:

$$L = \left(\frac{Q}{74.1} \right)^{0.562} + 261.5 \quad [4-1]$$

where;

Q = Volume of river flow in the Thompson River measured at Spences Bridge (m³/s)

L = Elevation of river surface adjacent to the Ripley Landslide (m.a.s.l.)

The measured water levels are presented in Figure 4-6 with the revised rating curve. The three river elevations used to calibrate the Hendry et al. (2015) rating curve are also shown.

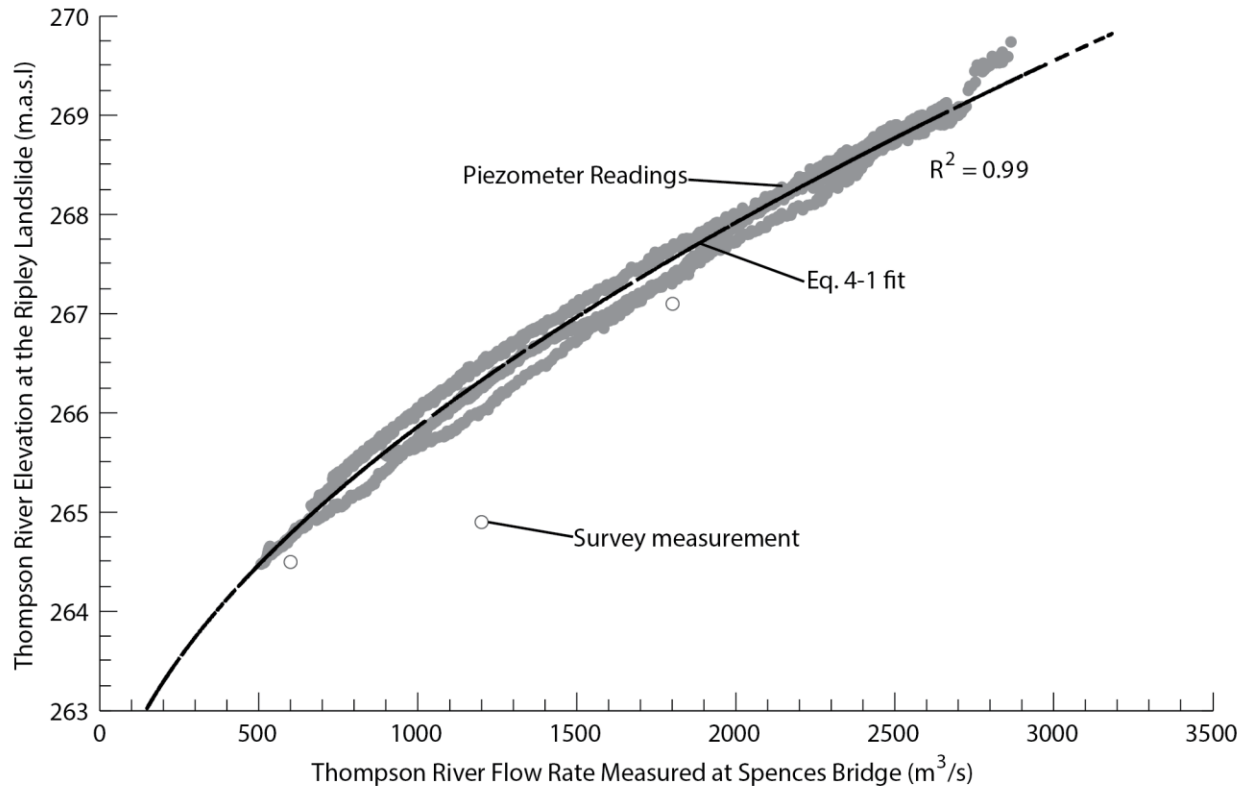


Figure 4-6 Correlation between the Thompson River elevation at the Ripley Landslide and the flow rate measured at Spences Bridge

The data at flow rates greater than 2700 m³/s departs from Equation 4-1. This could be attributed to unsteady flow conditions at high discharge volumes (Dottori et al. 2009). A comparison of the recorded river level to the level predicted by the revised rating curve yielded a maximum difference of 0.3 m for flow rates of 507 m³/s to 2864 m³/s. For the purposes of this research this range is adequate and Equation 4-1 can be used to estimate the river level throughout the year.

4.3 Comparison of Displacement Measurements from ShapeAccelArray, GPS Monitoring, and Slope Inclinometer

Slope inclinometers were installed in DH05-24 and DH05-27 (Figure 3-3) between October 25 and November 14, 2005 as discussed in Chapter 3. These were read initially on November 14, 2005 and during site visits on April 4, 2006 and March 21, 2007.

DH05-24 showed very little movement at the April, 2006 reading and was sheared off at a depth of 3 m below the top of casing when the March, 2007 reading. The April, 2006 inclinometer reading in DH05-27 showed two shear zones. There was a shallow shear zone located at an elevation of 267.6 m.a.s.l. which had a recorded displacement of 12 mm. The deeper shear zone, located at an elevation of 256.7 m.a.s.l, had a recorded displacement of 32 mm. This deeper sliding plane was defined as the primary shear plane by Hendry et al. (2015). Figure 4-7 shows the two well defined shear zones identified at DH05-27.

A ShapeAccelArray (SAA) was installed in BH13-02 (Figure 3-3) to monitor the shear displacements at the primary shear zone identified by Hendry et al. (2015). The second shallower zone of movement identified by Hendry et al. (2015) from the SI data which was not captured by the SAA installation. The SAA has been continuously recording since May 4, 2013. The trend of displacements with depth are shown in Figure 4-7. The shallow movement zone, identified by Hendry et al. (2015), is shown in Figure 4-7 and lies outside of the interval monitored by the SAA installation.

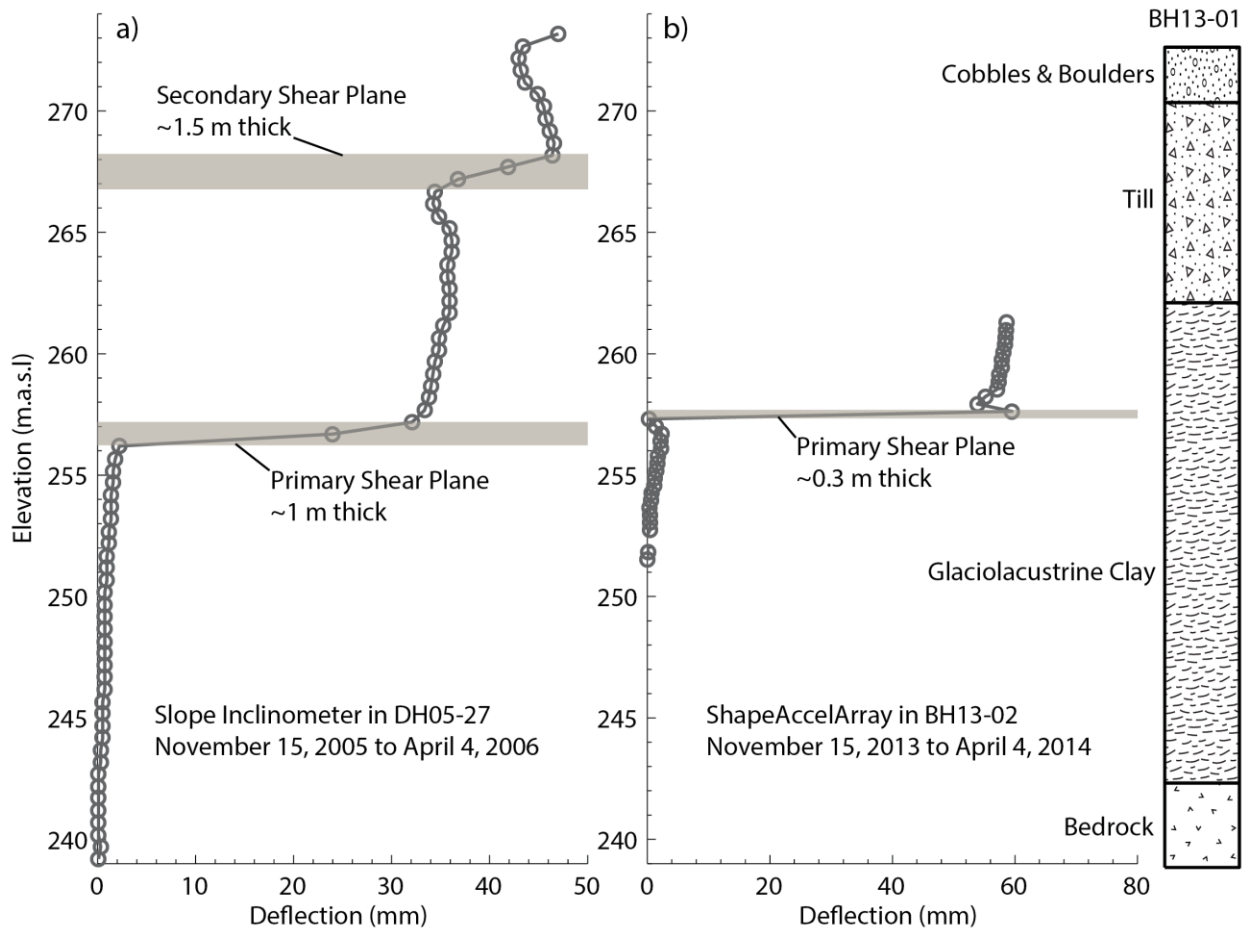


Figure 4-7 Deflection recorded at the Ripley Landslide by a slope inclinometer in DH05-27 (a) and a ShapeAccelArray in BH13-02 (b) for the same time period in different years

The Global Positioning System (GPS) discussed in Chapter 3 allows for monitoring of the surface displacements of the Ripley Landslide. The GPS system began recording displacements on April 11, 2008. Various instrument issues resulted in discontinuous recording until 2011. The locations of the GPS monitoring units can be seen in Figure 3-3. Figure 4-8 shows the inconsistency of the GPS monitoring results before 2011 and also shows the differences between GPS monitoring units.

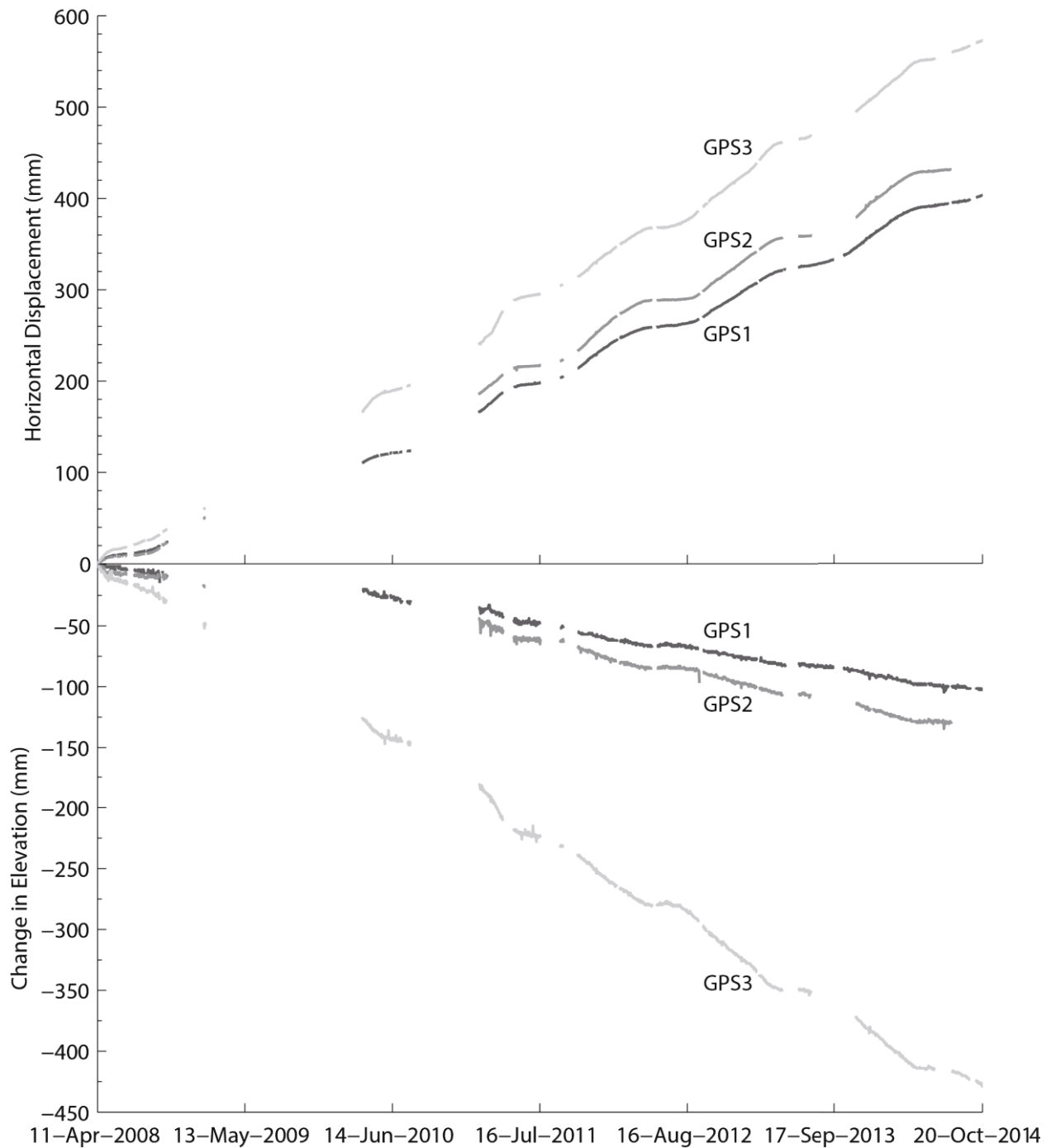


Figure 4-8 GPS surface displacements recorded on the Ripley Landslide

A comparison of the SI, SAA and GPS monitoring results is the ideal way to ensure that each of these techniques is providing results that are representative of landslide behaviour. However, the SI data, which is considered as a baseline to be compared to, was collected over a period where

there was no other method being used on the site. In addition, the differences between the GPS unit behaviours (Figure 4-8) are evidence that the location of monitoring has an effect on surface deformations. This means that, while the GPS units are reporting surface deformations over the same time period that the SAA is recording, these deformations may be different from the surface deformations at the location of the SAA.

One of the issues with the monitoring data from the SAA in BH13-02 is that it is only monitoring internal shear displacements over the more active of the two identified shear zones. Without concurrent ground surface deformation readings at that location, it is difficult to assess if the surface and internal shear movements are the same. If the surface movements were equal to the internal shear displacements, the landslide is purely translational along that single shear zone. If the surface movements are greater than the internal shear displacements, there are several possible explanations:

- 1) The base of the SAA is not installed into a fixed layer.
- 2) There are shear displacements occurring along other shear planes above the location of the SAA.

In the case of either of these explanations, the displacements recorded by the SAA would only represent a portion of the total landslide movement. This could limit the amount of interpretation which can be done using these results.

In addition, the river level variation has been previously linked to stability at the Ripley Landslide (Hendry et al. 2015). The year to year variation of river levels can make it difficult to compare monitoring from different years.

Despite the difficulties regarding monitoring location and time period, the results of the various methods for the annual period of November 15 to April 4 were compared. This period was chosen as it was the only time that slope inclinometer data was recorded at the Ripley Landslide. The results of this comparison are presented in Table 4-1. The river flows for each of the monitored years is shown in Figure 4-9.

Table 4-1 Comparison of horizontal displacement monitoring methods

Monitoring Method	Displacements in mm from November 15 to April 4					Comments
	Year of Monitoring					
	Nov 2005 to Apr 2006	Nov 2011 to Apr 2012	Nov 2012 to Apr 2013	Nov 2013 to Apr 2014	Nov 2014 to Apr 2015	
Slope Inclinometer	44	-	-	-	-	Monitors displacement of full depth to bedrock
GPS 1	-	35.4	35.1	38.9	-	Monitors surface displacement
GPS 2	-	44.4	39.9	45.1	-	Monitors surface displacements
GPS 3	-	42.2	51	48.9	-	Monitors surface displacements
ShapeAccelArray	-	-	-	58.3	38.2	Monitors displacements of primary shear zone at 257 m.a.s.l.

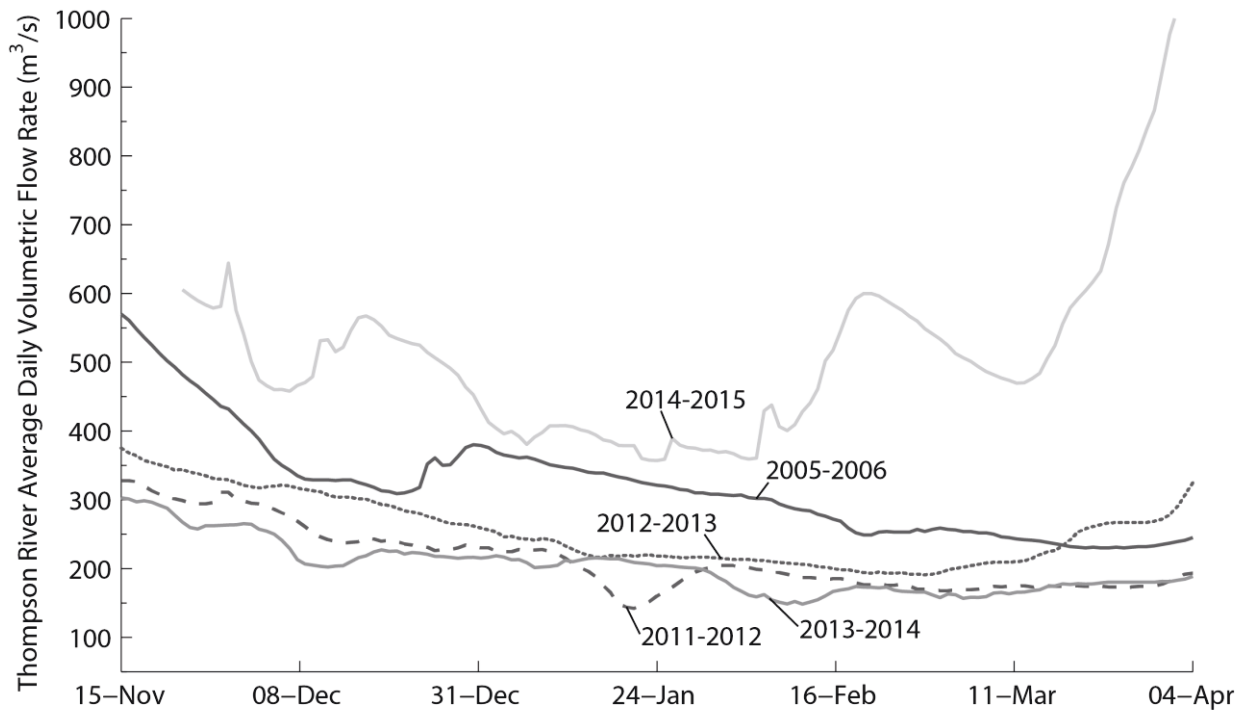


Figure 4-9 River flow in the Thompson River measured at Spences Bridge for the period of November 15 to April 4 for the various periods of slope monitoring compared in Table 4-1.

The comparison of the different monitoring results showed that the results for each method ranged from 35.1 mm to 58.3 mm of recorded displacement during the period of November 15 to April 4 in each year. There were differences from year to year which can be attributed to differences in river flow. There were also differences in a given year between monitoring methods which can be attributed to different locations of the monitoring equipment. The monitoring results shown in Table 4-1 did not provide adequate evidence to conclude if the internal shear displacements recorded by the SAA were the same as the surface displacements of the landslide.

Alternatively, if the SAA can be proven to be representative of the level of activity of the landslide, this data could still be useful for interpreting the landslide behaviour. If the SAA is not

capturing all of the displacements, but the amount it moves in a given time period is proportional to the surface displacements in that time period, the SAA can be considered representative of landslide activity.

The landslide activity has been characterized as seasonal by Hendry et al. (2015) with the majority of the annual movement occurring during the winter months. The SAA's ability to identify this seasonality and differentiate between periods of landslide activity and inactivity can be determined by comparing the SAA and GPS monitoring. This is assuming that the activity of the surface displacements is proportional at the location of the SAA and the location of the GPS units. This comparison can be done visually by observing the trends of displacement over time of the SAA and the various GPS units. Figure 4-10 shows a portion of the monitoring data recorded by the various systems. The apparent active and inactive periods of the landslide are highlighted.

The GPS units appear to record some displacements during the inactive periods while the SAA is recording essentially no movement. The SAA then records higher displacements during the active periods. Despite the differences in the magnitudes of displacements recorded in each period, the SAA does provide a good indication of the periods of activity.

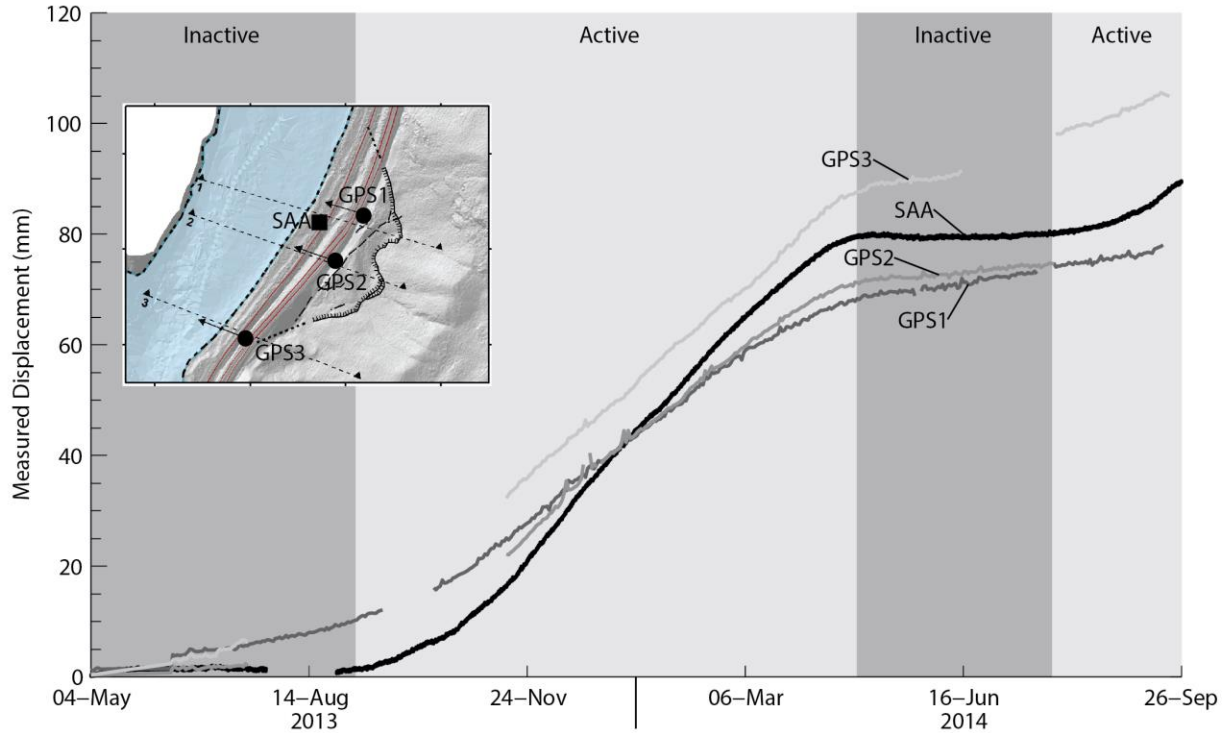


Figure 4-10 Comparison of displacement measurements of the SAA installed in BH13-01 and the GPS displacement units placed across the Ripley Landslide

Based on the comparison of these results presented in Table 4-1 and Figure 4-10, the SAA provides valid periods of active movement. The SAA data can be used to determine the relative amount of landslide activity in a given period.

4.4 Summary

The Measurand SAA and grouted-in piezometers were trialed at the Ripley Landslide to provide continuous hourly monitoring of the landslide movement and pore pressure changes. Review of this data has concluded that:

- 1) Interpreting the pore pressures required compensating for the barometric pressure variation.

- 2) A rating curve correlating river discharge at Spences Bridge and the measured river levels is adequate for estimating river surface elevation at the Ripley Landslide.
- 3) The shear displacements recorded by the SAA at the primary shear plane are considered representative of the overall slope activity.

5 Ripley Landslide Kinematics

The combination of all of the investigations discussed in Chapter 3 has yielded a large set of detailed geological information. The preliminary analysis of displacement monitoring data discussed in Chapter 4 has provided a better understanding of the way in which the landslide is behaving. Using the most recent geology and displacement data, the kinematics of the Ripley Landslide is better understood and incorporated into revised cross sections.

5.1 Previously Proposed Cross Sections

Geological cross sections of the Ripley Landslide have been proposed in the past (Hendry et al. 2015, Huntley and Bobrowsky 2014). The Hendry et al. (2015) cross sections were developed based on the borehole logs of DH05-26, regional surface geology information (Ryder 1976) and the landslide mechanism described in Eshraghian et al. (2007). Assumptions of horizontal shear planes and unit contacts were based on the previous observations by Eshraghian et al. (2007) from larger nearby landslides (CN50.9, South Landslide, Basque Landslide).

The surface profiles for these sections were taken from a digital elevation model developed using a ground based light detection and ranging (LiDAR) system. This surface topography was combined with bathymetry data which characterized the ground surface below the river. The location of these sections can be seen in Figure 3-3.

The Hendry et al. 2015 cross sections are shown in Figure 5-1 for reference.

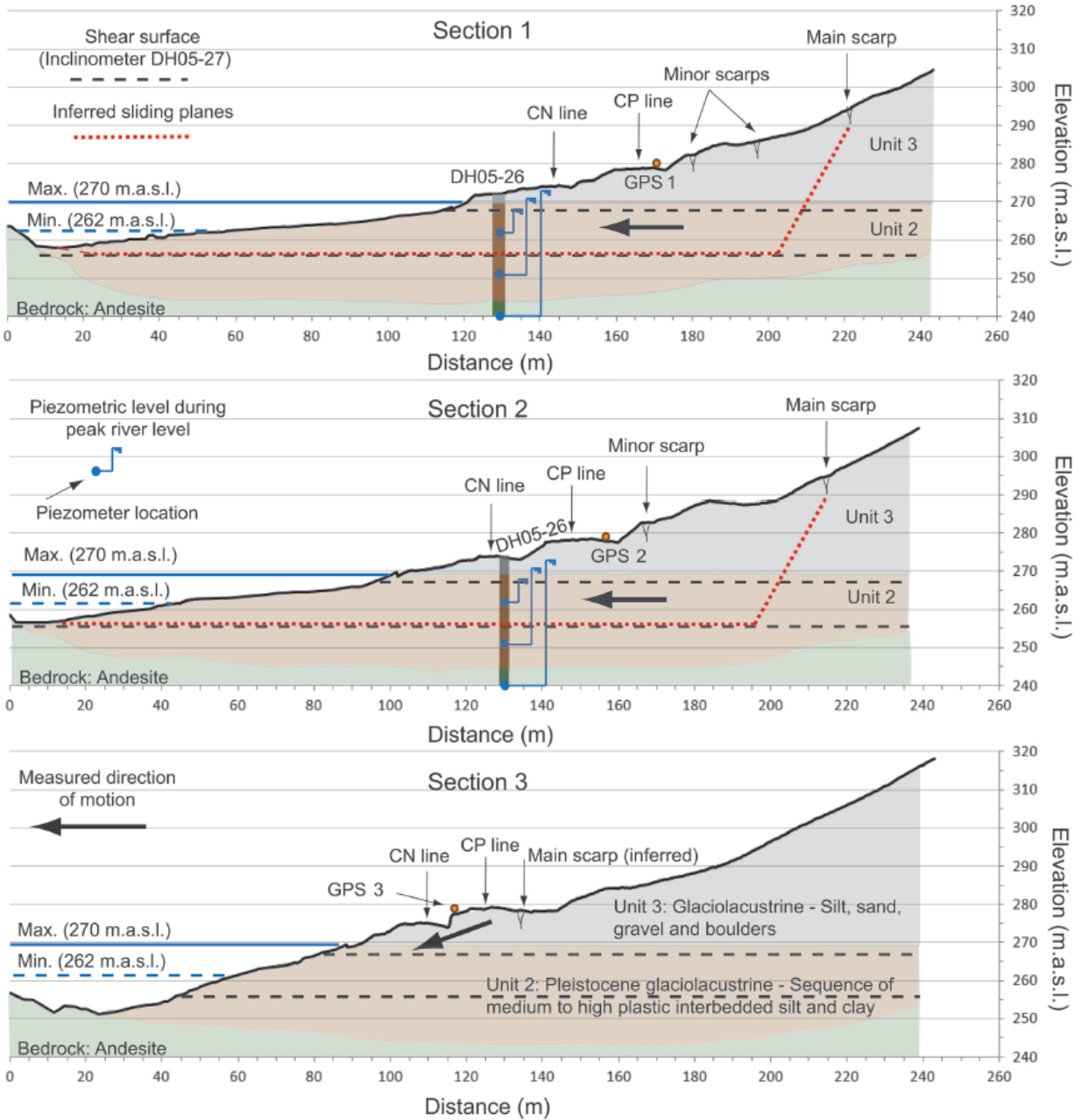


Figure 5-1 Cross sections of the Ripley Landslide by Hendry et al. (2015) showing rupture surfaces, estimated stratigraphy, measured piezometric elevations (see Figure 3-3 for locations)

5.2 The effect of bedrock profile on landslide mechanism

There are many boreholes across the Ripley Landslide which were discussed in Chapter 3 (Figure 3-6 and Figure 3-7). The additional boreholes drilled in 2015, in combination with the seismic refraction results (Figure 3-5), have yielded a better estimate of the bedrock profile beneath the Ripley Landslide than what was assumed in Figure 5-1.

The lateral extent of the landslide was previously described as being constrained by the bedrock outcrops on the north and south flanks of the landslide (Hendry et al. 2015). The bedrock profile moving up slope was not well defined and it was assumed to not be a factor controlling the landslide extent. The mechanism of a horizontal basal sliding plane extending back into the slope was assumed by Hendry et al. (2015). Many of the other landslides observed in the region experienced near horizontal deep seated movements which led to this assumption.

BH15-03 was drilled approximately 40 m upslope from BH13-01. The bedrock interface at the upslope location was found at an elevation of 261.1 m.a.s.l. compared to 242.4 m.a.s.l. at the location closer to the river. The shallow bedrock in the upslope areas of the Ripley Landslide was discussed in Chapter 3. The previously identified deep rupture surface in Unit 2, if assumed to be near horizontal, encounters this shallower bedrock. This bedrock profile therefore appears to limit the extent of the landslide.

5.3 Surface displacement vectors

Analysis of the GPS data from the site has provided information with implications on the kinematics and the basal shear surface of the Ripley Landslide. The GPS monitoring units provide both horizontal and vertical surface deformation over time. The vertical and horizontal

deformations can be compared to yield the displacement vector inclination. The trend of the displacement vector inclination over time for each GPS unit can lead to various conclusion:

- 1) If the angle is constant over time, the landslide is translating along a basal plane with an angle of inclination equal to displacement vector inclination. This could also mean that the landslide is moving over multiple planes but the rates along each plane are consistently proportional.
- 2) If the angle varies over time the landslide mechanism is most likely not purely translational.

There are other factors not related to landslide activity which could affect the displacement vector inclination such as surface settlements.

Figure 5-2 shows the observed angle of movement for the three GPS units on the Ripley Landslide. The data before 2011 was not included as this was much more sensitive to small changes in elevation as the cumulative horizontal movement at this point was small. The displacement vector inclinations for GPS 1 and GPS 2 are fairly consistent at 14 and 16 degrees, respectively, while GPS 3 is travelling at 37 degrees. In the case of all units the displacement vector inclination is relatively constant. There are three possible explanations for this behaviour:

- 1) The shear plane at the GPS locations is dipping towards the river with their respective recorded angles.
- 2) The displacements have not been observed over enough horizontal distance to record any variation in the displacement vector inclination.
- 3) The landslide is not purely translational but the different mechanisms result in a consistent displacement vector inclination.

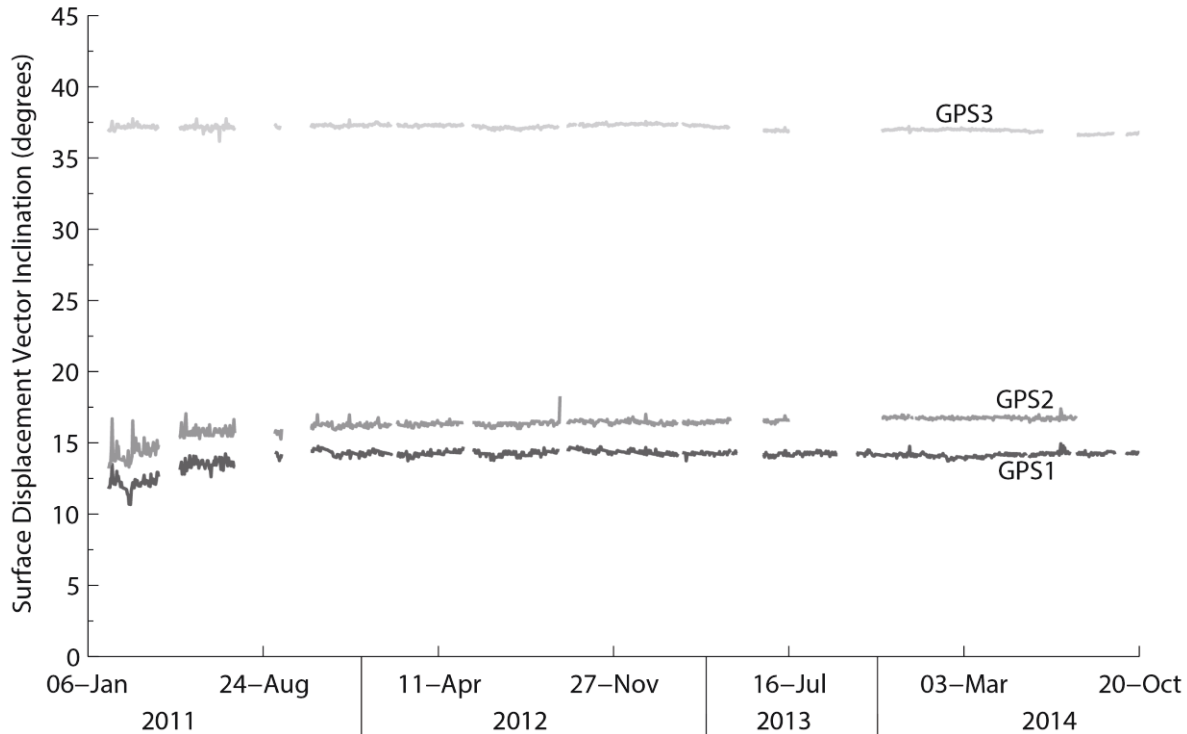


Figure 5-2 Surface displacement vector inclinations observed by three GPS monitoring units installed on the Ripley Landslide (see Figure 3-3 on p.28 for unit locations)

The displacement vector inclinations seen in Figure 5-2 do not support the horizontal shear zone beneath the tracks depicted in the previously developed sections. The shear zone beneath the GPS units is likely dipping significantly below horizontal. Based on this new information the mechanism and kinematics of the Ripley Landslide is discussed in the following sections.

5.4 Additional displacement data at the Ripley Landslide

The 2015 investigation provided additional SI data collected in BH15-04 before it was retrofitted with a ShapeAccelArray (SAA). The initial reading was performed on March 3, 2015 with additional readings during site visits on May 4, 2015 and July 13, 2015. These readings identified two shear planes. A deep sliding plane at approximately 268 m.a.s.l. and a shallow

zone at approximately 275 m.a.s.l. Cumulative horizontal deformations of 8 mm in the deep shear zone and 2 mm in the shallow zone were observed from March 3, 2015 to July 13, 2015.

During this same time period the SAA in BH13-01 recorded a cumulative horizontal movement of 10 mm along an isolated shear plane at an approximate elevation of 257 m.a.s.l. As discussed in Chapter 4, there was a shallow movement zone outside of the range that the SAA was observing. To estimate the amount of movement that the shallow plane would have had during this time period, the April 4, 2006 SI reading from DH05-27 was scaled down so that the primary shear plane showed 10 mm of cumulative displacement.

Scaling the SI reading from DH05-27 was done under the assumption that the two shear planes move a proportional amount during a given period. If this were not true we would expect to see a seasonal variation in the displacement vector inclination. None of the GPS monitoring units displacement vector inclinations showed any seasonality in Figure 5-2. Therefore, the assumption is considered valid.

Figure 5-3 shows a portion of Section 2 from Figure 5-1 with updated geology and the displacement data discussed above. The incremental displacements are plotted beside the boreholes to better identify the shear zones. The cumulative displacements for each zone are also indicated.

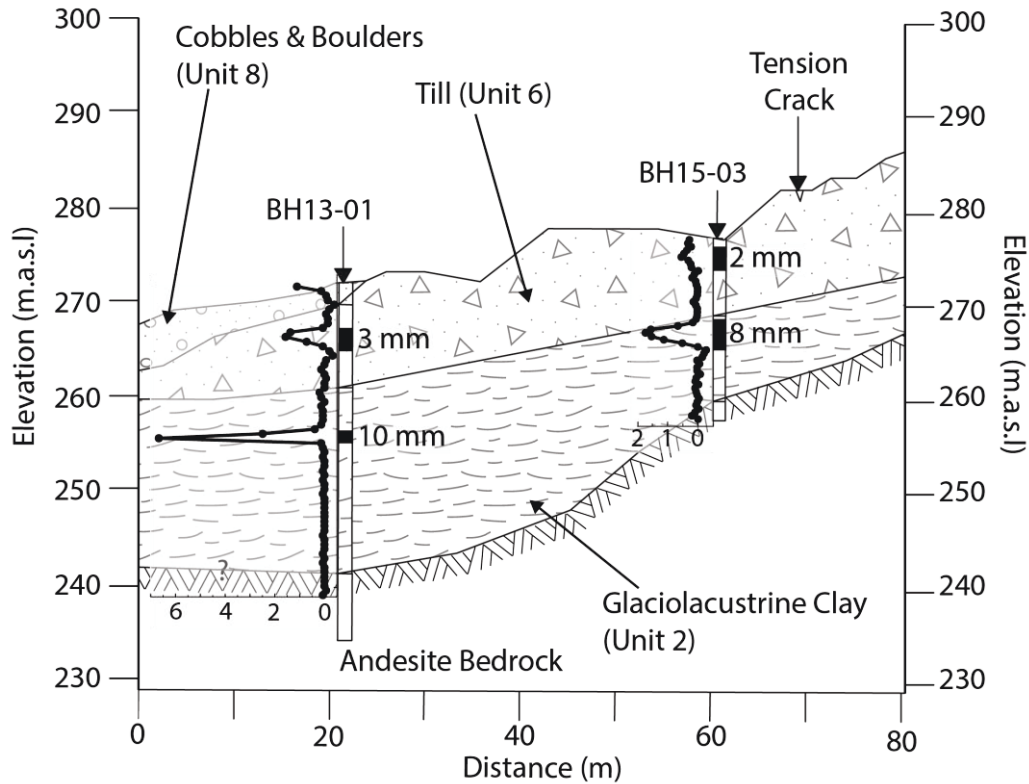


Figure 5-3 Incremental displacements (in mm) along Section 2 (Figure 3-3) between March 3, 2015 and July 13, 2015; Shear zones indicated in black with the cumulative displacement indicated beside them

The thickness of the observed shear zones ranged from 1 m to over 3 m. This thickness of the shear zone may be an indication of the mechanism occurring at that location. The deep shear zone in BH13-01 is the narrowest observed surface. This is what would be logically expected in the case of the landslide translating along a specific weak layer according to the mechanism proposed by Eshraghian et al. (2007). The deep shear zone observed at BH15-03 was approximately three times as thick. This indicates that the shear zone at this location is not following a single horizontal weak layer as the shear zone is not as narrow and well defined.

It appears that the deep seated movement at BH13-01 is following the mechanism of near horizontal movement along a weak layer. The deep movement zone observed at BH15-03 is likely the same shear zone based on the magnitudes of movement, but it is being constrained towards the surface by the shallowing bedrock profile. This also agrees with the steepness of the displacement vector inclinations of the GPS units which result from the shear zone interacting with the bedrock below the points they are monitoring.

The shallow movement zones moved similar amounts and are both occurring within Unit 6. These two zones are most likely connected and are part of a shallow and long rupture surface that extends up the slope. These shallow movements may have been caused by the movement of the deeper rupture surface and loosening of the till layer. This would explain why this shallow movement was not observed in BH15-02 and BH15-06 outside the southern edge of the landslide. The shallow movements could also be a much older failure which was caused by the original down-cutting of the Thompson River through Unit 6.

5.5 Vertical displacements of GPS 3

Since the installation of the GPS monitoring system, the vertical deformations observed at GPS 3 have been a cause for concern. The steepness of the displacement vector inclination seen in Figure 5-2 illustrates that GPS 3 is moving in a distinctly different fashion than GPS 1 and GPS 2. The existence of a secondary landslide uphill from GPS 3 was hypothesized by Hendry et al. (2015) based on this abnormal vertical displacement.

The high vertical deformation was observed during mobilization for the site investigation as mentioned in Chapter 3. There were isolated zones of track roughness due to vertical movement observed near GPS 3 and at the approximate northern margin of the landslide. These high

vertical deformations could be the result of the main scarp of the landslide crossing the tracks at these locations. The vertical deformation at the back of the landslide is expected to be higher than it would be midslope. This concept is illustrated in a simplified form in Figure 5-4. The vertical deformations at the surface of Block A would be expected to be higher than those observed on Block B.

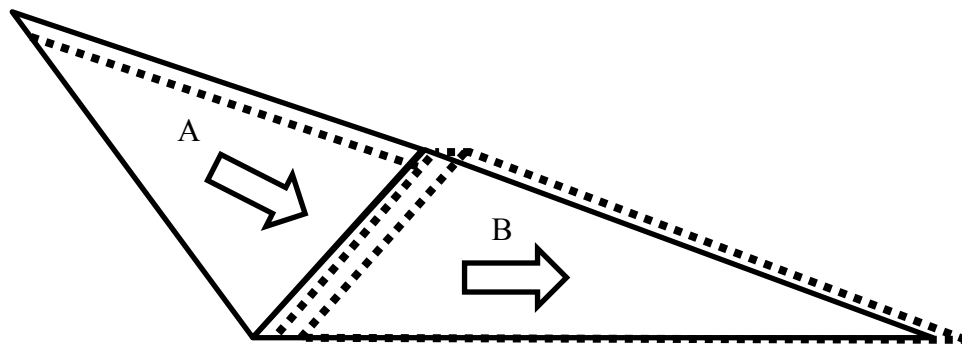


Figure 5-4 Simplified visualization of a compound landslide (after Norrish and Wyllie 1996)

As previously discussed, the bedrock outcrops observed just to the north and south of these points limit the extent of the landslide and would also indicate that the landslide back scarp crosses the tracks near these points. The lack of deformation observed at SI installations in BH15-02 and BH15-06 (Figure 3-3 p. 28) also indicate that the landslide does not extend further upslope behind GPS 3. This information explains the vertical deformations observed at GPS 3 without the existence of a secondary landslide.

In addition, as previously mentioned, the long shallow deformations in the till were not observed uphill from GPS 3. These shallow movements occur at a shallower angle which would further decrease the overall displacement vector inclination of the surface for the central portion of the landslide.

5.6 Cross sections of the Ripley Landslide

The updated geological information and mechanism observations discussed in this chapter were incorporated into a set of new cross sections of the Ripley Landslide. These cross sections were developed at the same locations as the sections depicted in Figure 5-1 and can be seen in plan view in Figure 3-3.

Each cross section shows the boreholes which were drilled closest to that section. The stratigraphy at these boreholes and the nearest seismic refraction results were used for determining the bedrock profile and placement of unit contacts.

The rupture surfaces indicated in the revised cross sections are based on borehole displacement measurements as well as the observation of tension cracks on the landslide surface. These sections depict a shallow sliding surface as well as a deep shear zone as discussed in the previous section.

The deeper shear zone follows the mechanism that has been observed at other landslides in the region while the shallower movement zone is a different mechanism. This deeper shear plane is horizontal at BH13-01 and then, as it approaches the bedrock, the back scarp is formed. Based on the shape of the bedrock, the backmost tension crack is not caused by this deeper shear plane. The backmost tension crack is either the original backscarp of the shallower movement zone or a retrogression of the shallower movement which formed over much shallower bedrock.

This combination of two mechanisms adequately explains the deformations and tension cracks which have been observed on the Ripley Landslide. The revised cross sections can be seen in Figure 5-5.

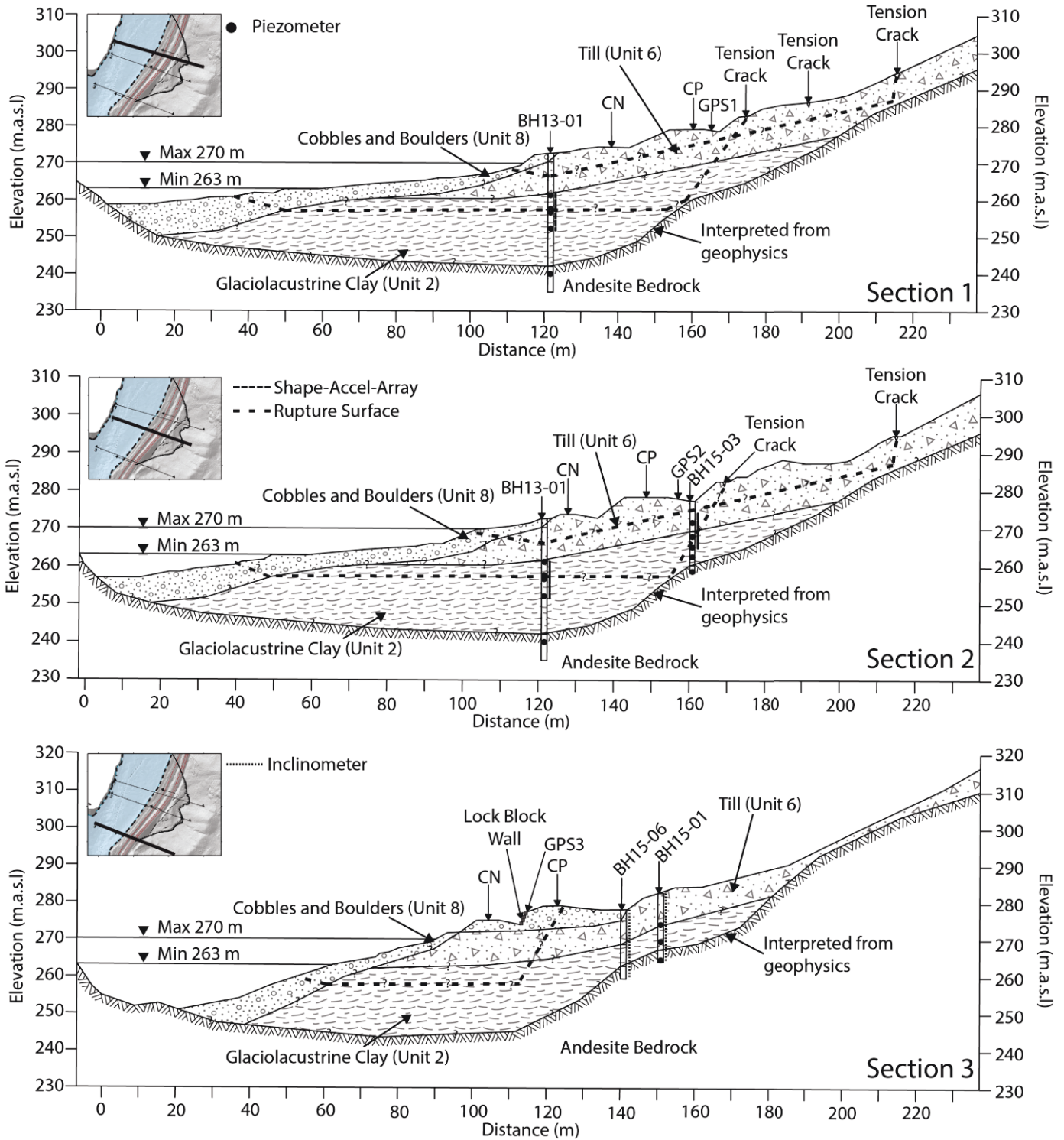


Figure 5-5 Revised cross sections of the Ripley Landslide showing rupture surfaces, river level range, instrumentation, and estimated stratigraphy

The revised cross sections in Figure 5-5 represent one possible hypothesis to explain the deformations observed on the Ripley Landslide. One of the main assumptions of this hypothesis is that the deeper rupture surface extends horizontally back into the slope. An alternative hypothesis is that the deeper rupture surface runs parallel to the interpreted upper boundary of Unit 2. This hypothesis assumes that the Unit 2 bedding within is inclined at approximately the same angle as the top surface of the deposit. This implies that the inclination of the top of the unit is a result of differential consolidation and the bedding planes, which the rupture surface formed along, are inclined. As the samples from the 2015 investigation are further examined, the inclination of the bedding at BH15-03 may provide additional insight, and aid in determining which hypothesis is correct.

5.7 Implications of revised cross sections

The revised sections of the Ripley Landslide have three major implications regarding future work and risk management of the site. These implications are (1) the likelihood of retrogression, (2) the difficulties of analyzing the landslide, and (3) the effects of changes of slope geometry on landslide activity.

All of the landslides characterized by Eshraghian et al. (2007) showed signs of having had retrogressive movements occur. If the bedrock channel that the river is flowing in is as narrow as our investigations would suggest, the weak layer in Unit 2 may have extended as far back as possible before encountering bedrock. The bedrock may restrict further retrogression along this plane. More investigation on the uphill portion of the slide would be required to confirm this. If the shallow movements in the till continue, ravelling of the till over the shallow bedrock uphill is possible which could result in another tension crack forming further uphill.

The presence of two different mechanisms at the Ripley Landslide is an interesting problem. The way that these two mechanisms interact is difficult to predict. As a result it may be difficult to capture this interaction in any analysis performed on the landslide.

Finally, the previous understanding of the landslide mechanism indicated that the shear plane was likely near horizontal beneath the CP and CN track at the Ripley Landslide. This assumption meant that any fill placement along the tracks would not have a significant effect on the factor of safety of the landslide. Based on the updated cross sections, the railway may be much closer to the back scarp than originally estimated. This could change the effect that any earth work would have. The shallow movement zone observed could also be more affected by changes to the surface. For this reason, further earthwork near the railway lines should be approached with caution.

5.8 Summary

GPS and traditional displacement data has been used to understand the mechanisms of slope instability at the Ripley Landslide. The analysis of this data in combination with previous sections and field observations have led to the following conclusions:

- 1) The GPS displacement vector inclinations are significantly different depending on their location on the landslide and were steeper than expected.
- 2) Displacement readings indicate that there are two shear surfaces active at the landslide; a deep surface within Unit 2 and a shallower failure zone in the till.
- 3) Updated geology and the presence of two different shear zones was able to explain the deformations and tension cracks observed on site.

- 4) Revised cross sections were produced showing updated understanding of geology and landslide mechanism.

6 Ripley Landslide Temporal Velocity

A seasonal variation in movement rates was previously observed in other studies (Macciotta et al. 2014, Hendry et al. 2015). Figure 6-1 shows the seasonality of the landslide activity with most of the movement occurring in the fall and winter months when the river level is low. As the river rises the landslide movement slows and can eventually stop (see Figure 6-1). Hence it appears high river level buttresses the landslide and suppresses movement (Bunce and Chadwick 2012).

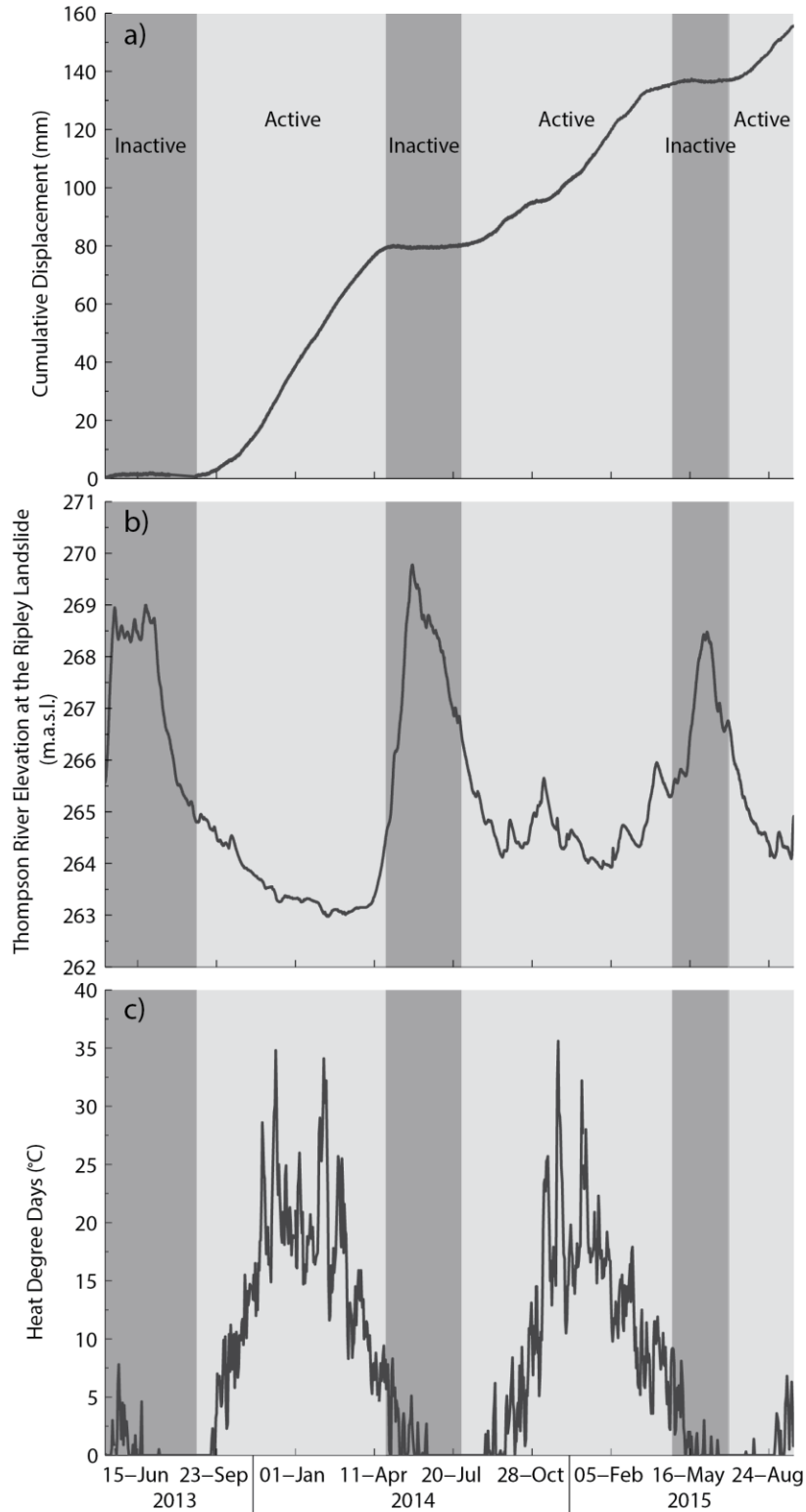


Figure 6-1 Seasonal variation of displacements recorded using SAA in BH13-02 (a), Thompson River Elevation (b), and Heat Degree Days (c) at the Ripley Landslide

Eshraghian et al. (2007) suggested that during the high river elevations, water infiltrates the landslides and the pore pressures come to equilibrium with the elevated river boundary. When the river level rapidly falls, the buttressing forces are removed and previously balanced forces are now unbalanced and so the landslide movement commences. Eshraghian et al. (2007) noted that this trend was similar to a rapid drawdown effect.

Rapid drawdown is defined as a reduction of water level within a water body adjacent to the slope without a corresponding equivalent reduction of pore pressure within the slope (Duncan and Wright 2005).

The monitoring results of the Ripley Landslide, are used in this chapter to evaluate if this drawdown mechanism is responsible for the seasonal variations in velocity of the Ripley Landslide.

6.1 Calculating landslide velocity

The variation of landslide velocity over time is required to determine which factors are controlling slope instability and validate the drawdown mechanism. A continuous record of the landslide velocity can be calculated from the ShapeAccelArray (SAA) readings. The SAA was determined to be a valid method of measuring the relative amounts of movement in different periods as mentioned in Section 4.3. It should be noted that the SAA only indicates the activity of the primary rupture surface.

The sampling rate for the SAA was changed from hourly to every 6-hours in January 2015. SAA readings from before January 2015 were trimmed to simulate a continuous 6-hour sampling rate throughout the data set. The trimmed displacement measurements were shown previously in Figure 6-1. The general trend of these displacements appears relatively smooth. If the velocity at

any point is calculated using the raw data the velocity is quite variable. The instantaneous velocity (v_n) at a point was calculated using:

$$v_n = \frac{d_{n+1} - d_{n-1}}{2} \times 4 \quad [6-1]$$

where; v_n = instantaneous velocity at timestep n ($\frac{\text{mm}}{\text{day}}$);

d_n = 6 – hour displacement measured at timestep n (mm)

The trend of instantaneous velocity over time can be seen in Figure 6-2.

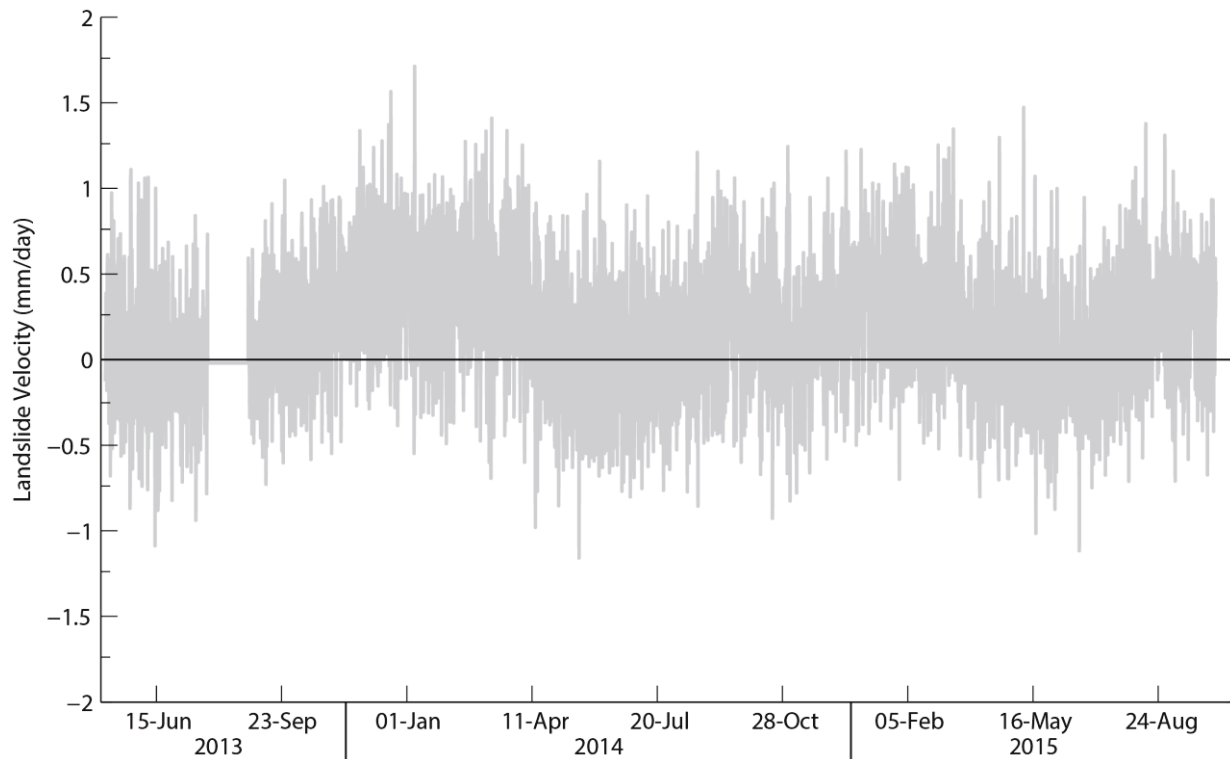


Figure 6-2 Instantaneous velocity calculated from 6-hour SAA readings from BH13-02 using Equation 6-1

The velocity trend in Figure 6-2 is difficult to analyze for various reasons. The first reason is that there are many points which have a negative velocity. This is not considered possible as this

indicates that the landslide is moving uphill. The high frequency variation and negative velocities are likely a result of instrument accuracy. Filtering the displacement data using a moving average before calculating the velocity is required to remove some of this high frequency variation. A filter threshold was proposed by gradually increasing the filtering window until the high frequency variation and negative velocities were removed from the velocity trend.

A frequency analysis was performed to determine if the proposed filter threshold would remove the high frequency variation from the velocity trend without oversmoothing the data. This would preserve as much real variation as possible while eliminating variation that results from noise in the displacement data. A fast fourier transform was performed on the entire velocity data set. This analysis yields the distribution of frequencies of variation within the data. The results of this analysis are shown in Figure 6-3.

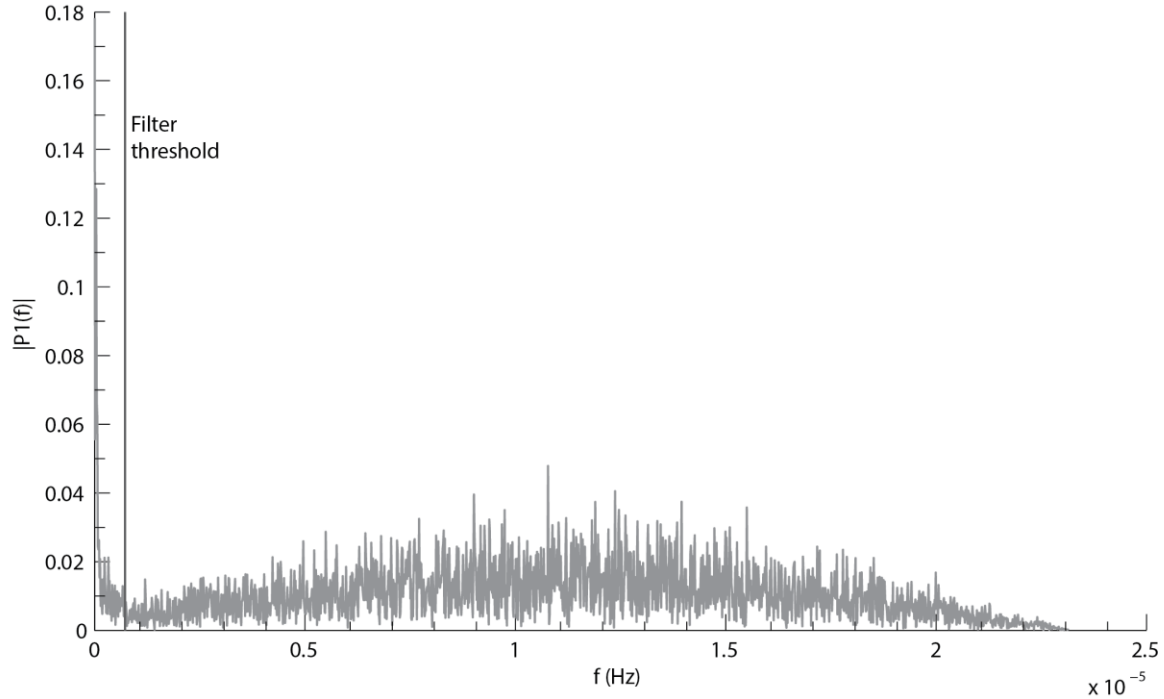


Figure 6-3 Fast fourier transform of instantaneous landslide velocity calculated from 6-hour SAA readings from BH13-02 using Equation 6-1

This frequency analysis was repeated for a period of landslide inactivity in 2014. This period of inactivity is highlighted in Figure 6-1. The frequencies of variation observed during this period are not changes in landslide activity as the landslide is inactive during this period. The results of the frequency analysis on this period is shown in Figure 6-4.

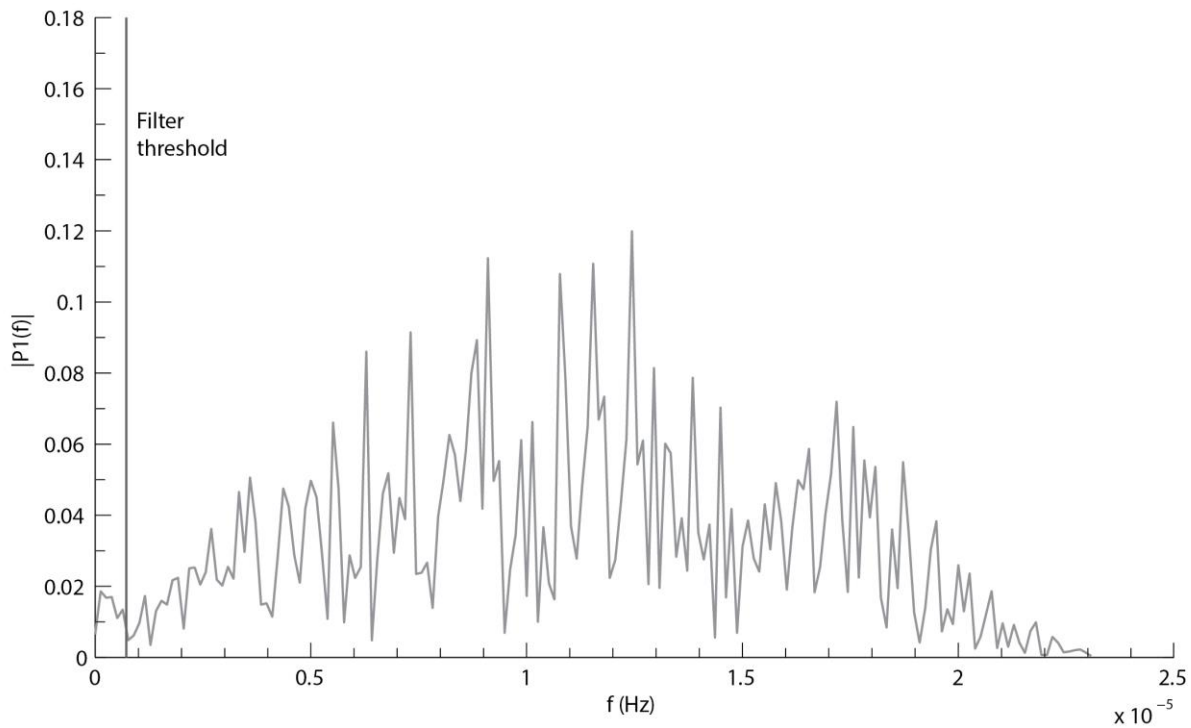


Figure 6-4 Fast fourier transform of landslide velocity during period of landslide inactivity in 2014 (Figure 6-1)

The frequencies higher than the proposed filter threshold lines in Figure 6-3 and Figure 6-4, were observed in both the entire data set as well as the period of inactivity. It can be concluded that these variations are not actual variations in the landslide velocity as they were present when the landslide velocity is constant during an inactive period. The proposed filter threshold lines are plotted at a frequency of 7.2×10^{-7} Hz which corresponds to a period of 16-days. Figure 6-5 shows the velocity trend calculated according to Equation 6-1 with the exception that the

displacement trend was smoothed using a 16-day moving average before the velocity was calculated.

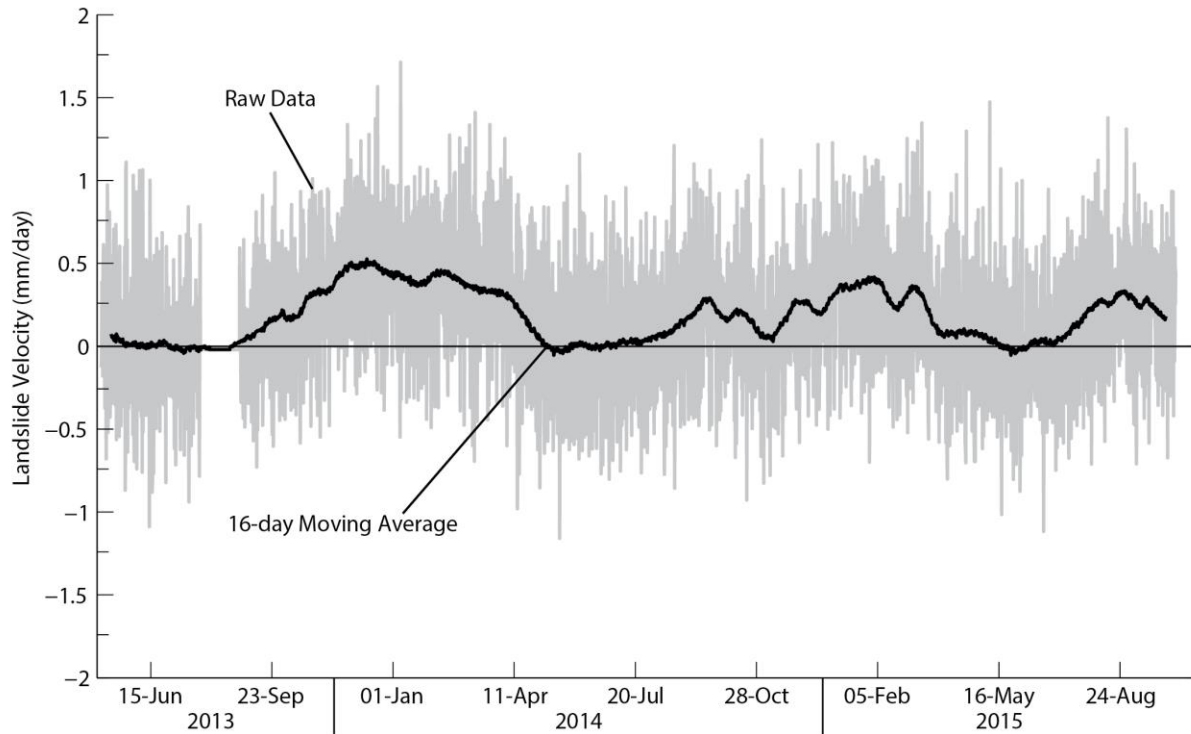


Figure 6-5 Instantaneous landslide velocity calculated from the 16-day moving average of 6-hour SAA readings from BH13-02

The filtered velocity trend from Figure 6-5 can be considered to be representative of the landslide activity on the primary rupture surface.

6.2 Interaction of the Thompson River and the Ripley Landslide

As previously mentioned, the Thompson River has been hypothesized to be a major factor in the stability of the landslide (Bunce and Chadwick 2012, Macciotta et al. 2014, Hendry et al. 2015). Insight into the mechanism by which the Thompson River influences the stability of the Ripley Landslide can be gained through analysis of the monitoring data from the 2013 investigation.

To visualize the effects of the river on the landslide, the landslide can be thought of as a block with weight and boundary forces acting upon it (Figure 6-6). The imbalance of these forces (F_s) is the cause of the landslide instability. A change in the river elevation must increase or decrease F_s to have an effect on the stability of the slope.

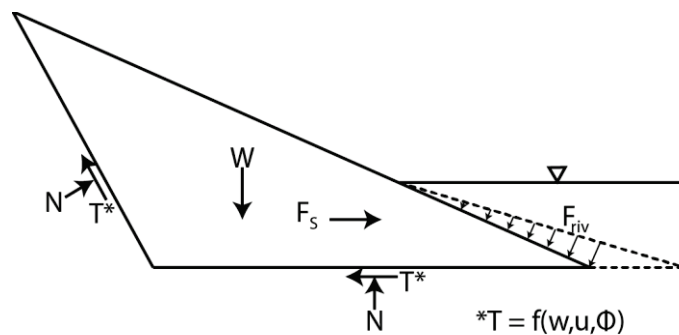


Figure 6-6 Forces acting on the landslide mass that produce a net instability (F_s)

A change in river elevation can have various effects on the landslide itself. Some of these effects depend on the permeability of the soils and drainage conditions in the landslide. These effects include the following and are shown in Figure 6-7:

- 1) Increased lateral resistance from the fluid force exerted by the river ($F_{riv,L}$).
- 2) Total stress change in soil below the river from the vertical component of the river fluid force.
- 3) Changes to pore pressures along the rupture surface (depends on permeability).
- 4) Infiltration of river water into the landslide mass changes weight of landslide (depends on permeability).

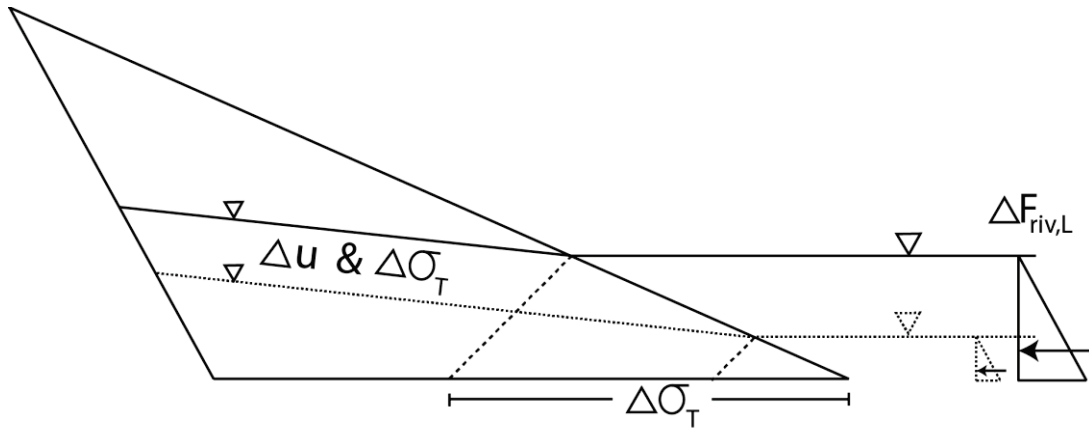


Figure 6-7 Changes to landslide mass caused by variation in the river elevation adjacent to the landslide

The permeability of the soils in the landslide affects the pore pressure caused by changes in the river elevation. These pore pressure changes in the landslide can be divided into two parts: 1) stress induced changes and 2) changes in the phreatic surface.

Pore pressures due to total stress change are determined using Skempton's B parameter which is linked to soil permeability (Skempton 1954). A low permeability soil will have a pore pressure response closer to the full amount of total stress change applied. Conversely, a high permeability soil will have a much smaller change due to the same change in total stress.

The changes in the phreatic surface are determined by how quickly water infiltrates or drains from the soil and subsequently changes the saturation of the soils around the phreatic surface. This change in saturation affects the total stress and pore pressures in that area of the landslide. This mechanism is shown for the river rising and the river falling in Figure 6-8.

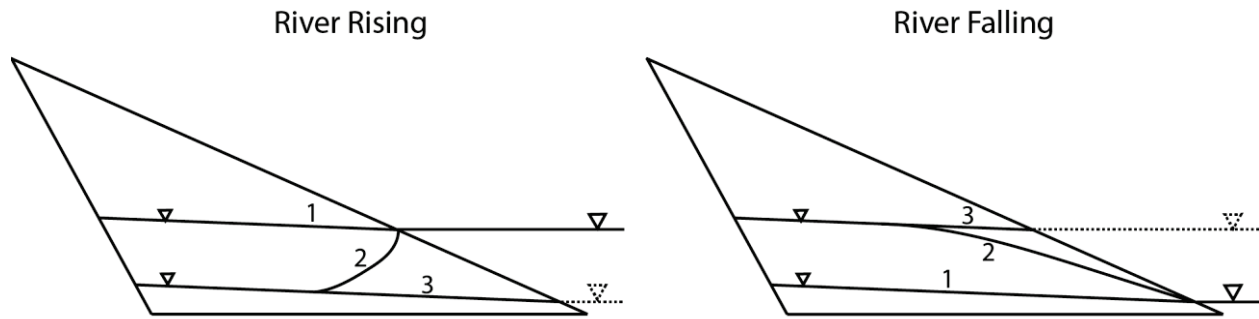


Figure 6-8 Phreatic surface resulting from an increase and decrease in river level for a landslide mass with (1) high permeability, (2) moderate permeability, and (3) very low permeability.

At the Ripley Landslide, the permeability of Unit 2 has been estimated to be 5×10^{-9} m/s for lateral flow and 5×10^{-10} m/s for vertical flow (Bishop 2008). Eshraghian et al. (2008) estimated the permeability of Unit 2 to be 1.8×10^{-11} m/s. Pore pressure changes in this layer would most likely be due to total stress change as the permeability is very low and this layer would behave as undrained. The till overlying Unit 2 was previously estimated to have a permeability of 5×10^{-7} m/s (Bishop 2008). There is also evidence in prairie region tills where fractures and weathering can cause a 3-order of magnitude increase in bulk permeability (Hendry 1982). Based on this it is likely that water from the river is able to move into and out of this layer over time.

When the river level adjacent to the Ripley Landslide increases, the loading of the river will increase the total stress at the shear surface, and cause an undrained response in Unit 2 increasing pore pressures along the shear surface. Assuming Skempton's B for Unit 2 is less than one, the increase in total stress will be greater than the increase in pore pressures, leading to an increase in effective stress. This increase in effective stress will increase the available shear strength along the shear surface. There will also be an increase in lateral resistance from the river.

Infiltration occurs into the sediments overlying Unit 2 while the river elevation is high. This further increases the total stress and pore pressures on the shear surface. This means that the available shear strength along the shear plane will gradually decrease while the river is high and the landslide is inactive. The weight of the landslide also increases as a result of this infiltration.

When the river level adjacent to the Ripley Landslide decreases, the pore pressures along the shear surface decrease immediately as a result of unloading. The lateral resistance from the river also decreases. The pore pressures which developed as a result of the water infiltration logically takes longer to change as drainage is required. This is the period where the landslide starts moving.

This mechanism explains the differences in movement for the river rising and the river falling. Hendry et al. (2015) observed a hysteresis between the river rising and river falling in the landslide velocity as a function of river elevation. The difference is a result of the seepage of water into the landslide mass. The difference in saturation changes for river rising and river falling can be seen in Figure 6-8. These different saturation profiles result in different stresses along the shear surface for the same river level and a change in the out of balance forces which lead to movement.

This mechanism also explains the trend observed by Eshraghian et al. (2005) where extended periods of high flow in the summer result in higher movements in the following winter. This increased movement is a result of more water which would have infiltrated the landslide during the extended period of high flow. This is the essence of the rapid drawdown mechanism.

This drawdown mechanism consists of two parts: (1) the effect of the river and (2) the seepage related changes in the landslide. The effect of the river incorporates undrained total stress

response along the shear plane and the lateral resistance exerted by the river. Seepage related changes include the changing phreatic surface due to the infiltration of water and the forces exerted on the landslide mass by the seepage of water. Separating these effects will provide insight into the factor dominating the landslide velocity.

6.3 Evaluating the proposed rapid drawdown mechanism of the Ripley Landslide

The effect of the river can be evaluated by comparing the landslide velocity to the river flow. The landslide velocity using the 16-day moving average was determined for the time period May 5, 2013 to November 19, 2015 in Figure 6-5. The volumetric flow of the Thompson River measured at Spences Bridge was then determined using the same 16-day moving average interval and time period. The results are plotted in Figure 6-9 and show that the landslide velocity increases significantly when the Thompson River flow is below 1034 m³/s. At this flow the river level at the Ripley Landslide is at Elevation 265.9 m.a.s.l. (see Figure 4-6).

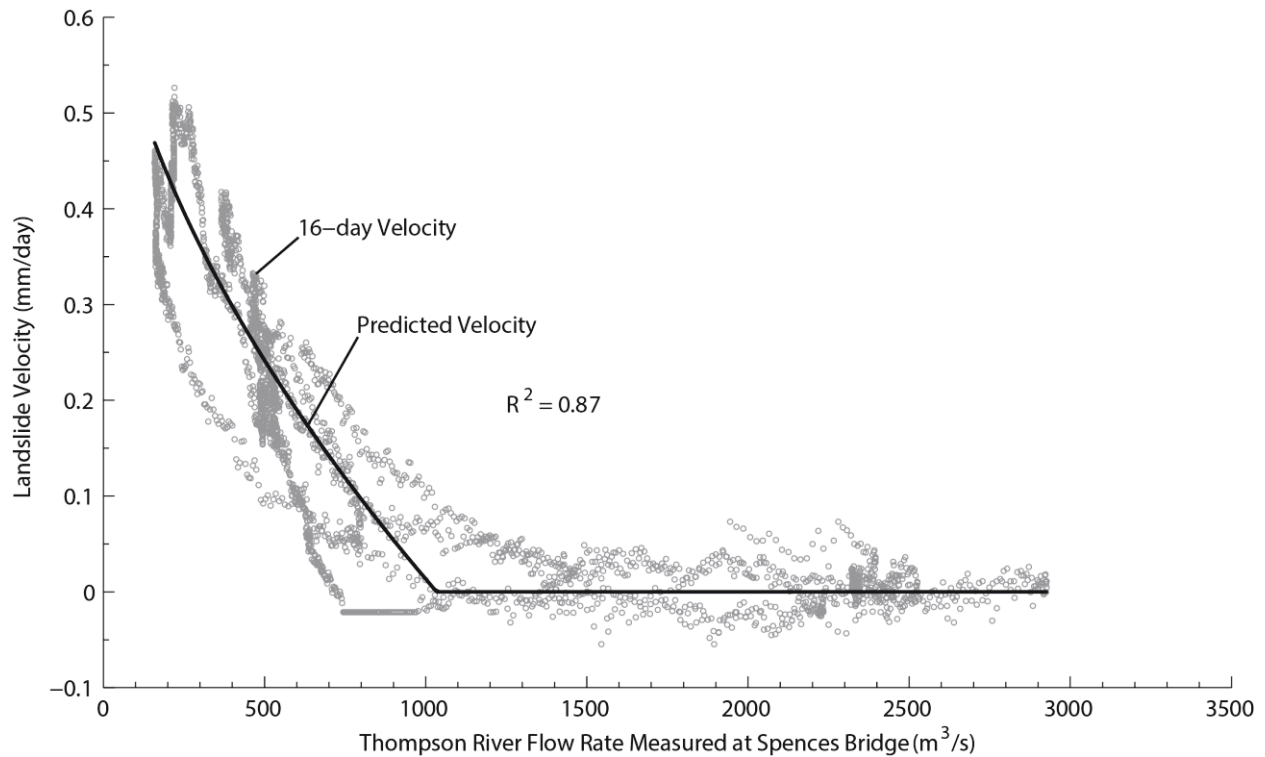


Figure 6-9 Trend of 16-day velocity with volumetric flow of the Thompson River as measure at Spences Bridge

The trend line in Figure 6-9 can be expressed as:

$$v'_n = (-0.164) * \left(\sqrt[1.78]{\left(\frac{Q}{74.1}\right)} - 4.4 \right) \quad \text{for } Q < 1034 \text{ m}^3/\text{s} \quad [6-2]$$

$$v'_n = 0 \quad \text{for } Q > 1034 \text{ m}^3/\text{s}$$

where; v'_n = anticipated velocity at timestep n ($\frac{\text{mm}}{\text{day}}$);

Q = volumetric flow of the Thompson River measured at Spences Bridge ($\frac{\text{m}^3}{\text{s}}$)

At any date, the landslide velocity can be estimated from Equation 6-2 using the Thompson River flow measured at Spences Bridge.

The displacements predicted by integrating the velocity trend illustrated in Figure 6-9 for a given time period can be seen in Figure 6-10a (July 1, 2013 to July 1, 2014) and Figure 6-10b (July 1, 2014 to July 1, 2015). The period of these figures was divided from July 1 to July 1 as this encompasses one season of landslide activity.

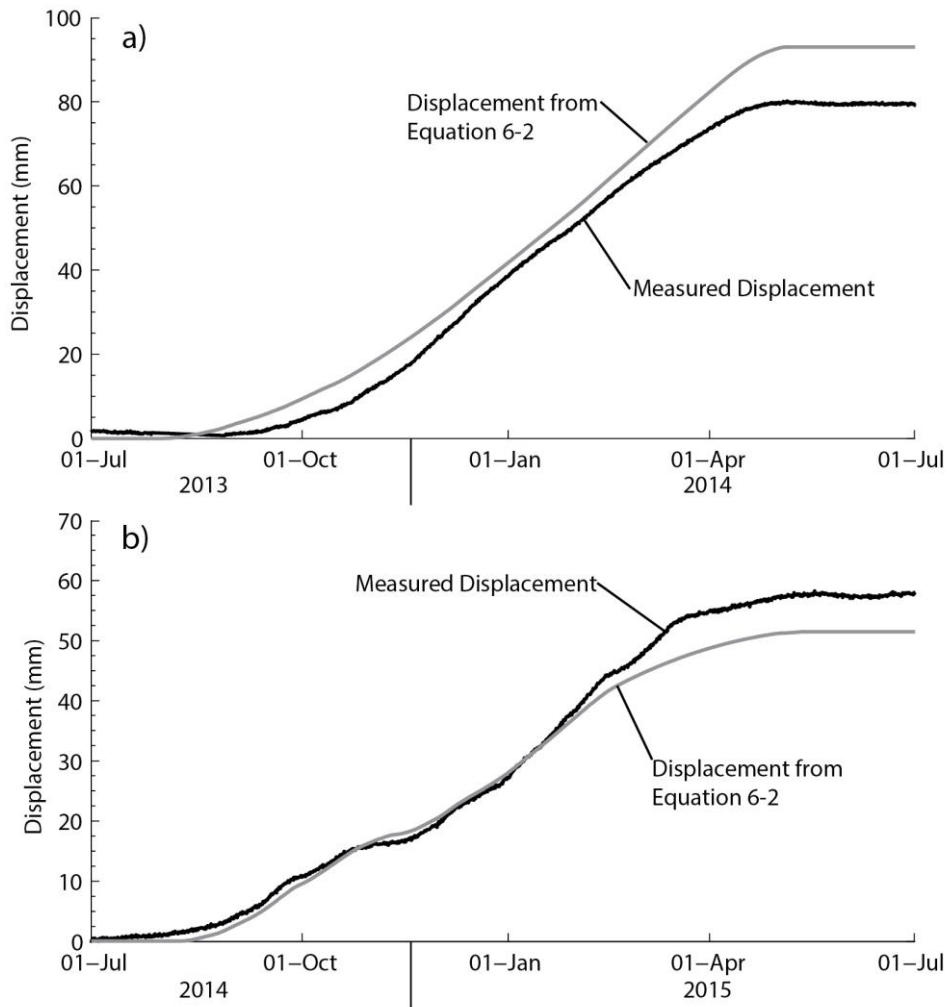


Figure 6-10 Displacements predicted based on river flow variation and the velocity trends presented in Figure 6-9 for the periods of July 1, 2013 to July 1, 2014 (a) and July 1, 2014 to July 1, 2015 (b)

A strong correlation between the river flow and the displacements of the Ripley Landslide is shown in Figure 6-9. This indicates that the river plays a significant role in the mechanism which controls the stability of the Ripley Landslide. This relationship is potentially useful as a risk management tool due to the readily available and reliable river discharge data.

The seepage related element of the drawdown mechanism can also be assessed. There are sufficient pore pressure measurements taken at the Ripley landslide to quantify the pore pressure changes related to the seepage of river water into the landslide mass. Differential pressure (DPr_n), a parameter that varies as a function of the drawdown effect, is defined as:

$$DPr_n = E_{SZ,n} - E_{River,n} \quad [6-4]$$

where;

DPr_n = differential pressure at time “n” (m)

$E_{SZ,n}$ = piezometric elevation of shear zone at time “n” (m.a.s.l.)

$E_{River,n}$ = elevation of Thompson River surface adjacent to the Ripley

Landslide at time “n” (m.a.s.l; from Equation 4-1)

The differential pressure is a measure of the difference between the pore pressures within the landslide mass and the buttressing effect of the river. Differential pressure also captures any undrained pore pressure changes resulting from river level fluctuation. This parameter will vary over time as the river levels and pore pressures change seasonally. When the river drops quickly and the seepage related pore pressures dissipate over time this will result in a high differential pressure immediately following the river level decrease.

The landslide movements were divided into the same seasons as presented in Figure 6-10 to minimize the effect of changes in other influencing factors such as changes in bathymetry or

other unknown factors. Figure 6-11 presents the relationship between the 16-day landslide velocity and the differential pressure for those seasons of movement. It should be noted that the trend in Figure 6-11c represents a partial year and the trend line may not be representative of the full year of displacement readings.

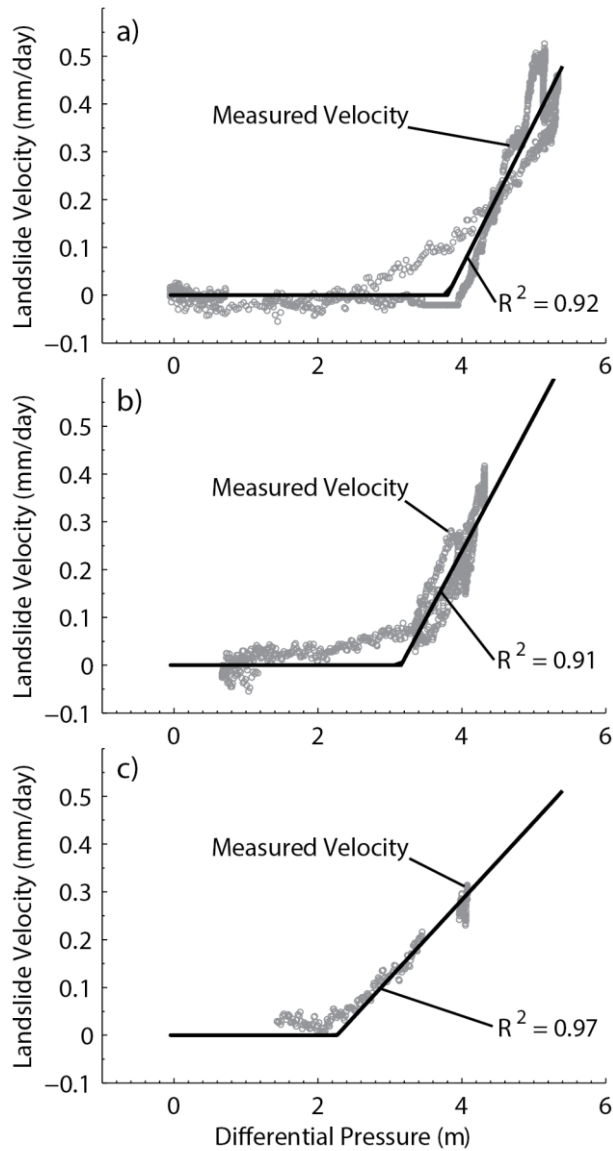


Figure 6-11 Landslide velocities for the movement seasons starting in 2013(a), 2014(b), and 2015(c) at the Ripley Landslide as a function of differential pressure as defined by Equation 6-4.

The trend lines in Figure 6-11 are given by:

$$v''_n = (DPr_n - a) * (b) \quad \text{for } DPr_n > a \quad [6-5]$$

$$v''_n = 0 \quad \text{for } DPr_n < a$$

where; v''_n = anticipated landslide velocity at timestep n $\left(\frac{\text{mm}}{\text{day}}\right)$;

DPr_n = differential pressure from Equation 6 – 4 at timestep “n” (m)

a = threshold differential pressure (m)

b = slope of landslide velocity trend

The values for the trendlines in Figure 6-11 are given in Table 6-1.

Table 6-1 Equation coefficients and coefficients of correlation for the trend lines in Figure 6-11

Season of Displacement	a (m)	b	R ²
July 2013 to July 2014	3.8	0.30	0.92
July 2014 to July 2015	3.2	0.28	0.91
July 2015 to December 2015 (partial year)	2.3	0.16	0.97

Splitting this trend into individual years and correlating to differential pressure increased the R² value for all cases when compared to the general trend in Figure 6-9 (R² = 0.87). The trends as a

function of river level should be recalculated on a season to season basis to determine the actual improvement of using differential pressure in place of river level.

Figure 6-12 presents the relationship between the 16-day landslide velocity and the river elevation for the previously defined seasons of movement. The river elevations were plotted in reverse order so the shape of the trends could be easily compared to those in Figure 6-11. It should be noted again that Figure 6-12c is a partial year of displacement readings.

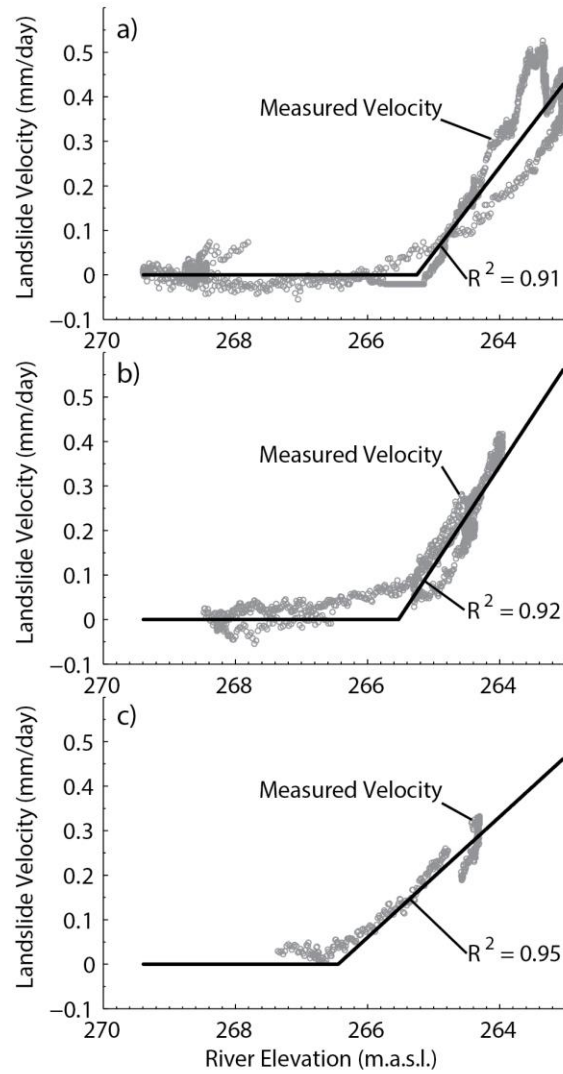


Figure 6-12 Landslide velocities for the movement seasons starting in 2013(a), 2014(b), and 2015(c) at the Ripley Landslide as a function of river elevation

The trendlines for landslide velocity in Figure 6-12 can be expressed as:

$$v'''_n = (c - E_{\text{river},n}) * (d) \quad \text{for } E_{\text{river},n} < c \quad [6-6]$$

$$v'''_n = 0 \quad \text{for } E_{\text{river},n} > c$$

where; v'''_n = anticipated velocity at timestep n $\left(\frac{\text{mm}}{\text{day}}\right)$;

$E_{\text{river},n}$ = Thompson River elevation at the Ripley Landslide
at timestep "n" (m. a. s. l)

c = threshold river elevation (m.a.s.l.)

d = slope of landslide velocity trend

The values for the trend lines in Figure 6-12 are summarized in Table 6-2.

Table 6-2 Equation coefficients and coefficients of correlation for the trend lines in Figure 6-12

Season of Displacement	c (m)	d	R ²
July 2013 to July 2014	265.3	0.19	0.91
July 2014 to July 2015	265.5	0.23	0.92
July 2015 to December 2015 (partial year)	266.4	0.14	0.95

The trends of landslide velocity with river level showed a similar improvement in correlation when split into multiple years. There was no significant improvement in correlation when considering the difference between the river elevation and the pore pressures measured along the shear plane at BH13-02 (Figure 3-3).

Based on the lack of improvement in correlation, there are two possible conclusions: (1) the seepage related changes to the landslide mass are not a significant factor controlling the overall

landslide stability, or (2) differential pressure is not an appropriate parameter to represent the seepage related effects on landslide stability.

Another conclusion of this analysis is that dividing the trends of landslide velocity and river elevation into separate years improved the correlation. Based on this improvement, there are factors which affect this relationship that change on a yearly basis. It is likely that the general trend presented in Equation 6-2 will need to be updated in the future as these changes continue.

6.4 Factors affecting pore pressure in the Ripley Landslide

Despite the lack of benefit when considering pore pressures in Section 6.3, the artesian pressures at the Ripley Landslide are undoubtedly related to the stability issues. Pore pressures are more difficult to monitor than river elevation as they require boreholes for instrument installation and these instruments are costly to replace when they stop functioning. Relating the measured pore pressures to various external factors which are easier to monitor would be very beneficial for the long term prediction of movement trends of the Ripley Landslide as well as other landslides in the valley. Understanding what factors control pore pressure variation within the landslide is also an essential step in estimating the effectiveness of any remedial measures involving the reduction of pore pressures.

6.4.1 The Ripley Landslide as part of a regional groundwater flow basin

The Ripley Landslide is located at the topographical low region of a large valley (Figure 6-13). Bishop (2008) modeled the Thompson River Valley as a regional groundwater system and concluded that pore pressures within the glaciolacustrine silt and clay are not significantly affected by the fluctuation of the Thompson River stage as maximum change in pressure head observed throughout the model simulation within this unit was less than one centimetre. Bishop

(2008) also concluded from modelling that the regional flow regime is capable of generating elevated pore pressures in the glaciolacustrine silt and clay, fractured bedrock and bedrock units in the lower region of the valley near the Thompson River but that these artesian pressures in the Thompson River Valley were difficult to predict with accuracy. Nonetheless, Bishop's modelling did demonstrate that the flow and pore pressure in the vicinity of the Thompson could be influenced by the regional flow system and that the landslide areas in the Thompson River are located in a discharge zone of a regional groundwater flow system. The upward gradient which was previously observed at the toe of the Ripley Landslide (Hendry et al. 2015) and at other landslides in the Thompson River valley (Eshraghian et al. 2008) is a characteristic trait of discharge zones (Toth 1962).

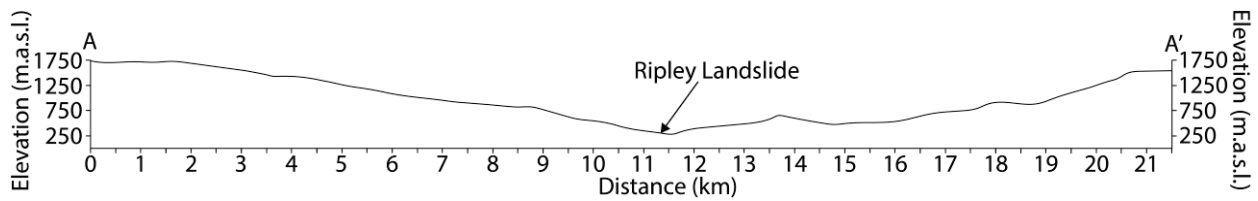


Figure 6-13 Regional map of the Thompson River valley and cross section A-A' centred at the Ripley Landslide (image and profile from Google Earth 2015)

To confirm the regional flow of groundwater at the Ripley Landslide, isotope samples were taken during the 2015 site investigation. Approximately 300 mm from the bottom of every core run was cut and trimmed to remove any contamination from drilling fluid. The samples were analyzed using a Picarro L1102-I isotopic water liquid analyzer. The method for laboratory sample preparation and testing follows the methodology presented in Hendry et al. (2013).

Figure 6-14 shows one of the isotopes tested as a function of depth. It appears that there is very little mixing occurring and the isotopes within the clay are quite consistent with depth. If water

was seeping upward (as the upward gradient would indicate) we would expect to see some sort of gradual slope as the enriched water from the bedrock mixes with the water in the clay. This lack of apparent mixing indicates that despite the upward gradient, there is very little upward flow of water from the bedrock into the clay.

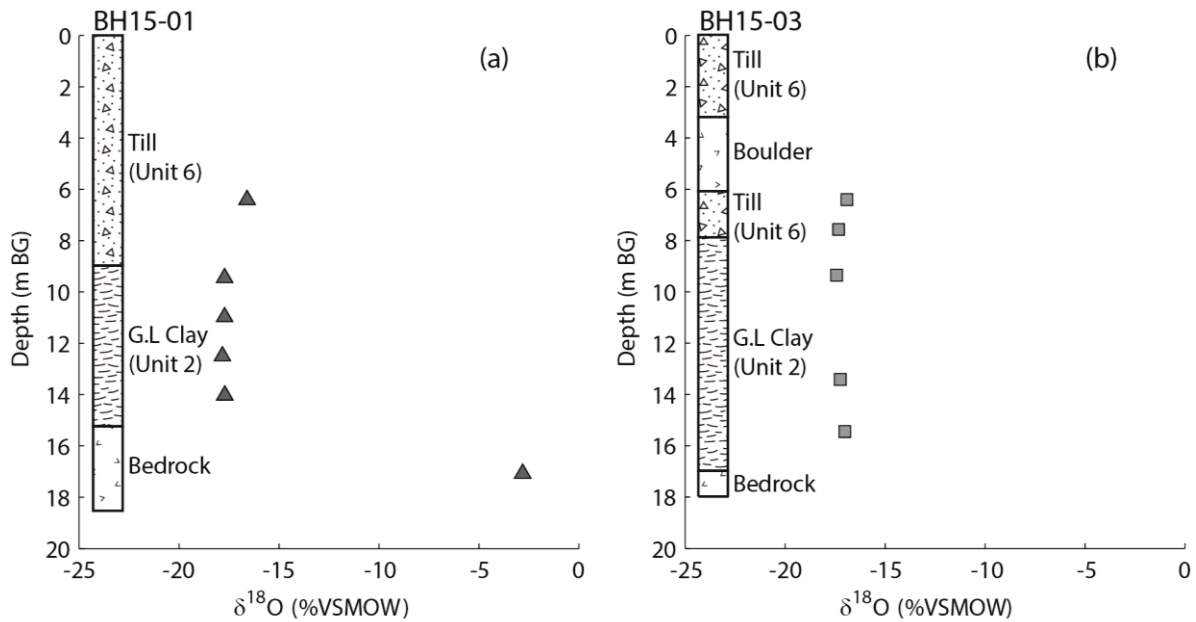


Figure 6-14 Isotope testing results with depth from BH15-01 (a) and BH15-03 (b) taken during the 2015 investigation of the Ripley Landslide (testing performed by Erin Schmeling)

When plotted with depth there is a slight enrichment curve observed in Figure 6-14a at 6-9 m below grade (BG). It is possible that this is representative of mixing with precipitation seeping from the ground surface. The precipitation in the Thompson River valley is less depleted than the water which was found in the clay (Bowen 2015). This is what causes the shallower samples to be slightly more enriched as the water in the till mixes with the precipitation that infiltrates over time.

The results from Figure 6-14 are compiled on a co-isotope plot in Figure 6-15. There is a significant difference in the isotope results of the water found within the bedrock compared to the other samples from within the glaciolacustrine clay. The enrichment of the water in the bedrock is likely the result of mineral transfer occurring as the water flows through fractured rock. This indicates that the water present in the bedrock has flowed a significant distance through the fractured bedrock layer. It is quite clear based on the topography and isotope data that there is a regional groundwater flow system that is affecting the landslide.

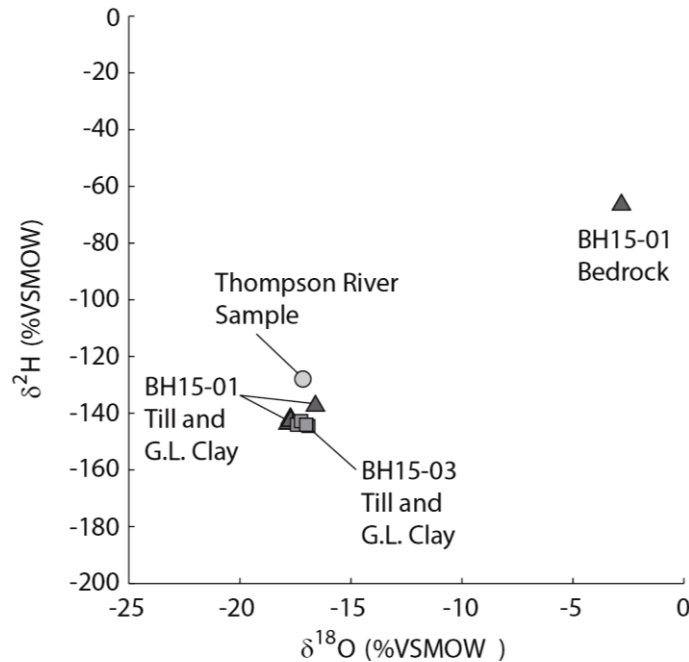


Figure 6-15 Co-isotope plot of testing results from the Ripley Landslide
(testing performed by Erin Schmeling)

6.4.2 The effects of river level fluctuation on pore pressures at the Ripley Landslide

The pore pressure and river level monitoring since 2013 has allowed for the real time comparison of the pore pressures within the landslide and river elevation. Bishop (2008), based on groundwater modelling, concluded that the fluctuation of the river had little to no effect on the pore pressures within the bedrock (less than 6 cm change in head). Figure 6-16 shows the seasonal variation of the river level by approximately seven metres during the monitoring period.

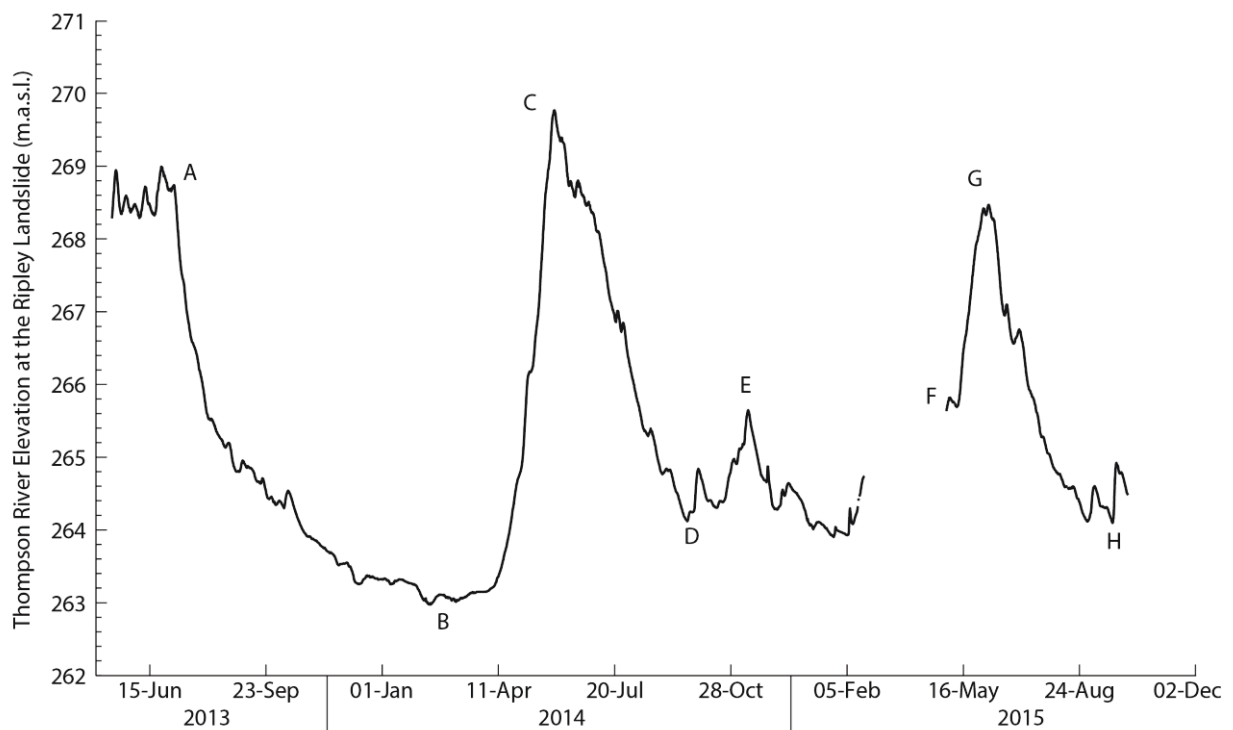


Figure 6-16 Seasonal variation of Thompson River elevation at the Ripley Landslide

Figure 6-17 shows the variation of the bedrock pore pressure as a function of river elevation. The seasonal changes in river elevation correspond to changes in bedrock pressure of approximately 2 m (A to B, C to D, and G to H). The trend has linear and parallel sections from A to B and from C to D. The linear trend shown in the figure is parallel to these linear sections. The pore pressures in Figure 6-17 can be expressed as:

$$E_{BRt,n} = E_{BRr,n} + 177 + 0.35 * E_{river,n} \quad [6-3]$$

where; $E_{BRt,n}$ = total bedrock pressure at time “n”

$E_{BRr,n}$ = regional bedrock pressure at time “n”

$E_{river,n}$ = river elevation at time “n”

The section of the trend from G to H appears to have a steeper slope and the cause of this variation is unknown. Nonetheless, the trend shows a strong correlation between the recorded pore pressures in the bedrock and the Thompson River elevations suggesting that the river is a significant factor controlling pore pressures in the bedrock.

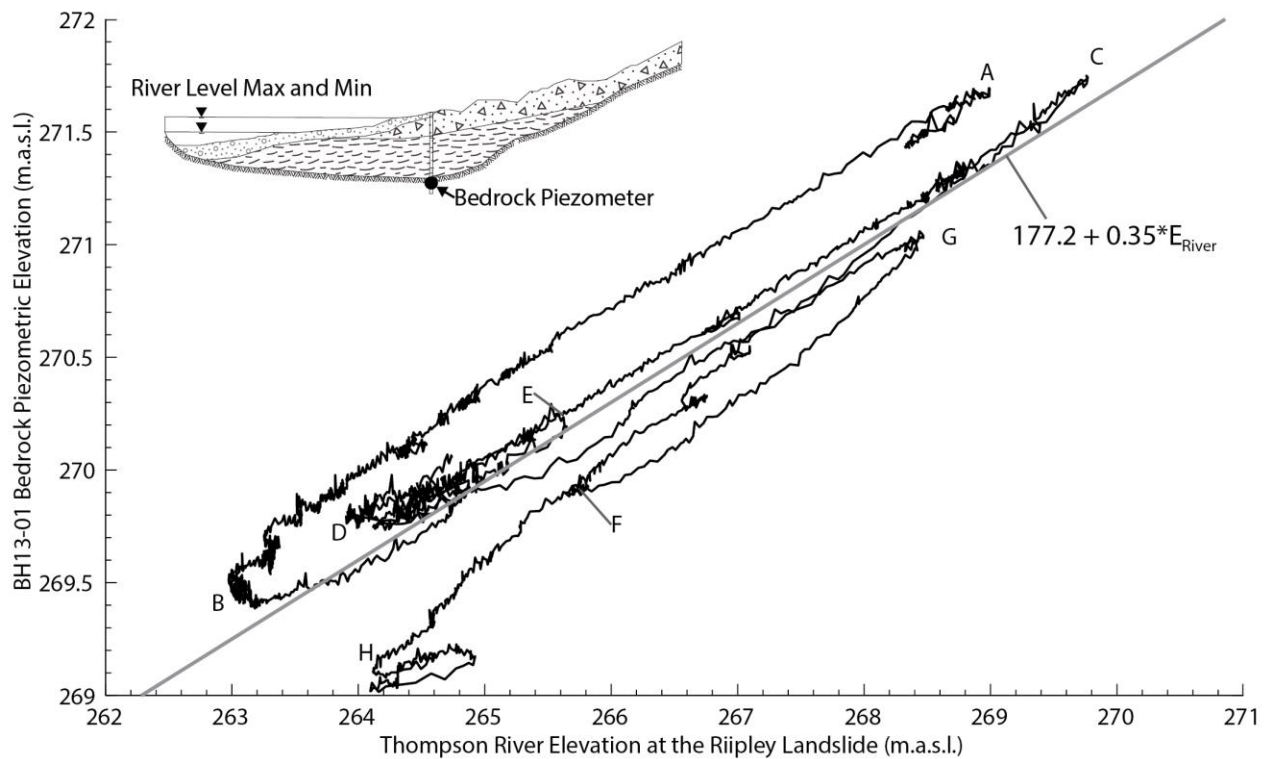


Figure 6-17 Variation of bedrock pressure as a function of river elevation

The Thompson River elevation at the Ripley Landslide varied between 263.0 m.a.s.l. and 269.8 m.a.s.l. during the monitoring period. The bedrock pore pressures had a range of 269.1 m.a.s.l. to 271.7 m.a.s.l. over the same monitoring period. Transient seepage modelling performed by Bishop (2008) predicted bedrock pore pressure changes of 6 cm in response to seasonal river level change which is nearly two orders of magnitudes lower than the observed pore pressure variation.

Assuming the river is causing changes in the bedrock pressure according to the linear trend in Figure 6-17, the non-linear portions of this trend could be the result of changes in regional groundwater system boundary conditions (e.g. precipitation, irrigation). In this case, seasonal variation or correlation with regional weather patterns is expected. These non-linear pressures could also be the result of seepage of river water into the landslide mass as discussed in Section 6.2. In this case, the non-linear pressures would be expected to correlate very strongly with the river levels and have some time lag.

The non-linear bedrock pressures can be determined by calculating the departure from the linear trend (Figure 6-17) given by Equation 6-3. Figure 6-18a shows the bedrock pore pressure varying with time with the apparent effect of the river elevation removed. The trend in Figure 6-18a represents the changes in bedrock pressures not related directly to the river. Figure 6-18b shows the river elevation change over the same period.

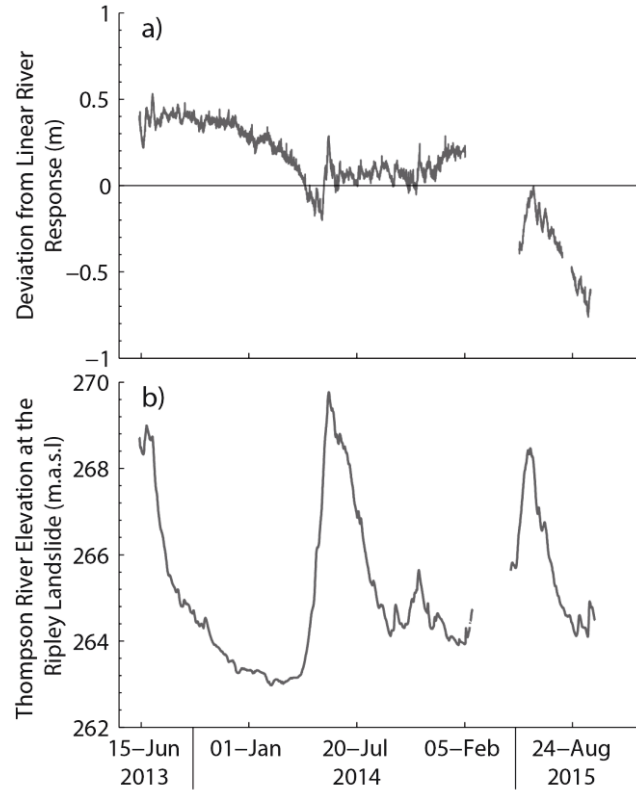


Figure 6-18 Deviation of bedrock pressures from linear river response over time as defined by Equation 6-3 (a) and Thompson River elevation adjacent to the Ripley Landslide with time (b)

The trend in Figure 6-18 shows a generally seasonal variation. This seasonal variation appears to have a low point each year in April to May with a generally parabolic shape. The increase in non-linear pressures from April to September occurs during the months where the spring melt begins and precipitation occurs as rain. The non-linear pressures then gradually decrease through the winter months until the low point in the following April.

The peaks in the non-linear pressures are relatively concurrent with peaks in river level variation at the landslide. This correlation to river elevation is evidence of the effects of seepage into the landslide but there are certain areas which indicate there are other mechanisms at work. In early 2014 the river levels were lower than they were in early 2015. This should result in more water

being trapped in the landslide and higher non-linear pressures in 2015. The non-linear pressures were actually significantly lower in 2015. This seasonal difference in non-linear pressures cannot be explained based on seepage alone.

The year to year differences in the range of this seasonal variation are likely also a function of the net recharge in the regional basin. The variables controlling this net recharge would likely include irrigation, the depth of snowpack, the rate of snowpack melt, and the amount of rainfall in the regional basin.

Irrigation within the region was also a factor considered in the groundwater modelling considered by Bishop (2008). Bishop found that changing the amount of irrigation did not significantly affect pore pressures. The amount of surface water used for irrigation is allocated and regulated by the B.C. Government (Province of British Columbia 2015). The actual amount used each year may vary but this regulation would remove some of the year to year variability inherent in weather trends such as precipitation. For these reasons, changes in irrigation in the upland area were not considered to be a major contributor to the year to year variability in regional pressures.

The drop in these non-linear pressures in 2015 should correspond to a lower amount of net recharge in the regional basin based on the work by Bishop (2008). In 2015 the Nicola region, which includes the upland area East of Ripley, was given a Level 4 drought classification. This is the highest drought classification which the B.C. government can declare (Province of British Columbia 2015). While the lower pressures in 2015 do suggest that regional climate controls these non-linear pressures, further correlation with weather data would be required to confirm this.

6.4.3 Analysis of weather data and its effects on regional bedrock pressures

Weather data within the recharge area of the regional basin is not available for the current monitoring period. A proxy weather station was not able to be used as the differences in temperature and precipitation were significant between the recharge area and other stations.

The Logan Lake weather station (Environment Canada 2015) is the best representation of the conditions in the recharge zone. It is located on the upland plateau adjacent to the Thompson River Valley. The location of Logan Lake relative to the Ripley Landslide is shown in Figure 6-13.

This station stopped reporting weather data in 2005. Data from years prior to the closing of the station can be examined to see if the typical seasonal trends in climate are concurrent with the seasonal trend from Figure 6-18 or staggered by some consistent time lag. This is assuming that the trend is fairly consistent from year to year.

Figure 6-19a shows the non-linear bedrock pressure trends from the Ripley Landslide in 2014 for reference. Figure 6-19b, Figure 6-19c, and Figure 6-19d show the yearly trends in mean daily temperature, precipitation, and snowfall, respectively, for 2003 and 2004 at the Logan Lake monitoring station (Environment Canada 2015).

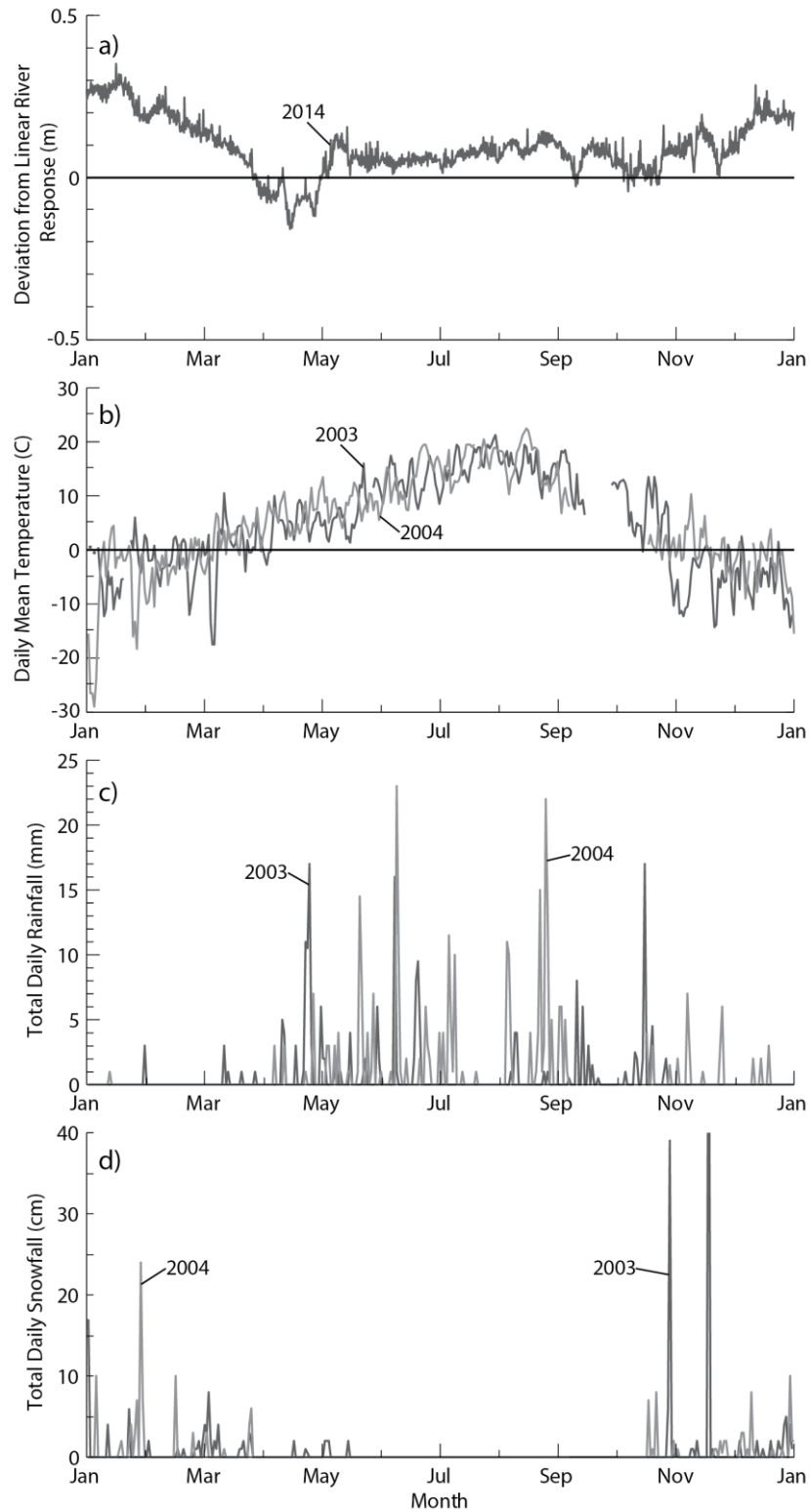


Figure 6-19 Non-linear pore pressures at the Ripley Landslide over time (a) and seasonal trends in temperature (b), rainfall (c), and snowfall (d) at Logan Lake

When considering the climate trends in Figure 6-19 it appears that the increases in non-linear pressures occurs approximately one month after the temperatures are consistently above freezing. The early periods of rainfall likely are falling on snowpack and would have a compound effect on the recharge rate into the regional groundwater basin. This correlates to a sharp upward spike in the non-linear pressures. Based on a visual comparison, the non-linear portions of the bedrock pressures are partially the result of changes in the recharge of the regional groundwater basin. It appears that there is approximately a one month lag between changes in the recharge zone and a corresponding change in pore pressures at the Ripley Landslide. The exact time lag cannot be confirmed without weather monitoring data concurrent with the pore pressure monitoring which is an area of possible future research.

6.5 Summary

The monitoring data from the Ripley Landslide has allowed for a more detailed analysis of the landslide behaviour. Continuous monitoring of displacements has allowed for calculation of landslide velocity as a function of time. These rates were then correlated to pore pressures and river levels to better understand the mechanism of the landslide. This analysis has lead to the following conclusions:

- 1) Displacements filtered to a 16-day moving average produced a landslide velocity trend that was representative of landslide activity along the primary rupture surface.
- 2) River elevation was inversely correlated to landslide velocity with a coefficient of correlation of 0.87.
- 3) The parameter differential pressure, used to represent the previously hypothesized drawdown mechanism, did not improve the correlation with landslide velocity when compared to the correlation with river flow.

- 4) The Ripley Landslide is located within the discharge zone of a regional groundwater flow system.
- 5) The river elevation has an apparent linear effect on pore pressures within the Ripley Landslide.

7 Summary and Recommendations

7.1 Summary

In this thesis, the Ripley Landslide in the Thompson River Valley near Ashcroft, British Columbia was investigated to better understand the instabilities which are common in that region. A site investigation and monitoring program were carried out as part of this research in February 2015. The information obtained during this 2015 investigation was combined with information from two previous site investigations to better understand the geology and behaviour of the Ripley Landslide.

The instrumentation results from the investigation in May 2013 were measured using technology that had not been used in this region previously. Monitoring data were analyzed to ensure that the readings from these instruments were representative of the landslide behaviour. Following this analysis it was concluded that the pore pressure monitoring data were correct but required compensation for barometric variation. The displacement data were determined to be representative of relative magnitude of landslide activity in a given period. A rating curve was also developed for the site to determine the elevation of the Thompson River at any given time based on flow measurements downstream at Spences Bridge.

The displacement data from the three site investigations and the GPS surface monitoring system on the site were analyzed to better understand the kinematics of the Ripley Landslide. This analysis showed that there were two active zones of movement. A deeper translational block in Unit 2 and a shallower failure in the till were identified based on the displacement results and tension cracks observed on the surface. This improved understanding of landslide kinematics and

the drilling information from all investigations was then incorporated into cross sections of the landslide.

Finally, the relationship between landslide velocity, pore pressures, and the Thompson River elevation was investigated. The landslide velocity and pore pressures in the landslide both correlated very strongly with the river level. The influence of other factors such as seepage of water into the landslide mass and regional climate variation were also identified. The Ripley Landslide was also determined to be located in the discharge zone of a groundwater flow system.

7.2 Contributions of the Thesis

The main contributions of this thesis to the studied subject are as follows:

- Validation of monitoring data obtained using fully grouted piezometers and Shape Accel Array on a moving landslide (Chapter 4).
- A rating curve was developed for determining the elevation of the Thompson River at the Ripley Landslide based on flow measurements taken at Spences Bridge (Chapter 4).
- Establishing the influence of the bedrock profile on the lateral extent and the possibility of retrogression (Chapter 5).
- Improved cross sections of the Ripley Landslide based on all available geology and displacement data (Chapter 5).
- Identified a shallow failure occurring in the central portion of the Ripley Landslide (Chapter 5).
- Calculated a continuous velocity trend of the Ripley Landslide based on high frequency displacement readings (Chapter 6)

- Found inverse correlation between the river flow and velocity of the Ripley Landslide (Chapter 6).
- Recognized the effect of river level fluctuation, seepage, and regional climate changes on the pore pressures within the Ripley Landslide (Chapter 6)

7.3 Conclusions

This research has increased our understanding of the Ripley Landslide and the other landslides in the Thompson River Valley near Ashcroft. The main conclusions of this thesis are as follows:

- The geology of the Ripley Landslide and other landslides in the region is complex. Developing cross sections requires information from multiple boreholes as bedrock and unit profiles vary laterally. An assumption of horizontal contacts is not advised given the key role that the bedrock plays in limiting the landslide extents.
- Fully grouted vibrating wire piezometers can be used to monitor pore pressures in a slow moving landslide provided the conditions allow for the validation of these results. A previously identified upward gradient would be an example of a condition where any vertical cracking of grout would be very evident. In the absence of any way of validating the monitoring results, fully grouted vibrating wire piezometers should be used with caution.
- The Ripley Landslide consists of two separate movements. The deep seated translational movement that is typical of the region is observed with a basal sliding plane in Pleistocene glaciolacustrine clay (Unit 2) at an approximate elevation of 257 m.a.s.l. A second shallower failure surface is inclined subparallel to the surface of the slope through

the Fraser glaciation till and extends upslope beyond the backscarp of the deep seated movement.

- The instability, as indicated by landslide velocity, is primarily a function of the Thompson River elevation. This strength of this relationship is a result of the lack of seepage that occurs into the landslide. This is evident as most of the pore pressure changes in the landslide can be explained directly based on the river elevation variation. As a result the variation of the river elevation is the main factor controlling slope movements.
- The pore pressures within the Landslide are controlled by multiple factors. The Thompson River variation has effects which are practically immediate in Unit 2. There are also changes related to water seeping into the more permeable layers overlying Unit 2. Finally, changes in the regional climate can have effects on the pore pressures as the Ripley Landslide is located in the discharge zone of a regional groundwater flow system.

7.4 Recommended Future Research

Several areas of the research in this thesis require additional investigation. Some of the potential areas for further investigation are as follows:

- Verify revised cross sections by logging bedding orientation in cores from the 2015 site investigation.
- Expand upon previous statistical analysis of the Thompson River and the correlations between river flow and slope displacement to determine the statistical distribution of displacements.

- Correlation of track geometry measurements taken during the monitoring period to quantify the cost and effect of slope movements on the track itself. This could then be expanded to the rest of the valley so that track geometry can be processed to assess the activity of known areas of instability and potentially discover new areas of concern.
- Use a coupled hydro-mechanical model of the Ripley Landslide to better understand the combined effects of river level variation, seepage, and regional groundwater flow. This model would be required if any remedial measures involving drainage or relieving the artesian pressure at the landslide toe were to be assessed.
- Evaluate remedial measures for the landslides in this region using a model calibrated to the displacement data. The improved understanding of the landslide mechanism and abundance of information on landslide deformation would hopefully eliminate some of the assumptions required when modelling the slope.

References

- Adeyeri, J.B. 2014. Technology and Practice in Geotechnical Engineering. Published by: IGI Global 2014. pp. 768.
- BGC Engineering Inc. 2006. THOM 54.50: Ripley Slide April 4, 2006 Monitoring Event. Memorandum dated July 20, 2006.
- BGC Engineering Inc. 2007. Thompson Mile 54.40 Landslide March 22, 2007 Site Visit Report. Memorandum dated March 24, 2007.
- BGC Engineering Inc. 2009. CPR THOM Sub Mile 54.4 (Ripley Slide) / CN Rail ASH Sub Mile 56.8 October 28, 2009 Monitoring Event. Memorandum dated December 4, 2009.
- Bishop, N.F., Evans, S.G., Petley, D.J., Unger, A.J.A. 2008 The geotechnics of glaciolacustrine sediments and associated landslides near Ashcroft (British Columbia) and the Grand Coulee Dam (Washington). *In* Proceedings of the 4th Canadian Conference on Geohazards. Presse de l'Universite Laval, Quebec, 594 p.
- Bishop, N.F. 2008. Geotechniques and hydrology of landslides in Thompson River Valley, near Ashcroft, British Columbia. M.Sc. thesis, University of Waterloo, Waterloo, Canada.
- Bobrowsky, P.T. and Dominguez, M.J. 2012. Landslide Susceptibility Map of Canada. Geological Survey of Canada, Open File 7228, scale 1:6 million. doi:10.4095/291902.
- Bowen, G. J. (2015) The Online Isotopes in Precipitation Calculator, version 2.2. <http://www.waterisotopes.org>.

- Bunce, C., and Chadwick, I. 2012. GPS monitoring of a landslide for railways. *In* Proceedings of the 11th International & 2nd North American Symposium on Landslides, Banff, Canada.
- Calvello, M., and Cascini, L. 2006. Predicting Rainfall-Induced Movements of Slide in Stiff Clays. *In* ECI Symposium Series <http://dc.engconfintl.org/geohazards/7>.
- Cartier G., and Pouget, P. 1988 Etude du comportement d'un remblai construit sur un versant instable, le remblai de Salledes. (Puy-de-Dome). Rapport de recherché LPC No. 153 Laboratoire Central des Ponts et Chaussees, Paris.
- Clague, J.J. and Evans, S.G. 2003. Geologic framework of large historic landslides in Thompson River Valley, British Columbia. *Journal of Environmental and Engineering Geoscience*, 9(3): 201-212. doi:10.2113/9.3.201.
- Contreras, I.A., Grosser, A.T., Ver Strate, R.H. 2008. Geotechnical instrumentation news – the use of the fully-grouted method for piezometer installation, Part 1 and Part 2. *Geotechnical News* 26(2): 30-37.
- Contreras, I.A., Grosser, A.T., Ver Strate, R.H. 2012. Geotechnical instrumentation news – update of the fully-grouted method for piezometer installation. *Geotechnical News* June 2012, 20-25.
- Cruden, D.M., and Varnes, D.J. 1996. Landslide types and processes. *In* Landslides: Investigation and mitigation. Transportation Research Board, Special Report 247, pp. 36-75.
- Cruden, D.M. 2016. Personal communication (Thesis defense comments). April 21, 2016.

- Dottori, F., Martina, M.L.V., Todini, E. 2009. A dynamic rating curve approach to indirect discharge measurement, *Hydrol. Earth Syst. Sci. Discuss.*, 6, pp. 859-896.
- Duncan, J.M., and Wright, S.G. 2005. *Soil strength and slope stability*. John Wiley & Sons, Inc., Hoboken, New Jersey.
- Eden, W.J. 1955. A Laboratory study of varved clay from Steep Rock Lake, Ontario, *American Journal of Science*, Vol.253, pp.659-674.
- Environment Canada. 2015. Barometric Pressure readings taken at the Kamloops AUT weather Station. <http://climate.weather.gc.ca/> [accessed October 15, 2015].
- Environment Canada. 2015. Flow rates and water elevations of the Thompson River measured near Spences Bridge, BC (08LF051). <http://www.wateroffice.ec.gc.ca> [accessed December 10, 2015].
- Environment Canada. 2015. Weather station data recorded at the Long Lake Station. <http://climate.weather.gc.ca/> [accessed December 12, 2015].
- Eshraghian, A., Martin, C.D., and Cruden, D.M., 2005. Landslides in the Thompson River Valley between Ashcroft and Spences Bridge, British Columbia. *In Proceedings of the International Conference on Landslide Risk Management, Vancouver, B.C. 31 May – 3 June 2005. Edited by O. Hungr, R. Fell, R. Couture, and E. Eberhardt. A.A. Balkema, London. Pp 437-446.*
- Eshraghian, A., Martin, C.D., and Cruden, D.M. 2007. Complex earth sides in the Thompson River Valley, Ashcroft, British Columbia. *Environmental and Engineering Geoscience*, 13(2): 161-181. doi:10.2113/gseegeosci.13.2.161.

- Eshraghian, A., Martin, C.D., and Morgenstern, N.R. 2008. Movement triggers and mechanisms of two earth slides in the Thompson River Valley, British Columbia, Canada. *Canadian Geotechnical Journal*. 45. pp 1189-1209. Doi:10.1139/T08-047.
- Evans, S.G. 1982. Landslides in surficial deposits in urban areas of British Columbia: a review. *Canadian Geotechnical Journal*, Vol.19, pp. 269-288.
- Evans, S.G., Cruden, D.M., Bobrowsky, P.T., Guthrie, R.H., Keegan, T.R., Liverman, D.G.E., and Perret, D. 2005. Landslide risk assessment in Canada; a review of recent developments, *In Proceedings of the International Conference on Landslide Risk Management*, Vancouver, B.C. 31 May – 3 June 2005. *Edited by* O. Hungr, R. Fell, R. Couture, and E Eberhardt. A.A. Balkema, Rotterdam. Pp. 351-434.
- Fulton, R.J., and Smith, G.W. 1978. Late Pleistocene stratigraphy of south-central British Columbia. *Canadian Journal of Earth Sciences* 15, pp 971-980.
- Google Earth. “Ripley Landslide and surrounding area” 50 33’24.81” N and 121 13’37.81” W. Google Earth. October 8, 2014. [Accessed December 2, 2015].
- Gundogdu, B. 2011. Relations between pore water pressure, stability and movements in reactivated landslides. Masters thesis, Middle East Technical University, Turkey
- Hendry, M.J. 1982. Hydraulic Conductivity of a Glacial Till in Alberta. *Ground Water*. Vol. 20, No. 2. pp 162-169.
- Hendry, M.J., Barbour, S.L., Novakowski, K., Wassenaar, L.I. 2013. Paleohydrogeology of the Cretaceous sediments of the Williston Basin using stable isotopes of water. *Water Resources Research*, vol. 49, 4580-4592, doi:10.1002/wrcr.20321.

- Hendry, M.T. 2011 The geomechanical behaviour of peat foundations below rail-track structures. Doctoral dissertation, University of Saskatchewan, Saskatoon, Canada.
- Hendry, M.T., Macciotta, R., Martin, C.D., Reich, B. 2015. Effect of Thompson River elevation on velocity and instability of Ripley Slide. *Canadian Geotechnical Journal*. 52: 1-11. doi: 10.1139/cgj-2013-0364.
- Huntley, D.H., Bobrowsky, P.T. 2014. Surficial geology and monitoring of the Ripley Slide, near Ashcroft, British Columbia, Geological Survey of Canada, Open File 7531.
- Hvorslev, M.J. 1951. Time-lag and Soil Permeability in Ground Water Observations. Waterways Experimental Station, Corps of Engineers, United States Army, Vicksburg, MS, USA, Bulletin 36.
- Leonoff, C., and Klohn Leonoff Ltd. 1994. A dedicated team: Klohn Leonoff Consulting Engineers 1951-1991. Klohn Leonoff, Richmond, Canada. pp. 19.
- Levesque, C. 2015. Personal communication. January 7, 2015.
- Macciotta, R., Hendry, M., Martin, C.D., Elwood, D., Lan, H., Huntley, D., Bobrowsky, P., Sladen, W., Bunce, C., Choi, E., Edwards, T. 2014. Monitoring of the Ripley Landslide in the Thompson River Valley, B.C., 6th Canadian Geohazards Conference, Kingston, Ontario, 15-18 June. doi:10.13140/2.1.2811.7125.
- Marefat, V., Duhaime, F., and Chapuis, R.P. 2015. Pore Pressure Response to Barometric Pressure Change in Champlain Clay: Prediction of the Clay Elastic Properties. *Engineering Geology* 198 (November): 16–29. doi:10.1016/j.enggeo.2015.09.005.

- Matheson, D.S., and Thomson, S. 1973. Geological Implications of Valley Rebound. Canadian Journal of Earth Sciences. Vol. 10, pp. 961-978.
- McKenna, G.T. 1995. Grouted-in Installation of Piezometers in Boreholes. Canadian Geotechnical Journal 32, pp. 355-363.
- Measurand Inc. 2013. Manual ShapeAccelArray. Fredricton, NB, Canada. <http://www.measurandgeotechnical.com/docs/saamanual21mar13.pdf>. [accessed April 23, 2015].
- Mikkelsen, P.E. and Green, E.G. 2003. Piezometers in Fully Grouted Boreholes. International Symposium on Geomechanics, Oslo, Norway, September 2003.
- Miller, B.G.N., and Cruden, D.M. 2002. The Eureka River landslide and dam, Peace River Lowlands, Alberta. Canadian Geotechnical Journal 39, pp. 863-878.
- National Atlas of Canada. Surveys and Mapping Branch, Energy and Mines and Resources. 1972. Glacial Geology, pp. 33-34.
- Norrish, N.I, Wyllie, D.C. 1996 Rock Slope Stability Analysis. Landslides : Investigation and Mitigation, Transportation Research Board Special Report 247, Washington, DC, edited by Turner, A.K. and Schuster, R.L. pp 391 to 425.
- Olson, R. 2015. Personal communication. June 16, 2015.
- Perry, N. 2016. Personal communication, January 6, 2016.

- Porter, M.J., Savigny, K.W., Bunce, C.M., MacKay, C. 2002 Controls on stability of the Thompson River landslides. In Proceedings of the 55th Canadian Geotechnical Conference, Niagara Falls, pp. 690-698.
- Province of British Columbia 2015 Regulations on the irrigation of crops in the Ashcroft area. http://www.env.gov.bc.ca/wsd/water_rights/ [accessed January 10, 2015].
- Province of British Columbia. 2015. Drought classifications and British Columbia region map. <http://www.livingwatersmart.ca/drought/> [accessed January 10, 2015].
- Quigley, R.M. 1980. Geology, mineralogy, and geochemistry of Canadian soft soils: a geotechnical perspective. Canadian Geotechnical Journal. Vol. 17, pp. 261-285.
- Ryder, J.M. 1976. Terrain inventory and quaternary geology, Ashcroft, British Columbia. Geological Survey of Canada, Paper 74-79, doi:10.4095/102556.
- Ryder, J.M., Fulton, R.J., and Clague, J.J. 1991. The Cordilleran Ice Sheet and the glacial geomorphology of southern and central British Columbia. *Geographie physique et Quaternaire*, 45: 365-377.
- Ryder, M. 2016. Personal Communication. January 7, 2016.
- Simeoni, L., De Polo, F., Caloni, G., Pezzetti, G., 2011. Field performance of fully grouted piezometers. *In Proceedings of the 8th International Symposium on Field Measurements in Geomechanics.*, Volume: ISBN: 3-927610-87-9.
- Skempton, A.W. 1954. The Pore-Pressure Coefficients A and B. *Geotechnique*, Vol. 4, Issue 4, pp.143-147.

- Skempton, A.W., Leadbeater, A.D., and Chandler, R.J. 1989. The Mam Tor Landslide, North Derbyshire. *Philosophical Transactions of the Royal Society A: Mathematical, Physical and Engineering Sciences*, 329: 503-547.
- Slope Indicator. 2013. *VW Piezometer Manual*. Mukiltea, Washington, USA. www.slopindicator.com/pdf/manuals/vw-piezometer-manual.pdf [accessed April 23, 2015].
- Smith, N.D., and Ashley, G. 1985. Chapter 4 Proglacial Lacustrine Environment. *Short Course 16: Glacial Sedimentary Environments*. The Society of Economic Paleontologists and Mineralogists. pp. 135-216.
- Stanton, R.B., 1898. The great land-slides on the Canadian Pacific Railway in British Columbia. *In Proceedings of the Institution of Civil Engineers, Session 1897-1898, Part II, Section 1*, pp. 1-46.
- Statistics Canada. 2016. Table 404-0014 – Railway transport survey, operating statistics, by mainline companies, annual (metric units). CANSIM (database). <http://www5.statcan.gc.ca/subject-sujet/result-resultat?pid=4006&id=4011&lang=eng&type=ARRAY&pageNum=1&more=0>. [accessed March 1, 2016].
- Toth, J. 1962. A Theory of Groundwater Motion in Small Drainage Basins in Central Alberta, Canada. *Journal of Geophysical Research*, 67(2): 4375 – 4387.
- Vaughan, P.R. 1969. A Note on Sealing Piezometers in Boreholes. *Geotechnique*, Vol. 19, No. 3, pp.405-413.